Dominic Jones
26/12/19

The use of Molecular and Physiological approaches to analyse GROUP VII ETHYLENE RESPONSE FACTORS (ERFVIIs) and the PRT6 N-degron Pathway

Project Supervisor:
Prof Michael Holdsworth

Keywords: Adaption to Environment, ERFVIIs, Protochlorophyllide

Number of Words in Abstract: 184
Number of Words in Main Text: 30,420

Thesis write-up submitted to The University of Nottingham in fulfilment of the requirements for the Masters of Research with Plant and Crop Science

Abstract:

Vast proportions of the earth are high altitude and mountainous terrain. For successful growth development at high altitude, seedlings must adapt to high altitude conditions in order to survive. The major difference in high altitude terrain to that of sea level is the difference in surrounding oxygen concentration (v/v). Oxygen concentration falls significantly as altitude elevation increases, resulting in an increasingly hypoxic environment. GROUP VII ETHYLENE RESPONSE FACTORS (ERFVIIs) have been shown to responsible for sensing oxygen and are substrates of the PRT6 N-degron pathway of proteolysis. Here, I investigate the adaption to altitude associated with *A. thaliana* accessions and the impact of growing *A. thaliana* accessions in a hyperoxic (27%) environment. In addition, I show the role of the RELATED TO APETALA2.3 (RAP2.3) ERFVII in regulating protochlorophyllide (PCH) accumulation following an extended period of darkness and etiolation of the seedling. Furthermore, I develop transgenic tools to enable further analysis of the PRT6 N-degron pathway. Observations show significant differences in responses of accessions to varying growth conditions, and show that altitude adaption is an essential component of ensuring successful growth and survival of seedlings.

Table of Contents:

2. Chapter Two: Materials and Methods

3. Chapter Three: Results

4. Chapter Four: Discussion

Abbreviations:

Term	Definition
PTMs	Post-translational modifications, e.g arginylation.
ATEs	Arginyl transferases.
PCOs	Plant cysteine oxidases.
Ubiquitin (Ub)	Ubiquitin is a small (8.6 kDa, 76-residue) eukaryotic protein that can be conjugated to a substrate protein, thereby marking it for degradation.
N-degron	A class of degradation signal targeted by the N-degron pathway. An N-degron has an either modified or unmodified destabilising N-terminal residue of a protein (Varshavsky, 2011).
C-degron	A class of degradation signal targeted by the C-degron pathway.
N-degron pathway	The half-life of a protein is determined by the residue exposed at its N-terminus.
Degron	A degradation signal (Varshavsky, 1991).
N-recognin	Specific binding proteins that recognise N-degrons with specialised binding sites (Dougan *et al.,* 2012).
PRT6 N-degron pathway	A eukaryotic protein degradation pathway that involves the Nt-arginylation of protein substrates targeting the protein for ubiquitination through the N-recognin E3 ubiquitin ligases and degradation via the 26S proteasome.
PCH	Protochlorophyllide. The pre-cursor to chlorophyllide in the tetrapyyrole chlorophyll biosynthesis pathway.
POR	Protochlorophyllide reductase. The enzyme responsible for converting PCH to chlorophyllide during the tetrapyyrole chlorophyll biosynthesis pathway.
ERFVIIs	Group VII ethylene response factors.
MetAPs	Methionine amino-peptidases. Responsible for the co-translational cleavage of Met at position 2 in the Arg/N-degron pathway and the Ac/N-degron pathway.
PRT6	The proteolysis N-recognin responsible for recognising the N-degron in the PRT6 N-degron pathway.

DUBs	Deubiquitinating enzymes. These are utilised during the URT.
URT	The ubiquitin reference technique. A technique based on the ubiquitin fusion technique enabling any amino acid to be exposed at the N-terminus of a protein rather than Met.
RAP	RELATED TO APETALA proteins. A subset of ERFVIIs.
HRE	HYPOXIA RESPONSIVE proteins. A subset of ERFVIIs.
PIFs	Phytochrome-interacting transcription factors. Repress chlorophyll biosynthesis during darkness.
ROS	Reactive oxygen species.
Hypoxia	<10% v/v oxygen concentration.
Normoxia	~21% v/v oxygen concentration.
Hyperoxia	>21% v/v oxygen concentration.

Table 1:

Glossary of terms regarding literature surrounding the various N-degron pathways.

Chapter One:

Introduction

1.01 Flooding and Submergence:

Oxygen sensing is essential for survival in plants. Oxygen is vital for photosynthesising organs, but oxygen sensing and response is equally important in non-photosynthetic organs such as roots, flowers and fruits (Drew, 1997; Bailey-Serres and Voesenek, 2008). Plants lack an active system to distribute oxygen (van Dongen and Licausi, 2015). This results in highly active metabolic tissues such as meristems and fruits developing hypoxic (oxygen concentrations below 10% v/v) cores, even at normoxic oxygen levels (21% v/v oxygen) (Rolletschek *et al.,* 2004; Armstrong *et al.,* 2009). A variety of factors can cause a decrease in external oxygen levels, for example winter ice encasement, poor ventilation in a green house, or being grown at altitude. However, the most common, and threatening, cause of hypoxic oxygen levels is flooding.

A huge variety of crop plants suffer from flooding, often caused through a combination of both heavy rain fall and poor irrigation (Hinz *et al.,* 2010). Flooding results in almost 60% of all crop losses worldwide and causes damage of approximately $7.8 billion (Food and Agriculture Organization of the United Nations, 2015). As it becomes more difficult to feed the rising population, finding a solution to decrease these crop losses is essential. Flooding causes oxygen concentration surrounding the plant to decrease by up to 10^4, resulting in a hypoxic environment. Responding to this flooding and submergence is critical for the survival of the plant, and plants have developed both metabolic and morphological strategies to overcome both short-term and long-term submergence (Kende *et al.,* 1998; Drew *et al.,* 2000).

During periods of flooding and expected long term submergence some species of plants can adopt a quiescent state. This involves the plant arresting development and growth to conserve the energy use of carbohydrates in order to maximise and extend chance of potential long term underwater survival (Bailey-Serres and Voesenek, 2008; Colmer and Voesenek 2009). The most famous and exciting use of the quiescent strategy is that of SUB1 rice (Xu *et al.,* 2006). *SUB1A* was introgressed into a high yielding variety of rice named Swarna. It was found that the rice was then tolerant to submergence, whilst maintaining its high yield. It has been shown that the response in this deep water Swarna-*SUB1A* was due to a specific group of ethylene response factors (ERFs) named GROUP VII ETHYLENE RESPONSE FACTORS (ERFVIIs). During submergence ERFVIIs rapidly accumulate in flooded tissues and control their response through altering gibberellin acid (GA) signalling. The induction of the SUB1A ERFVII increases the accumulation of SLENDER RICE1 (SLR1) and SLENDER RICE1 LIKE1 (SLRL1) (Fukao *et al.,* 2006; Gibbs *et al.,* 2015). SLR1 and SLRL1 are GA signal repressors that inhibit hypocotyl and stem elongation, whilst also promoting the catabolism of carbohydrates (Fukao and Bailey-Serres *et al.,* 2008; Hirano *et al.,* 2012). In the quiescent strategy GA 20-oxidase is also deactivated; reducing the levels of active GA and enhancing SLR1 stability (Jung *et al.,* 2010).

If the response is one of a morphological nature and the plant is trying to rapidly grow upwards to supersede the water line, then this is known as the 'escape' strategy. Some key morphological traits needed for the escape strategy include: shoot elongation, development of aerenchyma and adventurous root formation (Sauter, 2000; Drew *et al.,* 2000; Voesenek *et al.,* 2006). During the escape strategy ERFVIIs are also utilised; however, it is *SNORKEL1* and *SNORKEL2* that regulate escape (Xu *et al.,* 2006; Hattori *et al.,* 2009). When these ERFVIIs are triggered by ethylene, GA 20-oxidase is upregulated increasing GA levels and promoting internode elongation, helping the plant extend above the water line and escape submergence (Raskin and Kende, 1984; Hattori *et al.,* 2004; Ayano *et al.,* 2014). However, these processes are very energy intensive, hence why it has only arisen in species that encounter slow rising flood waters, and not plants that suffer from rapid submergence.

1.02 ETHYLENE RESPONSE FACTORS (ERFs):

ERFs are vital signalling components of plants. ERFs are transcription factors (TFs) that belong to the multigene family of APETALA2 (AP2)/ERF TFs (Muller and Munne-Bosch, 2015). This multigene family of proteins contains either one or two AP2 domains. The ERF or EREBP (ethylene-responsive element-binding proteins) family has one AP2 domain. The RAV (related to ABI3/VP1) family also contains only one AP2 domain, but also has a B3 domain, with the AP2 family having two AP2 domains (Okamuro *et al.,* 1997; Riechmann and Meyerowitz 1998; Nakano *et al.,* 2006; Hinz *et al.,* 2010). ERFs vary in the way that they act, with different types of ERFs binding as either activators or repressors to the GCC box (AGCCGCC) elements (Ohme-Takagi and Shinshi, 1995). However, recently it has been suggested that some ERFs act through binding to dehydration responsive elements (Muller and Munne-Bosch, 2015). Overall, ERFs act as a regulatory hub integrating other signals such as abscisic acid, jasmonate and cytokinin; and they are essential in the quick and effective response to a variety of abiotic stresses such as drought, salinity, and light intensity (Muller and Munne-Bosch, 2015).

1.03 GROUP VII ETHYLENE RESPONSE FACTORS (ERFVIIs):

Group VII ethylene response factors (ERFVIIs) are a specific group of ERFs that form a phylogenetic cluster (Giuntoli and Perata, 2018) conserved throughout all angiosperms (Licausi *et al.,* 2011). They are most notably defined for their response to oxygen sensing and flooding (Xu *et al.,* 2006) as described in 1.01. In *Arabidopsis thaliana* (*A. thaliana*) there are a variety of different members of the ERFVII family that contribute to oxygen sensing and survival during flooding, most notably: RELATED TO APETALA2.12 (RAP2.12) (Hinz *et al.,* 2010), RAP2.2, RAP2.3 (Licausi *et al.,* 2010), HYPOXIA RESPONSIVE1 (HRE1), and HRE2 (Xu *et al.,* 2006). All ERFVIIs are characterised by their highly conserved N-terminal motif that in the presence of oxygen and nitric oxide (NO) is recognised as a degradation signal for degradation via the PRT6 N-degron pathway of targeted proteolysis (Gibbs *et al.,* 2014a). All members of the ERFVII family have unique and diverse functions in order to coordinate responses.

1.03.1 RAP2.12:

RAP2.12 is an important ERFVII TF (Nakano *et al.,* 2006) which acts as an activator of the anaerobic response to hypoxia (Licausi *et al.,* 2011). Like other members of the ERFVII group in *A. thaliana*, RAP2.12 is constitutively expressed at the RNA level in a variety of different cell types but upon the presence of oxygen the protein is degraded (Licausi *et al.,* 2011; Kosmacz *et al.,* 2015). In normoxic conditions a small amount of RAP2.12 is stored at an inactive site at the plasma membrane. In the plasma membrane RAP2.12 is protected from degradation as it is bound to ACYL-COA BINDING PROTEIN 1 and 2 (ACBP1 and ACBP2) (Licausi *et al.,* 2011). However, following a decrease in oxygen levels (such as during flooding and submergence) RAP2.12 quickly moves from the plasma membrane to the nucleus (Gibbs *et al.,* 2011; Kosmacz *et al.,* 2015). This rapid movement ensures a quick and effective response to any hypoxic stress (Giuntoli and Perata 2018). RAP2.12's movement to the nucleus specifically activates the expression of genes involved with anaerobic metabolism such as: PYRUVATE DECARBOXYLASE 1 (PDC1) and ALCOHOL DEHYDROGENASE1 (ADH1) which are specifically involved in ethanol fermentation (Paul *et al.,* 2016). SUCROSE SYNTHASE1 (SUS1) and SUS4 genes are also expressed and these are involved in carbohydrate degradation, providing energy for plant growth and

development (Paul *et al.,* 2016). PHYTOGLOBIN1 (PGB1) is also expressed which is involved in scavenging nitric oxide to promote the conversion of NADH to NAD^+ (Licausi *et al.,* 2011; Paul *et al.,* 2016; Hartman *et al.,* 2019).

The role of RAP2.12 in controlling the induction of many of genes was confirmed by Paul *et al.,* 2016. Results also showed there was an increase in fermentation products such as ethanol, lactate and alanine in the overexpression of a PRT6 N-degron pathway insensitive form of RAP2.12 (Δ13RAP2.12 – does not contain the first 13 amino acids from the N-terminus, including the regulatory cysteine) (Licausi *et al.,* 2011). As Δ13RAP2.12 does not contain the regulatory cysteine, cysteine oxidation does not occur resulting in the stability of the protein. In the N-degron sensitive form of RAP2.12, Paul *et al.,* 2016 did not see the same increase in these fermentation products. Those results confirmed the essential role of RAP2.12 in preventing aerobic fermentation, as if RAP2.12 were absent then there would be rapid losses in energy and carbon reserves, resulting in a reduction of plant growth. This shows RAP2.12's particular importance in flood response as if the plant were to undergo aerobic fermentation during submergence the plant would rapidly use its carbohydrate reserves and be unable to survive if submergence persisted long-term.

RAP2.12 stabilisation also regulates a variety of other metabolic processes including: respiration, the tricarboxylic acid cycle (TCA), amino acid metabolism, and the regulation of immune-regulatory metabolites. However, it is not a central regulator in most of these processes and its prime role remains to be rapidly transported from the plasma membrane to the nucleus to promote anaerobic fermentation following submergence (Paul *et al.,* 2016).

1.03.2 RAP2.2:

RAP2.2 is an ERFVII that is expressed at high levels constitutively in the roots and in shoots, where RNA is induced by extended periods of darkness (Hinz *et al.,* 2010). Similarly to both RAP2.12 and RAP2.3, RAP2.2 accumulates constitutively under normoxic conditions and undergoes translation during hypoxia (Mustroph *et al.,* 2009; Juntawong *et al.,* 2014; Gasch *et al.,* 2016). However, unlike RAP2.12, RAP2.2 RNA expression is not induced by hypoxia but rather by ethylene (Hinz *et al.,* 2010). Hinz *et al.,* 2010 showed that following overexpression of RAP2.2 survival was significantly improved during darkness. This showed that while RAP2.2 and ERFVIIs main function is to respond to oxygen levels, they are also regulated in part by light. If the plant has higher existing levels of RAP2.2 it enables a faster response to hypoxia, allowing a more efficient response and a strengthened chance of survival.

RAP2.2 has a vast number of roles excluding that of its role during hypoxia. RAP2.2 can also bind the sequence 5'-ATCTA-3' which is present in the carotenoid synthesis pathway of *PHYTOENE SYNTHASE* (PSY) and *PHYTOENE DESATURASE* (PDS) genes (Welsch *et al.,* 2007). Carotenoids are essential during photosynthesis as they harvest light energy and protect from damage by excessive light energy (Szabo *et al.,* 2005).

RAP2.2 is also important in resistance to pathogens, particularly the necrotroph *Botrytis cinera* (Zhao *et al.,* 2012). It was shown in Zhao *et al.,* 2012 that RAP2.2 expression was induced by *B. cinera* infection and ethylene treatment; whereas, in the ethylene insensitive mutants that lack the transcription factors required to initiate the ethylene response (*ein2* and *ein3 eil1*) the induction of RAP2.2 was disrupted and the plant became susceptible. The role of RAP2.2 in resistance was further confirmed by overexpressing RAP2.2 and using a *rap2.2-3* mutant. The line overexpressing RAP2.2 showed increased resistance to *B. cinera,* whereas the mutant line showed increased susceptibility.

1.03.3 RAP2.3

RAP2.3 is a transcriptional regulator and is localised to the nucleus and activates via binding GCC-boxes. This was confirmed through identification of RAP2.3's ability to bind to a GCC-box containing promoter region of the ABI5 gene (Gibbs *et al.,* 2014), and was also confirmed by RAP2.3 being able to transactivate a promoter containing tandem GCC-box copies (Rosa *et al.,* 2014).

However, similarly to other RAP TF's, RAP2.3 plays an important role in the hypoxia response. RAP2.3 works in combination with other RAP TF's to activate genes involved in anaerobic metabolism such as SUCROSE SYNTHASE1 (SUS1) and SUS4, as well as ADH1 and PDC1 (Papdi *et al.,* 2015).

1.03.4 HRE1 and HRE2:

HRE1 and HRE2 ERFVIIs are expressed at low levels during aerobic conditions and upon hypoxia are strongly upregulated (Bui *et al.,* 2015). Like RAP2.12 and RAP2.3, both HRE1 and HRE2 are localised to the nucleus upon hypoxia. HRE1 and HRE2 differ from RAP-type proteins in that they are unable to activate natural anaerobic promoters (Bui *et al.,* 2015). Unlike RAP type proteins, HRE proteins are also unable to associate with the hypoxia responsive promoter element (HPRE), a proposed functional anaerobic promoter element (Gasch *et al.,* 2016). This suggests that t here is a deficiency in DNA binding of HRE type protein, even though they contain the fully conserved AP2/ERF domain, potentially meaning that there are specific domains present on RAP type ERFVII proteins that are required for the interaction with HPRE. This agrees with what has been suggested that HRE's are necessary to sustain anaerobic gene expression, but it is the RAP type proteins required to initiate the transcriptional responses (Licausi *et al.,* 2010).

HRE1 specifically acts as an enhancer but not the actual inducer of the anaerobic response, as shown by Licausi *et al.,* 2010 where the induction of ADH and other anaerobic genes still occurred in the *hre1* loss of function mutant. Many other anaerobic genes were not upregulated in the *hre2* loss of function mutant, but the response to hypoxia remained strong. However, it was only in the double mutant *hre1 hre2* that there was a severe reduction in the anaerobic response; suggesting that there may be a partial redundancy in the function of HRE1 and HRE2 in that they both upregulate anaerobic gene expression, despite the specific anaerobic genes that they upregulate being different.

The method in which HRE1 and HRE2 are regulated however relies upon different mechanisms. HRE1 requires *de novo* protein synthesis to be induced and is only transiently induced with peak levels 2-4 hours after induction of hypoxia; whereas, HRE2 is regulated post-transcriptionally via mRNA stabilisation and its expression is conserved for 8 hours following hypoxia induction (Licausi *et al.,* 2010).

HRE proteins are essential to hypoxia response. Even though they themselves do not solely induce and respond to hypoxia, their importance in regulation and enhancement of anaerobic genes is essential for a complete response to low oxygen, as well as inducing the expression of RAPs. Unlike some of the RAP proteins however, HRE proteins their function appears to be exclusively related to oxygen response; whereas RAP proteins have a diverse range of functions (Licausi et al., 2010; Rosa *et al.,* 2014).

1.04 N-Degron Pathways of Protein Degradation:

The first initial clues and discoveries of the PRT6 N-degron pathway existing was found in *Saccharomyces cerevisiae* in yeast where it was uncovered that chimeric ubiquitin- β-galactosidase reporters containing varying nucleotide amino acids have different stabilities when grown *in vivo* (Bachmair *et al.,* 1986; Varshavsky, 2011; Gibbs *et al.,* 2014b). This is the study gave the first indications that the half-life of a protein is dictated by the amino acid at its N-terminus either being one of stabilisation or destabilisation; therefore, uncovering the vital features of the PRT6 N-degron pathway (Varshavsky, 2011; Sriram *et al.,* 2011).

Since the initial uncovering of a proteins fate being determined by its N-terminus, various branches of N-degron pathways have been uncovered.

1.04.1 The Eukaryotic PRT6 N-Degron Pathway:

The N-degron pathway in eukaryotes (such as *A. thaliana*) begins with the cysteine (Cys) residue at the amino-terminus (N-terminal) being exposed upon methionine (Met) cleavage by MAP (Met aminopeptidase) enzymes, making the Cys residue be susceptible to oxidation. Once the Cys residue has been oxidised (*Cys), ARGINYL TRANSFEREASE (ATE) conjugate *Cys to arginine (Arg). The Arg-specific N-recognin is then recruited (PRT6) (Garzon *et al.,* 2007). PRT6 is an N-degron pathway specialised E3 ligase that labels the ERFVII for degradation via ubiquitination and the 26S proteasome.

However, it is only during the presence of oxygen and NO that ERFVIIs are degraded via the PRT6 N-degron pathway. This is because that the oxidation of Cys required for degradation of the substrate is promoted by specific thiol oxygenases called PLANT CYSTEINE OXIDASES (PCOs), which convert Cys into Cys-sulfinic acid, acting as an ATE substrate (White *et al.,* 2017). As PCOs are only able to do this conversion of Cys to Cys-sulfinic acid in the presence of oxygen, this means that ERFVIIs are targeted to the proteasome in an oxygen dependent manor (Giuntoli and Perata, 2018).

When ERFVIIs are stable (during normoxia), they are able to selectively accumulate and enhance the translation of a core set of transcripts (Branco-Price *et al.,* 2008; Mustroph *et al.,* 2009). The set of transcripts promoted aid in providing essential conditions to enhance survival in low oxygen stress, such as: the protection of subcellular components, altering cell metabolism for sustainable and efficient energy production, and the detoxification of harmful anaerobic metabolism products (Giuntoli and Perata, 2018).

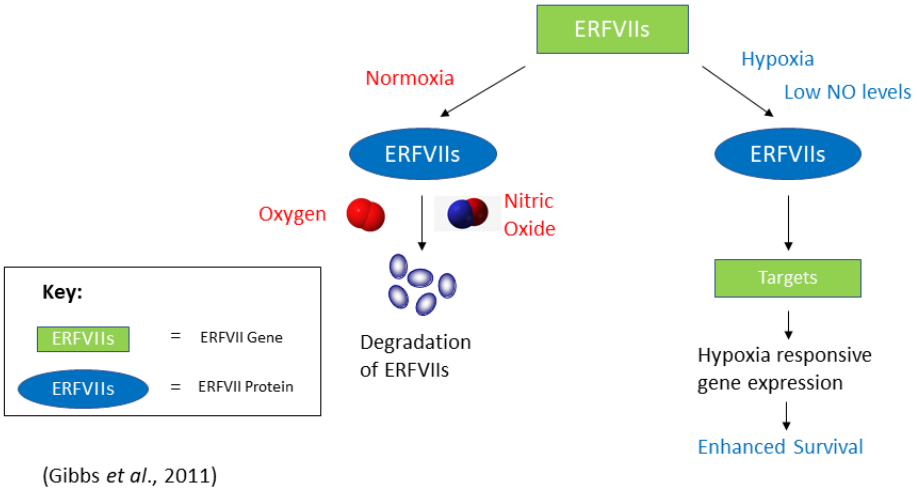

(Gibbs *et al*., 2011)

Figure 1:

Schematic of the fate of ERFVIIs in either normoxia or hypoxia (or low NO levels) via the PRT6 N-degron pathway.

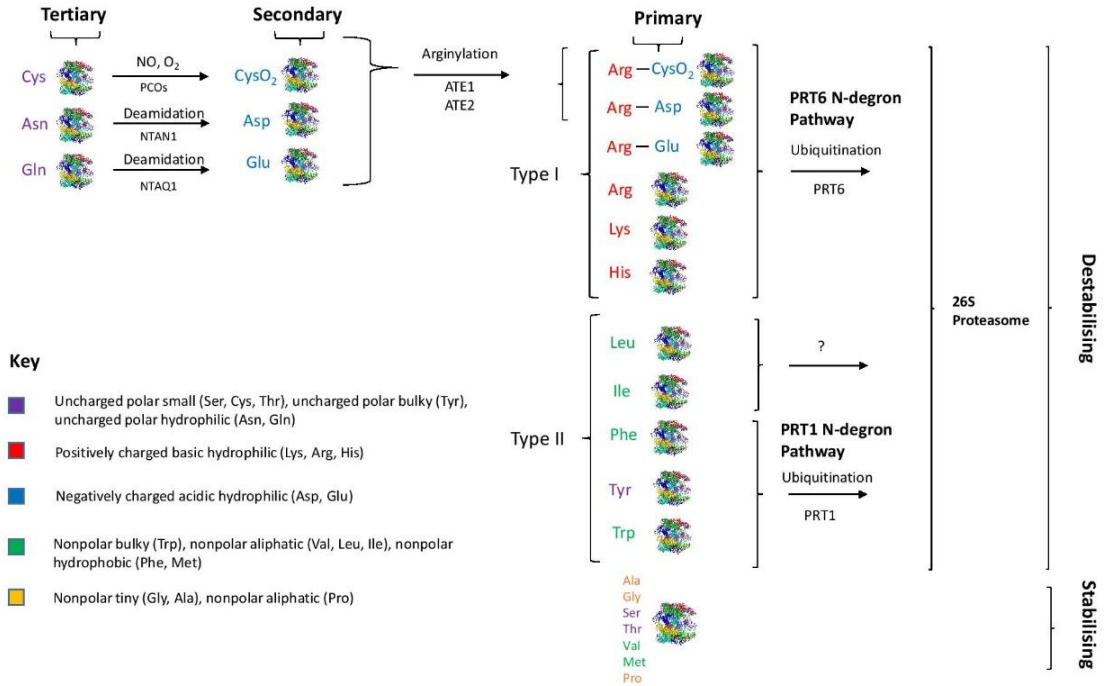

Figure 2:

The contemporary knowledge surrounding protein degradation via the N-degron pathways in plants. In plants the N-degron pathway is subdivided into two sections called the PROTEOLYSIS 6 (PRT6) and the PRT1 branches, addressing the type I residues (Arg, Lys and His) and type II residues (Leu, Ile, Phe, Tyr and Trp) residues respectively. The residue at the N-terminus of the protein classifies either stabilisation or destabilisation of the

protein. The three classes of destabilising residues are: primary, secondary and tertiary. Substrates bearing primary residues (e.g Arg) can be recognised by E3 ubiquitin (Ub) ligases: PRT6 or PRT1. In the PRT6 N-degron pathway the secondary destabilising residues can be formed via N-terminal acetylases (NTAs) for Asn and Gln or by Cys dioxygenases (PLANT CYSTEINE OXIDASES, PCOs) from Cys and O_2. Arginyltransferases (ATEs) attach an N-terminal Arg to secondary destabilising residues meaning the N-terminus now bears a highly Arg. Following this the protein is ubiquitinated by E3 ubiquitin ligase and is degraded via the 26S proteasome.

1.04.2 The Eukaryotic Ac/N-Degron Pathway:

In eukaryotic proteins the retained N-terminal Met residue is often cotranslationally N-terminally acetylated (Nt-acetylated) (Aksnes *et al.,* 2016). The Nt-acetylated Met residue acts as a degradation signal, targeted by E3 ubiquitin ligases (Hwang *et al.,* 2010). In yeast the E3 ubiquitin ligase (Ac/N-recognin) is the ER membrane-embedded Doa10 (Hwang *et al.,* 2010). In mammals the Ac/N-recognin is Teb4 and Not4 (Park *et al.,* 2015). Following recognition of the Nt-acetylated Nt-residues the protein is targeted for degradation via the 26S proteasome.

1.05 How Plants and Animals Differ in Oxygen Sensing:

Despite plants and animals both being obligate aerobes (they both respire through the mitochondria and require oxygen to do so) (Gibbs *et al.,* 2011), the way in which they sense oxygen is different. The oxygen sensing mechanism in mammals involves the TF hypoxia-inducible factor-1-alpha (HIF-1α). During normoxia, HIF-1α is degraded via the proteasome after they have been hydroxylated; whereas, during hypoxia, hydroxylation is strongly inhibited (due to it being oxygen dependent) and HIF-1α can then induce hypoxia responsive genes (Bruick, 2003; Haddad, 2004; Brihimi-Horn *et al.,* 2005). Due to a number of similarities in which oxygen is sensed through the degradation of proteins, it may be expected that animals also regulate their oxygen sensing via the PRT6 N-degron pathway. However, at this time only ERFVIIs, VERNALIZATION2 (VRN2) and LITTLE ZIPPER 2 (ZPR2) in *A. thaliana* have been identified as substrates of the PRT6 N-degron pathway (Gibbs *et al.,* 2011; Licausi *et al.,* 2011; Gibbs *et al.,* 2018 Weits *et al.,* 2019). Nevertheless, it is speculated that the role of the N-degron pathway in oxygen and NO sensing in animals is underappreciated and it may have a more significant role than currently expected (Gibbs *et al.,* 2014).

There are also other differences in the response to oxygen between plant and animals. Plants lack an active system to distribute oxygen, meaning highly active metabolic tissues such as meristems and fruits quickly develop hypoxic cores, even during normoxia (Rolletschek *et al.,* 2004; Armstrong *et al.,* 2009). This means that oxygen transport is reliant on diffusion, resulting in steep oxygen gradients occurring in tissues such as seeds (Borisjuk and Rolletschek, 2009), roots (Armstrong *et al.,* 1994; Mancuso and Boselli, 2002), and fruits (Ho *et al.,* 2010; Kosmacz *et al.,* 2015); unlike in animals where oxygen distribution is free.

1.06 Chlorophylls

1.06.1 What is Chlorophyll?

Oxygen is not the only molecular signal that plants must respond to, light is another critical development signal in plants. Chlorophylls are green pigments found in the chloroplasts of plants that allow plants to harvest energy from light through photosynthesis. Chlorophylls are arranged in photosystems which are embedded within the thylakoid membranes within chloroplasts. Chlorophylls absorb light most strongly in the red and the blue portion of the electromagnetic spectrum (Muneer *et al.,* 2014), and absorb least strongly and reflect in the green and near-green portions of the spectrum; hence the green appearance in leaves and chlorophyll containing tissues. There are two types of chlorophyll that exist in the photosystems of green plants: chlorophyll *a* and chlorophyll *b*, each absorbing different parts of the electromagnetic spectrum.

There are also two different pathways in which chlorophyll synthesis takes place through: the tetrapyrrole biosynthesis pathway and the methylerythritol phosphate (MEP) pathway. The tetrapyyrole pathway produces the chlorophyllide required for chlorophyll production, and the MEP pathway is responsible for the isoprenoid phytol tail of the chlorophyll, produced from geranylgeranyl diphosphate (GGDP) (Kim *et al.,* 2013).

1.06.2 The Chlorophyll Tetrapyrrole Biosynthesis Pathway:

Chlorophyll biosynthesis begins with the synthesis of 5-aminolevulinoc acid (ALA) from glutamic acid. Through a series of reactions ALA is then converted to protoporphyrinogen IX. Protoporphyrinogen IX is then oxidised to protoporphyrin IX through Protoporphyrinogen IX oxidase activity. Protoporphyrin IX can then either be converted Mg-protoporphyrin IX via Mg-chelatase, or can be converted to protoheme via Fe-chelatase. Mg-protoporphyrin IX is then esterified to form Mg-protoporphyrin IX monomethyl ester. Mg-protoporphyrin IX monomethyl ester is then converted to protochlorophyllide. Following illumination protochlorophyllide is converted to chlorophyllide via protochlorophyllide oxidoreductase. Chlorlorophyllide is then esterified to form chlorophyll (Aarti *et al.,* 2006) (Figure 3).

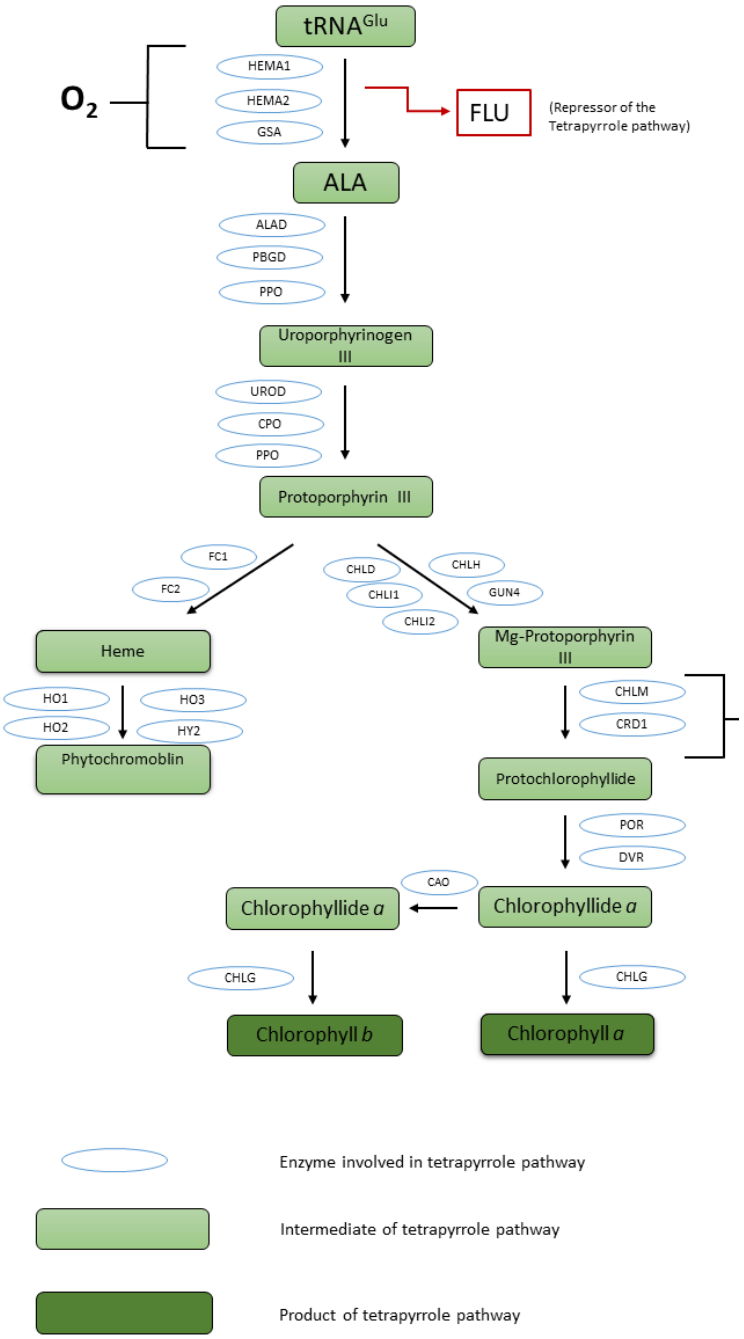

Figure 3:
The Plant Tetrapyrrole Pathway of Chlorophyll Synthesis Showing Key Enzymes.

ALA, 5-aminolevulinic acid; HEMA, glutamyl-tRNA reductase; GSA, glutamate-1-semialdehyde 2, 1-aminomutase; ALAD, 5-aminolevulinate dehydratase; PBGD, porphobilinogen deaminase; UROS, uroporphyrinogen III synthase; UROD, uroporphyrinogen III decarboxylase; CPO, coproporphyrinogen III oxidase; PPO, protoporphyrinogen IX oxidase; CHLH, Mg-chelatase H subunit; CHLI, Mg-chelatase I subunit; CHLD, Mg-chelatase D subunit; GUN4, regulator of Mg-chelatase; CHLM, Mg-proto IX methyltransferase; CRD1, Mg-proto IX monomethyl cyclase; POR, NADPH:protochlorophyllide oxidoreductase A, B and C; DVR, divinyl-protochlorophyllide reductase; CHLG, chlorophyll synthase; CAO, chlorophyllide a oxygenase; FC, ferrochelatase; HO, heme oxygenase; HY2, phytochromoblin.

1.07 Functions of the PRT6 N-degron Pathway:

It is not just flooding and submergence response that ERFVIIs and the PRT6 N-degron pathway respond to. There are a wide variety of functions that the PRT6 N-degron pathway is known to perform in, and they occur at multiple stages throughout plant development.

1.07.1 The PRT6 N-Degron Pathway's Role in Photomorphogenesis:

It is not just oxygen that ERFVIIs and the PRT6 N-degron rule pathway solely respond to, it has been shown that is essential for there to be an integrated response of oxygen sensing and light availability (Abbas *et al.,* 2015). When plants are below ground during darkness they must sense and respond to the darkness and follow a morphological plan of development that best suits them to survive in these conditions (skotomorphogenesis) (Wu, 2014). By recognising the periods of extended darkness it allows the plant to develop specific traits to adapt to this environment such as hypocotyl elongation, closed apical hook development (Abbas *et al.,* 2013; Mazzella *et al.,* 2014), suppressed chlorophyll biosynthesis, and cotyledon greening. Each of these traits serve specific roles to aid survival of the developing seedlings. Hypocotyl elongation takes place instead of cotyledon and root development as it allows the seedling to grow up to the surface at a much faster rate, allowing it to more actively seek the light it requires for photosynthesis. The closing of the apical hook develops to protect the small unfolded cotyledons and the underlying meristematic region from taking any damage whilst the seedling is attempting to push through the soil to the surface (Josse and Halliday, 2008). In flowering plants chlorophyll synthesis is supressed due to the enzyme required to make chlorophyll (protochlorophyllide reductase – POR) is light activated, and no light is present in the below ground environment during skotomorphogenesis.

However, the seedling only detecting the absence of light is not an ample environmental signal for the development of key skotomorphogenic traits (Sperling *et al.,* 1997; Raz and Ecker, 1999). Oxygen sensing through ERFVIIs and the PRT6 N-degron pathway is also essential for directing the development of traits as a response to the below ground environment (Abbas *et al.,* 2015). Through using mutants of the PRT6 N-degron pathway and evaluating their effect on the development of skotomorphogenic traits Abbas *et al* 2015 confirmed the role of ERFVIIs and the PRT6 N-degron pathway in both apical hook development and survival rates of etiolated (dark grown) seedlings (Abbas *et al.,* 2015).

Confirmation that survival of etiolated seedlings was in part controlled by ERFVIIs was an extremely important discovery. Survival of etiolated seedlings has primarily been linked to be due to photo-oxidative damage caused by high reactive oxygen species (ROS) levels. High ROS levels cause photo-oxidative damage to DNA, proteins and lipids; seriously damaging plant metabolic functions and ultimately causing death of the plant (Apel and Hirt, 2004). These high ROS levels are caused by high accumulation of protochlorophyllide (PCH) in darkness (Sperling *et al.,* 1997). PCH is a precursor of chlorophyll. The enzyme that converts PCH to chlorophyllide is protochlorophyllide reductase (POR) (Fujita and Bauer, 2000); however, this enzyme requires light to operate meaning that in the dark grown etiolated seedlings and during skotomorphogenesis this conversion cannot happen, meaning PCH accumulates and levels rise. Chlorophyll biosynthesis during darkness is also repressed by phytochrome-interacting transcription factors (PIFs) which prevent the conversion of PCH to chlorophyll *a* (Huq *et al.,* 2004). In darkness in the etiolated seedlings PCH accumulation is not an issue; however, it is when the seedlings are transferred to light that this accumulated PCH can go on to either form chlorophyll *a* or form ROS. If the seedling has spent longer in darkness it will accumulate more PCH. If high amounts of PCH are accumulated in darkness, it means that upon transfer to light that the production of ROS is much greater as much of this PCH is free and not bound to PORs, meaning it is converted to ROS upon induction of light. However, if the seedling is only in darkness for a short period of time it means that less PCH has accumulated, most of which being bound

to POR meaning that chlorophyllide production is favoured, leading to the production of chlorophyll and thus the greening of the cotyledons.

Survival related to PC and ROS accumulation is directly linked and dependent on ERFVIIs (Abbas *et al.,* 2015). It was shown that oxygen is sensed via ERFVIIs during early seedling development and this sensing of oxygen is critical for seedling survival. Abbas *et al.,* 2015 investigated *prt6* and *prt6erfVII* ability to survive following long-term exposure to darkness during normoxia. It was found that following long term exposure to darkness only *prt6* and not *prt6erfVII* survived. This confirms ERFVIIs involvement in survival because the only difference between *prt6* and *prt6erfVII* is that the sextuple mutant (*prt6erfVII*) lacks ERFVII activity; therefore, if it is unable to survive it must be due to ERFVII activity. The results of survival were further confirmed to be due to the activity of ERFVII activity following analysis of PCH levels in *prt6*, WT, *erfVII* (pentuple mutant that lacks all ERFVII activity) and *prt6erfVII*. What the analysis showed was that PCH levels were significantly lower in that of *prt6* in comparison to that of the other genotypes. This confirms that PC accumulation is ERFVII dependent because *prt6* is an N-end mutant that lacks E3 ligase meaning that its ERFVIIs are always stable, even during normoxia. As these lines were grown in normoxia all other genotypes ERFVIIs would become destabilised even though they were grown in darkness, whereas ERFVIIs in the *prt6* mutant would remain stable. *Abbas et al.,* therefore concluded that stabilised ERFVIIs aid in protecting seedlings from long term exposure to darkness by preventing PCH and subsequent ROS accumulation and then permit subsequent growth of the apical meristem following transfer to suitable light conditions (Abbas *et al.,* 2015).

1.07.2 The PRT6 N-Degron Pathways Role in Pathogen Response:

Plants must respond quickly and efficiently if they want to counteract pathogen infection. The immune response must be tightly regulated to ensure the correct time of activation, duration and amplification occur; as if not correct it could leave the plant susceptible to infection (Adam *et al.,* 2019). Plants vary in the way in which they respond to either biotrophic (feed on living material) or necrotrophic (kill parts of the plant to feed on dead material); however, it has been known that the way in which the plant controls the immune response always requires the ubiquitin/proteasome degradation system (Sharma *et al.,* 2016). However, the response to a range of both bacterial and fungal pathogens has been shown to be regulated by a specific branch of the N-degron pathway (de Marchi *et al.,* 2016). Ubiquitination and the PRT6 N-degron pathway has a vast number of roles in the regulation of plant immunity, for example: regulation of TF accumulation or receptor abundance related to pathogen-associated molecular patterns (PAMPs) (Lu *et al.,* 2011; Marino *et al.,* 2013;) and the regulation of defence pathways (Trujilo and Shirasu 2010; Marino *et al.,* 2012; Duplan and Rivas, 2014; Vicente *et al.,* 2019).

There have been a wide variety of pathogens that have specifically shown the action of ERFVIIs in pathogen response. In *Plasmodiophora brassicae*, following infection there was shown to be an upregulation of genes involved with fermentation as well as an upregulation of targets of ERFVII and N-degron degradation (Gravot *et al.,* 2016). Additionally, protection against root gall formation caused by *Plasmodipohora brassicae* has been shown to be enhanced under ERFVII stabilisation (Gravot *et al.,* 2016)

Individual ERFVIIs have also been shown to aid response to pathogens. *Botrytis cinerea* is a necrotrophic fungus that affects many plant species and is typically characterised by its grey mould appearance on the plant. When *A. thaliana* is subjected to the fungus, the ERFVII RAP2.2 and its partner Med25 participate in the plant defence downstream of ethylene signalling (Ou *et al.,* 2011; Zhao *et al.,* 2012). These signalling partners then activate the resistance genes *PDF1.2* and *ChiB,* providing protection and resistance against the fungal pathogen (Ou *et al.,* 2011; Giuntoli and Perata 2018).

However, despite knowledge of this ERFVII stabilisation under stress, the exact mechanism and pathway enabling this stabilisation and operation is still unknown (de Marchi *et al.,* 2016; Vicente *et al.,* 2019). There are however hypotheses on how the PRT6 N-degron pathway and ERFVIIs are involved in controlling this resistance. It is known that upon interaction with a pathogen plants undergo PAMP triggered immunity (PTI) and if PTI is unsuccessful then effector triggered immunity (ETI) takes place; however, how the duration and amplitude of this response is determined remains something relatively unknown (Kliebenstein 2014; de Marchi *et al.,* 2016). de Marchi suggests that it is the PRT6 N-degron pathway that determines the duration and scale of this amplification. By using the *ate1 ate2* mutant line of *A. thaliana* which lacks Arg-transferase activity (Graciet *et al.,* 2009) it was shown that these mutants lacking critical molecules for successful degradation via the PRT6 N-degron pathway were more susceptible to pathogen infection. de Marchi tested a wide variety of pathogens including biotrophs, necrotrophs, hemi-biotrophs (begin as biotrophs then switch to a necrotrophic lifestyle) and obligate pathogens. Pathogenesis tests confirmed that the PRT6 N-degron pathway is involved in plant defence against a range of pathogens. However, during tests where various parts of the PRT6 N-degron pathway were inactivated in mutant lines the change in susceptibility of the plant following inoculation increased slightly. However, the increase in susceptibility was not as dramatic or significant as you would expect if the PRT6 N-degron pathway were to be the master regulator of pathogen immune response. It is therefore hypothesised that the PRT6 N-degron pathway is a component of the plant defence response, with its primary role not triggering but rather promoting the defence response to pathogens (de Marchi *et al.,* 2016). However, for a complete immune response and full amplification of resistance to a pathogen, like many other functions and roles of the PRT6 N-degron pathway, this requires cross talk and regulation of many different signalling components such as abscisic acid (ABA), salicylic acid (SA) and jasmonic acid (JA) (Kim *et al.,* 2014).

1.07.3 The PRT6 N-Degron Pathways Role in Nitric Oxide Response:

Nitric oxide (NO) is a gaseous ROS that is a critical signalling component in plants. If plants are to ensure successful survival, they must effectively respond to NO (Domingos *et al.,* 2015). NO is an important signal for plants and coordinates many different processes including: seed dormancy, senescence, flowering and pathogen response (Mur *et al.,* 2013). NO is highly reactive, and most NO synthesised in plants is thought to be synthesised from either redundant nitrate reductases (NIAs) or via the action of nitric oxide-associated protein 1 (AtNOA-1) (Gibbs *et al.,* 2015). Previously, despite protein modifications (Kovacs and Lindermayr, 2013) being identified in plants no mechanism that coordinates NO sensing had previously been identified. Like oxygen sensing, NO sensing is also coordinated through the proteolytic control of ERFVIIs and the PRT6 N-degron pathway (Gibbs *et al.,* 2014).

Gibbs *et al* 2014 examined a wide variety of abiotic stresses that were suspected to be regulated by NO. Seed dormancy is a mechanism in which germination of the seed is prevented in order to stop the seed germinating in to unsuitable environmental conditions (Baskin and Baskin, 2007), and is removed by after-ripening of dry seeds or chilling of the imbibed seeds (Holdsworth *et al.,* 2008). The endosperm is the layer surrounding the embryo which maintains dormancy and responds to NO (Bethke *et al.,* 2004; Liu *et al.,* 2009). NO activates germination by reducing sensitivity to ABA (Gibbs *et al.,* 2014). Gibbs *et al* 2014 confirmed the involvement of NO and the PRT6 N-degron pathway in this germination process as WT seeds germinated following exposure to NO donors SNAP (S-nitroso-N-acetyl-DL-penicillamine) and SNP (sodium nitroprusside); however, the PRT6 N-degron pathway mutants *prt6*, and *ate1 ate2* were shown to be completely insensitive to SNAP and SNP and were unable to germinate.

The role of ERFVIIs and the PRT6 N-degron pathway in controlling known NO dependent processes such as hypocotyl elongation (Lozano-Juste and Leon, 2011) and stomatal closure (Desikan *et al.,* 2002) was also investigated in Gibbs *et al.,* 2014. Following periods of darkness and presence of NO gas, hypocotyl elongation is inhibited (Beligni and Lamattina 2000; Lozano-Juste and Leon, 2011). Similarly to that of seed germination, WT responded as expected and showed inhibition of hypocotyl elongation in these conditions, whereas the N-degron mutants' *prt6* and *ate1 ate2* did not show any inhibition of the hypocotyl; confirming the role of the N-degron pathway for NO inhibition of hypocotyl growth.

Stomatal closure is also known to be regulated by NO. As NO is a ROS, plants do not want to accumulate large amounts as despite its benefits in coordinating signalling, as high levels of ROS are toxic. This means that in response to extended periods of NO, stomata must close to minimalize NO uptake and ROS exposure. Following exposure to the NO donors SNAP and SNP, WT stomata close; however, following exposure to the same NO donor's *prt6* stomata were insensitive and remain open. This once again shows that the PRT6 N-degron pathway is responsible for responding to NO and coordinating morphological responses. However, for stomatal closure the PRT6 N-degron pathway mutant *ate1 ate2* did respond to SNAP and closed, which Gibbs *et al.,* 2014 suggested that this is because *prt6*-related substrates may not always require arginylation.

1.08 ERFVIIs Interactions with Hormones

Stabilised ERFVIIs are part of a wide protein network hub containing many different facets and individual molecules, and it is the integration of the response of ERFVIIs with other signals that allows ERFVIIs to be involved in so many different pathways and processes.

1.08.1 How do ERFVIIs and ABA Interact?

Abscisic acid (ABA) is an essential phytohormone in plants. ABA is an essential regulator in a wide variety of aspects in plant growth and development, and is important for the response to both biotic and abiotic stresses (Cutler *et al.,* 2010). It has been reported that ABA is perceived through four types of receptors and the resulting actions following binding are extremely diverse (Gonzalez-Guzman *et al.,* 2012). Recent evidence shows that features thought to be solely regulated through ABA may also be in part regulated through ERFVIIs and the PRT6 N-degron pathway (Zhang *et al.,* 2018). The action of ERFVIIs may not always be solely responsible for ABA regulation, but cross-talk between these molecules is vital for complete coordination of response to stresses.

ABA plays a variety of important roles in responding to submergence. ABA's role in the signalling network of *SUB1A* in rice is essential (Xu *et al.*, 2006; Fukao *et al.,* 2011). ABA levels decline following submergence as it is an antagonist of GA, meaning enhancement of the response to GA allowing for elongation of shoots (Hoffman-Benning and Kende, 1992; Fukao and Bailey-Serres, 2008). However, during submergence the *SUB1A* ERFVII increases ABA responsiveness (Xu *et al.,* 2006). This is an essential ERFVII-ABA interaction as often when flooding subsides, foliage of the plant become rapidly dehydrated (Setter *et al.,* 2010; Fukao *et al.,* 2011). SUB1A promotes the expression of genes associated with preventing dehydration response, desiccation and limiting the spread of ROS (Xu *et al.,* 2006).

It has also been revealed that RAP2.2 can control ABA sensitivity (Lumba *et al.,* 2014). Lumba *et al.,* 2014 showed that RAP2.2 is actually part of a type 2C phosphatases – subclass 2 of Snfl-related kinases (PP2C-SNRK3) complex. This complex is an essential component of the ABA signalling pathway. Lumba *et al* 2014 showed that ERFVII functions

are able to be altered and tuned via posttranslational modifications such as partner selection. For example, RAP2.2 being phosphorylated by SNRK3.15/22 isoform enables RAP2.2 to mediate negative ABA responses.

It has also been shown that ERFVIIs enhance abiotic responses though interactions with the chromatin remodelling ATPase BRAHAMA (BRM) (Vicente *et al.,* 2017). BRM integrates plants responses to abiotic stresses through controlling the interaction and responses of plant hormones, such as ABA (Han *et al.,* 2012; Peirats-Llobet *et al.,* 2016; Vincente *et al.,* 2017). As previously described, ERFVIIs and ABA both regulate seed dormancy and germination via enhancing *ABI5* activity to promote dormancy (Gibbs *et al.,* 2014). It was found that the double GCC *cis* element within the ABI5 promoter that is bound to ERFVIIs to promote dormancy is actually targeted by BRM for ABI5 repression when germination is to be promoted (Vincente *et al.,* 2017). It has also been shown that ERFVIIs were shown to interact with BRM, potentially enhancing this repression (Efroni *et al.,* 2013). However, the effects of BRM on ABA has been shown to be the opposite of what is observed in ERFVIIs, with BRM being shown to inhibit ABA sensitivity and ability to respond to drought, as well as enhancing root growth (Han *et al.,* 2012; Archacki *et al.,* 2013; Yang *et al.,* 2015). Vincente *et al.,* 2017 investigated the nature of this potential interaction between ERFVIIs and BRM using bimolecular fluorescent complementation (BiFC). This confirmed the interaction of RAP2.12 and RAP2.3 with the C-terminal domain of BRM, however there was no interaction found with RAP2.2. As ERFVIIs and BRMs regulate opposite growth strategies it is possible that BRM-ERFVII interactions are in competition for the same *cis* elements, both competing control ABA activity for desired development.

1.08.2 How do ERFVIIs and GA Interact?

Gibberellins (GAs) have a diverse range of effects on promotion and regulation of plant growth (Rodrigues *et al.,* 2012). GAs are responsible for responding to a wide variety of both biotic and abiotic environmental factors, and the whole GA pathway is modulated by various other hormones such as auxins, ethylene and cytokinins (Jasinski *et al.,* 2005; Frigerio *et al.,* 2006; Archard *et al.,* 2007; la Rosa *et al.,* 2014). DELLA proteins are the master regulators of GA signalling. DELLAs are transcriptional regulators that act immediately downstream of the GA receptor (Eckardt, 2007). DELLAs negatively regulate GA by accumulating in the nucleus when GA levels are low, and when GA levels rise the DELLAs are degraded via the 26S proteasome. DELLAs act as the central hub regulating the activity of diverse range of TFs and regulatory proteins, connecting many different signalling cascades (la Rosa *et al.,* 2014). la Rosa *et al.,* 2014 determined one of the TF interactions controlled by the DELLA protein GIBERELLIN INSENSITIVE (GAI) is to the ERFVII that is RAP2.3, suggesting a role for ERFVIIs in the gibberellin pathway. GAI was confirmed to either prevent or repress DNA binding of RAP2.3 to the GCC box in order to prevent RAP2.3's capacity to activate transcription.

la Rosa *et al.,* 2014 also discovered that the DELLA-RAP2.3 interaction mediates apical hook opening. Apical hook opening in etiolated seedlings is regulated by both GA's and ethylene (Abbas *et al.,* 2013). DELLAs inhibit ethylene during apical hook development through inhibition of ETHYLENE INSENSITIVE3 (EIN3), a TF acting as a positive regulator of ethylene (An *et al.,* 2012). Through using a loss of function *rap2.3* mutant, it was shown to have a significantly reduced hook angle in comparison to WT, suggesting an interaction between RAP2.3, GA and ethylene. Other ERFVII members were also analysed, and *rap2.12* mutants showed the same apical hook phenotype as that of *rap2.3*. This once again suggests an interaction between ERFVIIs to GAs and ethylene.

The ERFVII *Sub1A* in rice has also been shown to be involved in GA signalling during submergence, forming an important part of the quiescent strategy to survive long term submergence. SUB1A increases the accumulation of Slender Rice-1 (SLR1) and SLR1 Like-1 (SLRL1) proteins, both acting as GA signalling repressors (Fukao and Bailey-Serres, 2008). Subsequently, this heavily diminishes GA expression during submergence and hypoxia. This inhibition of GA also prevents further hypocotyl and stem elongation, whilst also promoting the catabolism of carbohydrates (Fukao and Bailey-Serres, 2008; Hirano *et al.,* 2012). SUB1A also upregulates GA 2-oxidase following submergence (Jung *et al.,* 2010). GA2-oxidase is a GA deactivating complex so decreases the accumulation of active GA.

1.08.3 How do ERFVIIs and Auxin Interact?

Auxin is a coordinator of growth and development in plants, transferring information and coordinating responses over both long and long distances. The main form of auxin in higher plants exists as indole-3-acetic acid (IAA). Auxin is a very diverse hormone, having a key role in plants is coordination of root growth; and recent evidence suggests that there may be cross-talk with ERFVIIs in this coordination, especially during periods of hypoxia (Eysholdt-Derzso and Sauter, 2017).

Plants that are subjected to frequent flooding such as *Oryza sativa* have been shown to form adventitious and lateral root formation through changing primary and lateral growth rates, and also by altering the angle of their growth (Sauter 2013; Daewood *et al.,* 2014; Eysholdt-Derzso and Sauter, 2017). However, Eysholdt-Derzso and Sauter 2017 found that not all plants will form these adventitious roots and thus there must be an alternative strategy for the root system to respond to flooding and the resulting hypoxia.

Under normoxic conditions it is auxin that determines root architecture and the directionality of root growth. However, Eysholdt-Derzso and Sauter 2017 discovered that when the oxygen conditions are lowered during hypoxia, root architecture is governed by ERFVIIs and functionally linked to polar transport of auxin. The role of ERFVIIs in regulating root development was confirmed using *HRE2:GUS5* in order to analyse HRE2 expression in the roots. No activity of HRE2:GUS5 was observed under normoxic conditions; however, following a period of 2% oxygen for 24 hours induction of HRE2 gene expression was observed in the root tip and the lateral roots. This induction of HRE2 only during hypoxic conditions confirmed that HRE2 (as well as other ERFVIIs) mediate root adaption specifically during hypoxia. Knockouts of HRE2 further confirmed HRE2's role specifically in the regulation of root slanting and root growth direction.

RAP2.12 was specifically confirmed to have a role in controlling auxin and root bending. Auxin transport to control root bending is mediated through auxin transport proteins, predominantly through PIN proteins which are membrane proteins that transport the anionic form of auxin across membranes (Krecek *et al.,* 2009). PIN2 is a particularly important member of the protein family and is involved in root-specific auxin transport and mediating the root gravitropism (Ganguly *et al.,* 2010). Eysholdt-Derzso and Sauter initially found that the PIN2 gene did not appear to be regulated by hypoxia, and expression of PIN2 did not change in the *erfVII* pentuple mutant suggesting PIN2 is not regulated via transcription during hypoxic conditions. However, when evaluating PIN2 protein abundance and distribution it was found that following 5 hours of hypoxia PIN2 abundance significantly decreased in comparison to controls. Further experiments were done in relation to PIN2 protein abundance and ERFVIIs and it was revealed that there was an antagonistic effect of hypoxia and RAP2.12 on PIN2 protein abundance, indicating the role of ERFVIIs controlling auxin activity in the root during hypoxic conditions. Genetic data gained from Eysholdt-Derzso and Sauter also suggests that RAP2.12 is ERFVIIs that also limit slanting during hypoxia via control of auxin distribution.

1.09 Altitude Sensing:

Altitude sensing and adaptation is a novel and under researched area of plant ecological development. As vast portions of the earth are covered in mountainous areas, with a wide variety of species of plants growing there, it is an extremely important area of research. However, how altitude is sensed in plants is still not fully understood, with there being no published literature of the actual mechanism in which altitude sensing in plants is taking place. This is in comparison to in animals where altitude sensing and adaption is fully understood and has shown to be due to the Hypoxia-inducible Factor 1 (HIF-1) system (Jiang *et al.,* 2011). The HIF pathway is the master regulator of hypoxia response in animals and is essential in responding to a decrease in oxygen levels (Bigham and Lee, 2014). Animals that live at high altitude have been shown to adapt to the elevated altitude through selecting for alleles within the HIF system that enable the animal to sense and respond to altitude effectively. However, for plants there is still questions around how altitude is sensed.

Sensing and response to oxygen has been shown to be controlled through ERFVIIs and the PRT6 N-degron pathway (Gibbs *et al.,* 2015). However, this has yet to be directly linked to if plants adapt to altitude through the ERFVIIs that they are using to sense oxygen.

1.10 Age Dependent Activity of ERFVIIs:

It has recently been uncovered by Giuntoli *et al.,* 2017 and Vicente *et al.,* 2019 that ERFVII activity in oxygen sensing and oxidative stress may also be influenced by the age of the *A. thaliana* plant. Giuntoli *et al.,* 2017 shows that induction of ERFVIIs was not solely controlled by oxygen, but the age of the *A. thaliana* also influenced ERFVII stability and response. It was shown that mature *A. thaliana* plants had a significantly lower induction of core hypoxia responsive genes (controlled by ERFVIIs) in comparison to that of younger seedlings, with induction of oxidative stress-response genes declining as the seedling ages.

Despite plant or tissue age playing a factor in induction of genes responsible for ERFVIIs, it remains the PRT6 N-degron pathway that controls the stability of ERFVIIs and is controlled by factors such as hypoxia and oxidative stress. However, through analysis of mutants of the PRT6 N-degron pathway Giuntoli *et al.,* 2017 showed additional control mechanisms that decrease ERFVII activity and reduce the amplification and impact of both the hypoxic and oxidative responses. Giuntoli *et al.,* 2017suggests that age dependent activity of ERFVIIs is mediated by ERFVII recruitment in a transcriptionally inactive complex, or potentially via the induction of transcriptional antagonists themselves. However, this is still contested as other theories on why ERFVIIs may have age dependent activity suggest that ERFVIIs harbour degrons, meaning that as their age increases there is greater amounts of ubiquitin-mediated proteolysis and thus will cause ERFVII activity and induction of ERFVII responsive genes to decrease (Abbas *et al.,* 2015; Papdi *et al.,* 2015; Holdsworth, 2017).

1.11 Non ERFVII Oxygen Sensors May Exist:

A recent study by Wang *et al.,* 2017 suggests that ERFVIIs may not actually be the true oxygen sensors, and it is ion channels that are the true sensors of oxygen. Wang *et al.,* 2017 still recognises the role of ERFVIIs and the PRT6 N-degron pathway in the coordination of a response to variable oxygen conditions; however, Wang et *al.,* 2017 suggests that the timescales in which stabilisation of ERFVIIs occurs in response to hypoxic conditions is too slow to be solely responsible for the changes in plant tissues such as:

membrane depolarisation (Zeng *et al.,* 2014), changes in transporter activity (Shabala *et al.,* 2014) and ROS production (Pucciariello and Perata 2017). These responses occur in a matter of seconds upon hypoxia and Wang *et al.,* 2017 suggests that ERFVIIs are rather the "transducers" of the response to hypoxia, rather than the absolute sensors themselves. However, we cannot completely rule ERFVIIs out as the true sensors due to this reason, as the speed and timings in which ERFVIIs act in response to a change in oxygen level has yet to be tested and reported (Holdsworth 2017).

Wang *et al.* 2017 suggests the possibility that oxygen sensing is working through ion channels. It is suggested that hypoxia stress is regulated via plasma membrane channels (AKT and KCO), tonoplast ion channels (TPC1) and ROS. It is proposed that it is a combination of all of these ion channels that collectively act as sensors, and it is not ERFVIIs as thought previously.

Wang *et al*. 2017 also used non N-degron oxygen sensing associated domains from archaebacteria, and ion channels from mammalian oxygen sensors to attempt to use bioinformatics to try and identify similar domains in *A. thaliana*. This identified a variety of other sequences that may be responsible for oxygen sensing, other than both ERFVIIs and ion channels. More than 250 proteins in *A. thaliana* that have the Met-Cys domain, like ERFVIIs, at their N-terminus. It is proposed that these could act as the true sensors of oxygen if an N terminal degron is present following Met cleavage. It is also possible that oxygen sensors may be from proteins cleaved by endopeptidases to reveal amino-terminal Cys as part of an N-degron (Holdsworth 2017). However, even if ERFVIIs are not the absolute and sole sensors of oxygen, their importance in the coordination of response to varying oxygen conditions is undeniable.

Gene	Phenotype(s) of Mutants
Development	
ATEs	Delayed leaf senescence phenotype (Yoshida *et al.,* 2002). The double mutant (*ate1* and *ate2*) exhibits abnormal shoot and leaf development (Graciet *et al.,* 2009). Reduced seed germination and inhibition of seedling establishment by sucrose (Holman *et al.,* 2009).
PRT6	Hypersensitive to ABA during germination (Holman *et al.,* 2009) Slower germination and lipid breakdown (Holman *et al.,* 2009) Abnormal shoot and leaf development (Graciet *et al.,* 2009) Increased sugar sensitivity and oil body breakdown during germination (Zhang *et al.,* 2018)
PCOs	The double mutant (*pco1* and *pco2*) impact growth and development during normoxia (Weits *et al.,* 2014).
Abiotic Stresses	

PRT6	The novel PRT6 mutant *greening after darkness1* (*ged1*) allows seedlings to withstand long periods of darkness (Riber *et al.,* 2015). Increased tolerance of seedlings to submergence and starvation (Riber *et al.,* 2015). Reduced germination following NO treatment (Gibbs *et al.,* 2014b). Increased resistance to hypoxia (Gibbs *et al.,* 2011). Decreased resistance to submergence (Mendiondo *et al.,* 2016). Increased resistance to salinity and drought (Vicente *et al.,* 2017). Increases survival during hypoxia through decreasing PCH accumulation (Abbas *et al.,* 2015).
Biotic Stresses	
ATEs	Impacts defence and JA responsive genes (de Marchi *et al.,* 2016).
PRT6	Increases resistance to pathogens through enhancing pathogen induced stomatal closure (Vicente *et al.,* 2018). Decreases resistance to pathogens (Davydov and Varshavsky, 2000).
Molecular	
PRT6	Accumulation of Arg-initiated GUS (R-GUS) (Garzon *et al.,* 2007).
ATEs	Accumulation of Met-, Gln-, Asn-, Cys- and Asp-initiated Luc (Graciet *et al.,* 2010).
PCOs	The double mutant (*pco1* and *pco2*) accumulates RAP2.12 protein (White *et al.,* 2017)

Table 2:
Mutant phenotypes of essential genes in the PRT6 N-degron pathway

1.12 Ubiquitin Reference Technique (URT):

The ubiquitin reference technique (URT) is an essential component of much of the molecular work done throughout this project. Ubiquitin (Ub) is part of a family of proteins that regulate many processes within eukaryotic cells (Pickart and Eddins, 2004). Ubiquitination of a protein signal can signal degradation of the protein by via the 26S proteasome, for example when the E3 ligase ubiquitinates in the PRT6 N-degron pathway (1.4) (Finley *et al.,* 2012). Ub fuses to either itself (poly-Ub) or to other proteins, targeting them for degradation (Piatkov *et al.,* 2013). These fusions are cleaved by deubiquitinating enzymes (DUBs), which yields mature Ub (Piaktov *et al.,* 2013).

A method named the Ub fusion technique was initially used in 1986 through utilising the properties of DUBs (Bachmair *et al.,* 1986). This was also the initial method which uncovered the PRT6 N-degron pathway of protein degradation and the discovery of N-degrons in short-lived proteins (Bachmair *et al.,* 1986; Varshavsky, 2011). The Ub fusion technique takes advantage of the reversible ubiquitination by DUBs that allows the generation of an N-terminal residue at the N-terminus of the protein of interest (Piaktov *et al.,* 2013). The development of this technique was extremely important as being able to alter the amino acid at the N-terminus, as normally at the N-terminus the starting codon is the initiation codon (AUG) for methionine, meaning that without the Ub fusion technique all proteins would begin with methionine. Prior to the development of the Ub fusion

technique it meant that other residues (e.g leucine) were unable to be cleaved and made to be N-terminal. By utilising DUBs, this problem was overcome in the Ub fusion technique to allow the generation of any desired N-terminal residue at the N-terminus (Piaktov *et al.,* 2013).

This project utilises the URT to aid in the measurement and analysis of proteins degraded via the PRT6 N-degron pathway. Following the production of an N-degron, polyubiquitination of the protein occurs and targets the protein for degradation via the 26S proteasome. Through the URT it allows us to expose specific N-terminal residues at the end of the desired protein of interest and also allows measurements of the rate of protein degradation. The URT utilises the fusion in which Ub is positioned between a downstream test protein and an upstream reference protein (Piaktov *et al.,* 2013).

The reference protein in which I chose to use was the triple tagged FLAG-DHFR-HA, which is a derivative of dihydrofolate reductase. The use of a FLAG tag aided detection of the reference protein. The FLAG tag is also hydrophilic, meaning that it is normally found on the surface of the protein of interest, making it easier to detect with antibodies. The FLAG tag is also beneficial as it when at the N-terminal, the tag is easily removed using the protease enterokinase. The addition of the HA-tag (human influenza hemagglutin) aids in the detection, isolation and purification via HA-tag specific antibodies. Another benefit of the HA-tag is that it does not interfere with the bioactivity of the tagged protein of interest.

1.13 Research Justification:

Work carried out throughout the thesis is on the genetic model plant species *A. thaliana*, with the eventual objective is to translate the work to high value crop species such as barley or rice.

There are great amounts of literature surrounding ERFVIIs and the PRT6 N-degron pathway and its many functions, however I believe the biggest impact of this research is in relation to submergence tolerance. Recent models predict that by 2050 approximately 450 million people will be exposed to an increased risk of flooding and there will be over 1.7 billion hectares of land being affected (Arnell *et al.,* 2016; Wang *et al.,* 2017); resulting in annual damage from flooding estimated to be over €60 billion (Voesenek and Sasidharan, 2013). In order to combat this jeopardizing issue of food security and crop loss it is going to be critical to create stress-tolerant cultivars in response to flooding. Further understanding the mechanism in which plants sense low-oxygen, and having the ability to manipulate this pathway, is going to be essential in the creation of these stress-tolerant cultivars to aid in reducing crop loss.

Altitude sensing is another key area of application of work done on ERFVIIs and the PRT6 N-degron pathway. Further understanding of ERFVIIs and the ability to manipulate them may allow us in the future to be able to optimise ERFVIIs in crops to the specific altitudes in which they're being grown at. This will enable us to grow crops in areas previously thought to be non-arable due to such low oxygen concentrations in which the crops are not adapted at, for example at mountainous land. This utilisation of land previously

thought uninhabitable for crops to grow at would allow for an increase in food production to combat the growing risk of securing global food security. This optimisation may show potential success for some crops, however the utilisation of this baron land may not work for many of the crops as the environmental conditions in these areas is often not farmed just solely due to the oxygen concentrations making crops being unable to grow at, there are a variety of other environmental factors such as temperature and rainfall that make the land non-arable.

Despite the PRT6 N-degron pathway's importance in many signal transduction pathways and cellular processes, the knowledge of the extent of the protein targets and processes potentially regulated by the PRT6 N-degron pathway remains relatively limited. As this is a relatively new area of research, there may be other vital processes that will be revealed that are regulated by the PRT6 N-degron pathway that could be manipulated to increase both yield and survival of crop plants.

As research in ERFVIIs and the PRT6 N-degron pathway continues to grow and expand with more laboratories seeing the importance and potential of this area of research it is essential to maximise the tools needed to research effectively. Throughout this thesis, I develop the some of the transgenic tools that will further enable this research.

1.14 Objectives and Hypotheses:

1.14.1 Hypotheses:

i) *A. thaliana* accessions are adapted to altitude and this impacts their growth and development when grown at a different altitude to their habitat.

ii) Elevated oxygen levels (hyperoxia) impacts growth and development of *A. thaliana* accessions.

iii) RAP2.3 stability is essential in the chlorophyll tetrapyrrole pathway and its stability impacts PCH accumulation.

iv) Expression of RAP2.3 under its promoter is regulated in part through light availability.

1.14.2 Molecular Objectives:

Through the research described in this thesis, I focus on using molecular biology techniques in order to further enhance the understanding of ERFVIIs through practices such as gene cloning and protein analysis. Through work presented, I develop and analyse transgenic tools to further study and analyse ERFVIIs in wild type and mutant *A. thaliana*, as well as analysing ERFVII stability of accessions originating at various altitudes. The experimental approaches designed to do this were as follows:

i) Using the RAP2.12 coding region transformed into a Ubiquitin reference technique plasmid to create the construct ^{FLAG}DHFR^{HA} –UBIQUITIN-C^{2} - RAP2.12^{HA} to carry out *in vitro* analysis of its stability.

ii) Gateway ^{FLAG}DHFR^{HA} –UBIQUITIN-C^{2} –RAP2.12^{HA} into a plant transformation vector and transform Col-0, *prt6*, *prt6erfVII*, *erfVII* and Sha.

iii) Carry out site-directed mutagenesis of ^{FLAG}DHFR^{HA} –UBIQUITIN-C^{2} –RAP2.12^{HA} to produce ^{FLAG}DHFR^{HA} –UBIQUITIN-A^{2} –RAP2.12^{HA} stabilising the construct.

iv) Using *A. thaliana* accessions from varying altitudes transformed with ^{FLAG}DHFR^{HA}-UBIQUITIN-C^{2} –RAP2.3^{HA} and developing independent transgenic lines from first generation seeds (T1) and take these to homozygous third generation seeds (T3).

1.14.3 Physiological Objectives:

I also analyse the physiological consequences of ERFVII stabilisation on seedling survival during the transition from skotomorphogenesis to photomorphogenesis. To do this, I proposed to conduct the following environmental studies to better understand the physiological responses of this transition:

i) Assess the survival of etiolated seedlings of different genotypes grown on agar plates when transferred to high levels of light.

ii) Examine chlorophyll and ROS accumulation of etiolated seedlings following transfer to high levels of light.

iii) Assess and compare survival of etiolated seedlings of different genotypes grown in soil when transferred to high light.

iv) Analyse PCH accumulation of seedlings from varying altitudes and ERFVII stability.

Chapter Two:

Materials and Methods

2.01 Plant Material:

Arabidopsis thaliana (*A. thaliana*) seeds were obtained from the Nottingham *Arabidopsis* stock centre (NASC), unless otherwise stated, and were grown for propagation. Mutants used were in the Col-0 (wild-type) and Sha background. Mutants used were *prt6-1*, *erfVII*, *prt6erfVII*(Garzón *et al.,* 2007; Gibbs *et al.,* 2011; Gibbs *et al.,* 2014). The mutant line Sha *prt6 was* obtained from Professor Michael Holdsworth, and is an PRT6 N-degron pathway mutant containing *prt6* back crossed to Sha 8 times.

Accession Name	Meteres above Sea Level (masl)	Country of Origin
Sha	3400	Tajikistan
Sne	2662	Spain
Bdm	2124	Spain
Vaz	1670	Spain
Bay-0	400	Germany
Bea	140	Spain
Col-0	100	USA
Ler-0	48	Germany

Table 3:
Comparison of masl and country of origin of *A. thaliana* accessions from different altitudes used throughout the experiments.

NUMBER	ACCESSION
1	Sha
2	Sne
3	Bdm
4	Vaz
5	Bay-0
6	Bea
7	Ler-0

Figure 4:
Comparative geolocation of accessions used throughout experiments.

2.02 *A. thaliana* Seed Sterilisation, Cold Treatment and Growth:

A. thaliana seeds were sterilised using 5% (v/v) parazone bleach and then plated on half strength Murashige and Skoog medium (Sigma-Aldrich) (Murashige and Skoog, 1962) supplemented with 1% (v/v)sucrose. Following plating seeds were incubated in 4°C in the dark for 4 days. Seeds were then exposed to white fluorescent light (90-100 µmol m^{-2} sec^{-1}) at 22°C for 8 hours in order to synchronise germination.

Dark grown seedlings were covered in aluminium foil to prevent the seeds being further exposed to light and were then transferred to complete darkness for the stated days.

Plants grown in soil were grown on: 1 part compost (provides organic matter for growth) (Levy and Taylor, 2003), 1 part vermiculite (helps the soil retain air, plant food and moisture) (Aristov *et al.,* 2000) and ½ a pot of perlite (aids in ensuring water retention in the soil) (Maxim *et al.,* 2014). After planting in soil plants were transferred to white fluorescent light (90-100 µmol m^{-2} sec^{-1}) at 22°C. Trays containing the soil and plant material were initially covered with a plastic cover containing air holes in order to replicate

the humid conditions the seeds were previously experiencing, and after 3 days this cover taken off. The plants were watered when required at intervals of 2-3 days.

2.03 Optical Microscopy:

Images of seedlings were captured using a Leica DC480 microscope using Leica Application Suite. Images were captured at 3.2x magnification, brightness 100%, and exposure 129.6 and gain 1.0x.

2.04 ROS Staining and Fluorescence Microscopy:

Col-0 and Sha seeds were plated on half strength MS medium containing 1% (v/v) agar. Seeds were stratified and germinated and exposed to 10 days of complete darkness. Seedlings were placed at different light intensities within the same chamber at light levels of: 365 µE m^{-2} s^{-1}, 225µE m^{-2} s^{-1}, 175 µE m^{-2} s^{-1}, 122.5µE m^{-2} s^{-1} and 57.5µE m^{-2} s^{-1}**.**

Fluorescence microscopy images of cotyledons were captured of seedlings after the seedlings had been exposed to extended periods of darkness followed by growth in light. Dichlorofluorescin diacetate (H_2DCFDA) is de-esterified intracellularly and turns to highly fluorescent 2',7'-dichlorofluorescein upon oxidation (Denton *et al.,* 2006). Seedlings from each sample population were incubated with 100*µL* H_2DCFDA, 10 *µL* Tris-HCL (acts as a buffering agent) (Durst and Staples, 1972) and 890*µL of distilled water* at room temperature whilst being regularly shaken. The seedlings were then washed 3 times with Tris-HCL to ensure that any unspecific staining was removed. Images were then captured using a fluorescence microscopy and Leica Application Suite.

2.05 Chlorophyll and Anthocyanin Extraction, and Assay:

Col-0 and Sha seedlings were grown in 6, 7, 8 days darkness then transferred to light intensities of 621 µE m^{-2} s^{-1} and 460 µE m^{-2} s^{-1} within the same chamber**.** Six seedlings from each line (WT and Sha) and light intensity were placed in 1mL of cold 80% acetone. Seedlings cotyledons were then crushed and ground in the Eppendorf tube whilst in the cold acetone in order to release the chlorophyll. The tubes were then placed on a tube shaker/rotator for 3 minutes in order to fully mix the solution. 1mL of the solution was then extracted and placed in a spectrophotometer cuvette, ensuring no plant material was taken up. The cuvette was then placed into the spectrophotometer and absorbance was measured at 645nm and 663nm, in order to measure for chlorophyll *a* and chlorophyll *b* respectively (Kume, 2017). Anthocyanin absorbance was measured at 530nm and 657 nm (Hughes *et al.,* 2008). Physiological phenotype was also scored relating to the colour of the seedlings cotyledons, as well as survival measured**.**

2.06 Measurement of PCH Levels:

Col-0 and Sha seeds were plated on half strength MS medium containing 1% agar.
Seeds were stratified and germinated and exposed to 5 days of complete darkness, then transferred to light for 5 days.

20 seedlings from each line were removed from each plate and homogenised into 1mL of 80% cold acetone. This was repeated 3 times for each line. Seedlings were then placed into the fridge and left overnight for 24 hours. In complete darkness seedlings underwent vortex mixing for 60 seconds and subsequent centrifugation at 22,000 xg for 10 seconds. 200μl of the solution was then aliquoted into wells and relative fluorescence measured (excitation at 440 nm; emission between 600-700nm) at room temperature using a gradient HPLC fluorescence detector.

2.07 Hyperoxia Oxygen Chamber Experiment:

Col-0, Sha, Sha *prt6-1*, *prt6-1*, *prt6erfVII*, Bdm and MA-HRE2 seeds were grown in darkness for 6 days on agar plates in a hyperoxic oxygen chamber at approximately 27% (v/v) oxygen. This chamber was then transferred to a light chamber and the plates placed in 460 μE m^{-2} s^{-1}. Chlorophyll and anthocyanin levels were measured as described (2.05) and ROS was stained and imaged using H_2DCFDA and fluorescence microscopy (2.04).

2.08 PCR Amplification of Truncated RAP2.12:

The polymerase chain reaction (PCR) was carried out to amplify truncated RAP2.12 starting at C^2 in *A. thaliana* cDNA (Sup 1 for primers). This included a master mix of 37μl sterile H_2O, 10μl of fusion buffer (5x), 1μl of deoxyribonucleotide triphosphates (dNTPs) (10mM), 0.1μl specific primers (10μM) , 0.1μl Taq polymerase (2mM). These samples were gently mixed using a mixer and 50μl of the master mix was extracted and placed into thin walled 0.2mL PCR tubes. 1.8μl (~20 ng/μl) of DNA was then added to each PCR tube. PCR conditions were 1 cycle of 5 minutes at 98°C for initial denaturation, followed by 35 cycles of: 30 seconds at 98°C for further denaturation, 1 minute at 57°C for primer annealing, 2 minutes at 72°C for extension and finally 7 minutes at 72°C for final extension. After the 35 cycles have been complete the sample is then cooled at 10°C until removed from the machine in order to prevent any further denaturation.

2.09 Gel Electrophoresis of Amplified C^2-RAP2.12:

Gel electrophoresis was carried out on the amplified C^2-RAP2.12 sample. 1% (v/v) agarose gel was made using Tris/Borate/EDTA (TBE) buffer (0.5X). Ethidium bromide (0.5μg/ml) was then added in order to bind to the DNA allowing visualisation under ultraviolet (UV) light (Biorad Universal Hood II Gel Doc System).

2.10 Gel Extraction and Purification of C^2-RAP2.12:

The amplified C^2-RAP2.12 was extracted from the agarose gel using the QIAquick Gel Extraction Kit. Amplified C^2-RAP2.12 was extracted from the agarose gel using a clean, sharp scalpel. Buffer QG was then added and the sample incubated for 10 minutes with vortexing every 3 minutes in order to ensure the gel was dissolved. Buffer QG was then added to the sample and then the sample was centrifuged for 1 minute and any flow through was discarded. 750μl of buffer PE was then added, and the sample centrifuged for 1 minute and any flow through once again discarded. Elution buffer was then added to the sample and soaked for 2 minutes. The purified C^2-RAP2.12 was then collected.

2.11 SacII Restriction Digest of Amplified C^2-RAP2.12:

The UFT-XHA vector and the C^2-RAP2.12 insert were digested using the SacII restriction enzyme (NEB). In a 1.5mL Eppendorf tube, 40μl of PCR product, 2μl SacII restriction enzyme, 6μl CutSmart Buffer (50mM Potassium Acetate, 20mM Tris-acetate, 10mM Magnesium Acetate, 100μg/ml BSA) (pH 7.9) and 4μl of H_2O were added. This master mixture was then vortexed to ensure full mixing. The mixture was then incubated at 37°C for 2 hours.

2.12 Ligation of UFT-3xHA-RAP2.12 and C^2-RAP2.12:

In a PCR tube, 2μl of vector DNA, 6μl of insert DNA, 2μl of ligase buffer, 1μl of T4 DNA Ligase (NEB) and 9μl of H_2O was added. The material was mixed gently using a shaker. The mixture was incubated at 16°C for 16 hours.

2.13 *Escherichia coli* (*E. coli*) Transformation of UFT-C^2-RAP2.12:

Firstly, 25μl of competent cells (ThermoFisher) were thawed on ice. 5μl of the ligation mixture (2.12) was added to the competent cells. The mixture was then placed on ice for 30 minutes after which the mixture was then heat shocked at 42°C in a water bath for 30 seconds. 950μl of the room temperature media was then placed into the tube. The tube was then incubated at 37°C for 30 minutes whilst being shaken vigorously and rotated. Zeocin selection plates were then warmed to 37°C and 100μl of the cells and ligation mixture were spread onto the plate. The mixture was incubated at 37°C overnight and number of transformants were counted and transformation efficiency calculated the following morning.

2.14 LR Cloning Reaction of UFT-C^2-RAP2.12:

The LR cloning reaction (Invitrogen) was utilised to generate an expression clone. To a 1.5mL microcentrifuge tube the following were added: 5μl entry clone (~200ng), 1μl destination vector (100-250ng), 2μl LR clonase reaction buffer (5X), 1μl TE buffer (pH 8.0). 2μl of LR clonase mix (Invitrogen) was added and the material mixed well by vortexing and spun down. The mixture was then incubated at 25°C overnight. The reaction was then stopped by adding 1μl of Proteinase K and incubated for 10 minutes at 37°C.

2.15 DNA Extraction and Purification of Plasmid DNA to Check for Transformation Success of UFT-C^2-RAP2.12 3xHA

Firstly, liquid lysogeny broth (LB) was prepared by combining 4g NaCl, 4g Tryptone, 2g Yeast extract and 400mL dH_2O. The mixture was then autoclaved for sterilisation. 5mL of liquid LB and 5μl of zeocin (100μg/ml) (InvivoGen) antibiotic was then added to a sterile culture tube. Using a sterile inoculation loop, a single colony was selected from the LB selection plates from the *E.coli* transformation and were dropped into the LB + zeocin (100μg/ml) (InvivoGen) mixture and swirled. The culture was loosely covered and placed in a 37°C shaking incubator at 200rpm for 18 hours. Growth confirmation was confirmed by the presence of a cloudy haze in the falcon tube.

A miniprep (DNA extraction and purification) of the DNA was then carried out using the QIAprep Spin Miniprep Kit. Firstly, overnight cultures were spun for 5 minutes and the supernatant removed. Pelleted bacterial cells were then re-suspended in 250μl of Buffer P1 (resuspension buffer) in a micro-centrifuge tube. 250μl of Buffer P2 (denaturing solution) was then added to the tube and mixed thoroughly by inverting the tube 6 times. 350μl of Buffer P3 (renaturing solution) was then added to the tube and once again the mixture thoroughly shaken by inverting 6 times. The tube was then centrifuged at 13,000 rpm in order to get rid of the cell debris (the precipitant) which was discarded. 800μl of the DNA supernatant was then pipetted into the spin column. The spin column was centrifuged for 60 seconds and the flow-through discarded. The spin column was then washed using 0.5μl Buffer PB and centrifuged for 60 seconds, with the flow through being discarded. The spin tube was again washed using 0.75μl buffer PE and centrifuged for 60 seconds, with the flow-through discarded. The spin-tube was centrifuged again for 60 seconds in order to remove any residual wash buffer, as any residual ethanol from Buffer PE may inhibit subsequent enzymatic reactions. The spin column was then placed in a clean 1.5mL micro centrifuge tube. The DNA was then eluted by adding 50μl of Buffer EB (10mM Tris Cl, pH 8.5) to the spin column, let stand for 60 seconds, and then centrifuged for 60 seconds.

2.16 NanoDrop Quantitation of UFT-C^2-RAP2.12 3xHA:

DNA obtained via plasmid miniprep was quantified using a NanoDrop (Thermo Fisher NanoDrop 2000) NanoDrop allows for DNA concentration to be identified through measuring the absorbance of UV-visible light through the sample (Desjardins and Conklin, 2010). The samples absorbance were measured from 220nm to 340nm and the nucleic acid and purity ratios were calculated using the software. Concentrations were then used to calculate DNA amount required for *in vitro* assays.

2.17 *In vitro* Assay of UFT-C^2-RAP2.12 3xHA and UFT-A-RAP2.12 3xHA to Compare Protein Degradation Levels:

A master mix was made using the following components: 12.5μl rabbit reticulocyte extract, 1μl TnT buffer, 0.5μl T7 polymerase, 0.25μl amino acids (leucine), 0.25μl amino acids (methionine), 0.5μl RNAse OUT. In a separate tube 1μg of plasmid DNA was aliquoted. 1μl of bortezomib (bortz) was added to one tube containing UFT-C^2-RAP2.12. The other tube of UFT-C^2-RAP2.12 was left without. The total volume in this tube was then made up to 10μl using water. To the 10μl DNA, 15μl of the master mix was added and mixed gently.

Samples were then placed in a 30^{o}C incubator for 30 minutes to allow for translation and then cycloheximide (2.6mM) was added to prevent further translation occurring. Samples were then taken at 0, 30 and 120 minute intervals respectively. 7μl of these samples were added to a tube containing 7μl protein loading buffer and 21μl water. These samples were kept on ice until the final 120 minute sample had been collected. The samples were then incubated at 95^{o}C for 10 minutes, put on ice for 5 minutes, spun for 1 minute and finally frozen for storage at -20^{o}C.

2.18 Western Blotting:

Western blotting was used to compare protein abundance and degradation of UFT-C^2-RAP2.12 3xHA and UFT-A-RAP2.12 3xHA samples from at the 30, 60 and 120 minute time points.

Preparation of Gels Required for Sodium Dodecyl Sulfate-Polyacrylamide Gel Electrophoresis (SDS-PAGE):
A running gel was produced containing: 3.3ml water, 4 mL acryl, 2.5mL Tris-HCl (10mM) buffer (pH 8.8), 0.1mL SDS (10%), 0.1mL ammonium persulfate (APS) (10%) and 4μl TEMED. A stacking gel was produced containing: 3.4mL water, 0.83mL acryl, 0.63mL Tris-HCl buffer (10mM) (pH 6.8), 0.05mL SDS (10%), 0.05mL APS (10%) and 4μl TEMED.

Electrophoresis of Proteins using SDS-PAGE:
SDS-PAGE was carried out using an electrophoresis cell using an ultra-pure 10x Tris/Glycin/SDS (TGS) buffer. 15μl of the samples were loaded into wells, and 6μl of Invitrogen loading buffer was added to both sides of the samples. A lid was placed on to the tank and the gels were originally run at 80V for 20 minutes. After 20 minutes the samples were run for 1 ½ hours at 120V.

Electrophoretic Transfer:
A running buffer was prepared comprised of: 700mL water, 200mL MetOH and 100mL 10x TG buffer. Proteins from the running gels were transferred to a nitrocellulose membrane (Bio Rad, Immune Blot pVDF membrane) using a sandwich in the presence of the running buffer at 4°C. The transfer was carried out at 80V for 2 hours.

Detection of Proteins:
A PBS buffer was prepared comprising: 500mL water and a phosphate-buffered saline (PBS) tablet (Thermofisher). This was stirred for 2 hours before use. 5% (v/v) milk in PBS buffer was prepared and poured into square petri dishes and TWEEN added (100μl in 100mL). In order to stop the electrophoretic transfer, the nitrocellulose membrane was removed from the membrane placed in the petri dish containing the 5% (v/v) milk blocking agent. This was then shaken for 1 hour at 45rpm. The blot was then incubated with the mouse antibody α-HA antibody (stock at 4μl per 10mL) at a dilution of 1/2,500 in blocking buffer at 45rpm for 2 hours. The blot was then washed 3 times with 10mL of 5% (v/v) milk in TBS buffer. The secondary antibody (Goat αmouse) (Intvitrogen) was used at a dilution of 1/10,000 in blocking buffer. The membrane was incubated for 2 hours without shaking.

Visualisation of the Blot:
PBS buffer was first removed from the membranes. 2mL of Pierce ECL Western Blotting Substrate was then applied to the membrane. The membrane was then wrapped in cling film and taped to the inside of the cassette. High Performance Chemiluminescence Film was then placed in the cassette and the film exposed for 1 minute. TBST was then added to the film and subsequently washed with water. ECL Reagent (Thermofisher) was then added to the film and subsequently washed and the film let dry.

2.19 *Agrobacterium tumefaciens* Competent Cell Transformation:

Firstly *Agrobacterium tumefaciens* (*A. tumefaciens*) competent cells were left to thaw for 1 hour. 5μg of plasmid was added to the competent cells and it was mixed gently and left on ice for 30 minutes. The competent cells and plasmid mix was then placed in liquid nitrogen for 5 minutes until completely frozen. The solution was then placed in a 37°C

water bath for 5 minutes. 900μl of LB medium was added to the solution and the competent cells revived on 28°C shaking incubator for 3 hours.

The competent cells were then plated on selection plates containing rifampicin (25μg/ml), spectinomycin (50μg/ml) and gentamicin (10μg/ml) (RGS plates). Once plated, the plates were incubated at 37°C for 3 days.

2.20 Overnight Cultures of *A. tumefaciens*:

50μl Liquid LB was prepared, and appropriate concentration of RGS antibiotics added to the solution. Using a sterile pipette tip, a singly colony was selected from the LB + RGS selection plates (2.19) and dropped into the LB + RGS mixture and swirled. The culture was loosely covered and stored in a 37°C shaking incubator for 24 hours. Growth was confirmed by the presence of a cloudy haze in the tube.

2.21 Mini-Prep of *A. tumefaciens*:

A miniprep of *A. tumefaciens* DNA was then carried out using the QIAprep Spin Miniprep Kit. Firstly, overnight cultures were spun for 5 minutes and the supernatant removed. Pelleted bacterial cells were then re-suspended in 250μl of Buffer P1 (resuspension buffer) in a micro-centrifuge tube. 250μl of Buffer P2 (denaturing solution) was then added to the tube and mixed thoroughly by inverting the tube 6 times. 350μl of Buffer P3 (renaturing solution) was then added to the tube and once again the mixture thoroughly shaken by inverting 6 times. The tube was then centrifuged at 13,000 rpm in order to get rid of the cell debris (the precipitant) which was discarded. 800μl of the DNA supernatant was then pipetted into the spin column. The spin column was centrifuged for 60 seconds and the flow-through discarded. The spin column was then washed using 0.5μl Buffer PB and centrifuged for 60 seconds, with the flow through being discarded. The spin tube was again washed using 0.75μl buffer PE and centrifuged for 60 seconds, with the flow-through discarded. The spin-tube was centrifuged again for 60 seconds in order to remove any residual wash buffer, as any residual ethanol from Buffer PE may inhibit subsequent enzymatic reactions. The spin column was then placed in a clean 1.5mL micro centrifuge tube. The DNA was then eluted by adding 50μl of Buffer EB (10mM Tris Cl, pH 8.5) to the spin column, let stand for 60 seconds, and then centrifuged for 60 seconds.

2.22 Preparation of *A. tumefaciens* Culture:

Large conical flasks containing 200μl liquid LB were prepared. The following antibiotics were added to the tube: rifampicin (25μg/ml), spectinomycin (50μg/ml) and gentamycin (10μg/ml). Prior overnight cultures containing 50μl *A. tumefaciens* and liquid LB were then poured into the large conical flask. The mixture was then incubated overnight at 37°C in a shaking incubator.

The following day the culture should have grown to mild-logarithmic phase and will be approaching, or at, the stationary phase. The liquid culture was transferred to micro

centrifuge tubes and the cells pelleted by spinning for 20 minutes at 22,000xg. The supernatant was poured off leaving the pelleted *A. tumefaciens* in the bottom of the tube. The pelleted cells were then suspended in 5% sucrose solution and the *A. tumefaciens* pellet mixed in. Prior to dipping. Silwet L-77 was added to a concentration of 0.05%.

2.23 *A. tumefaciens* Transformation via Floral Dipping:

The *A. tumefaciens* solution was poured into a shallow box and the *A. thaliana* inflorescences were dipped into the solution for 60 seconds and swirled gently to remove bubbles and ensure full coverage. A plastic dome cover was then placed over the plants for 72 hours in order to maintain humidity for successful transformation. The cover was then removed and plants returned to the growth room (Bent, 2006.

2.24 Site-directed Mutagenesis:

Primers were designed to substitute the cysteine in the UFT-C^2-RAP2.12 construct to remove the cysteine and replace it with a stable alanine (UFT-A-RAP2.12) (Sup 1 For primers). A PCR was carried out with the 30ng UFT 3xHA plus the insert template using the following mix: 1μl of forward primer, 1μl reverse primer, 1μl dNTPs, 10μl HF buffer (5x), 0.2μl Phusion Taq polymerase and 6μl of water. 3 repeats were carried out for each construct. The cycling conditions were 98°C for 30 seconds, 98°C for 10 seconds, 56°C for 30 seconds, 72°C for 1 minute and finally 72°C for 7 minutes. This cycle was repeated 16 times.

2.25 Hygromycin Selection to Select for Transformed Seedlings:

To 500mL of half strength MS media, 500μl of 50mg/ml hygromycin was added. 45mL of this media was poured onto square petri dishes and cooled at 4°C. 7mL of molten agar was added to sterilised seeds and this mixture was then poured onto square agar plates and cooled at room temperature for 30 minutes before covering and storage. High volumes of seeds were used in hygromycin selection as these seeds were straight from transformation and T1 seeds, meaning the chance of one individual carrying transformed DNA was low, meaning larger numbers of seeds were required to increase probability of finding transformed seeds.

Following plating for hygromycin selection and stratification seedlings were exposed to darkness for 5 days and subsequently exposed to light for 3 days. Hygromycin-resistant transformants were identified by their long hypocotyls (approximately 0.8-1 cm), whereas non-transformed seedlings had shorter hypocotyls (approximately 0.2-0.4 cm). Hygromycin resistant seedlings also had differences in greening of the cotyledons which allowed identification of resistance and transformants.

2.26 GUS Staining:

Growth Conditions:
4 lines of *promRAP2.3:MC-RAP2.3* in Sha and 4 lines of *promRAP2.3:MA-RAP2.3:GUS* in Sha were plated, chilled, and germinated as described (2.02). Seedlings were either

exposed to 5 days of darkness, 7 days of darkness, or were left in light as a control. Following growth GUS staining was carried out.

Stain Preparation:
GUS staining was carried out on *promRAP2.3:MC-RAP2.3* in Sha and *promRAP2.3:MA-RAP2.3:GUS* in Sha. First a phosphate buffer of pH 7.0 was made by mixing 1M sodium monophosphate and 1M sodium diphosphate in a 39:61 ratio respectively. The 20mg of X-gluc substrate and 10μl Triton X-100 were then added and the solution mixed.

Performing GUS Staining:
A master mix of the staining solution was made by adding 100mM potassium ferricyanide and 100mM potassium ferrocyanide. The solution was mixed thoroughly and the stain distributed to the individual tubes used for GUS staining. In 2mL tubes, 1mL of the GUS stain solution was added to the plant material. The plant material and GUS staining was then incubated overnight for 24 hours at 37°C to have an absolute idea of where GUS is present. Following the appearance of the blue colour of successful staining, tubes were centrifuged and the staining solution removed. Stained plant material was then placed in 70% ethanol and placed on a shaker for 16 hours. Stained plant material was placed in water for stored at 4°C.

Imaging GUS Stained Samples:
GUS stained samples were imaged using a Leica DFC320 microscope.

2.27 Data Analysis:
GraphPad Prism 7 was used to record, analyse and present quantitative data. Statistical differences were determined using a one-way analysis of variance (ANOVA) test and results were determined significantly different from one another if the p-value was less or equal to 0.05.

Chapter Three:

Results

3.01 Adaption to Altitude Impacts ROS Accumulation

I compared the responses of two accessions from very different altitudes to varying light intensities, and investigated the impact that this had on ROS and chlorophyll accumulation. Col-0 and Sha seedlings are adapted to grow at very different oxygen concentrations. Sha is an accession adapted to growth in the Tajikistan mountains at 3400 masl. This is an extreme difference in altitude compared to the 65 masl that Sha is being grown at during these experiments. At Sha's natural grown altitude, oxygen levels are significantly lower (~18% (v/v)) than that to which it was grown during experiments (~21% (v/v)). I hypothesised that the adaption of Sha to a hypoxic environment would impact plant development, and ROS and chlorophyll accumulation. Seedlings in Figure 5A-C underwent a 10-day period of etiolation and were subsequently transferred to 5 days of light intensities varying from 57.5 μE m^{-2} s^{-1} to 365 μE m^{-2} s^{-1}. H_2DCFDA staining was carried out to indicate ROS levels throughout the cotyledon, indicated by the green stain (Figure 5A-C). 5 seedlings were from each line and each treatment were imaged, and the image shown is the most representative seedling that had the median amount of staining. The red staining indicates chlorophyll levels throughout the cotyledon (Figure 5A-C). Results show (Figure 5A-C) elevated ROS levels in Sha in comparison to Col-0, throughout all light intensities (57.5 μE m^{-2} s^{-1} - 365 μE m^{-2} s^{-1}). Results also show that following an increase in light intensity, ROS production increases for both Col-0 and Sha Figure 5A-C). The vast differences in ROS and chlorophyll accumulation between accessions show that altitude adaption impacts growth and development of *A. thaliana* seedlings, and this adaption causes vast amounts of ROS and chlorophyll to be produced when grown if not adapted to growth in elevated oxygen concentration. Quantitative fluorescence intensity was measured in ImageJ, and the mean fluorescence is shown from 5 seedlings (Figure 5E-F), proving quantitative confirmation of the results shown in Figures 5A-C.

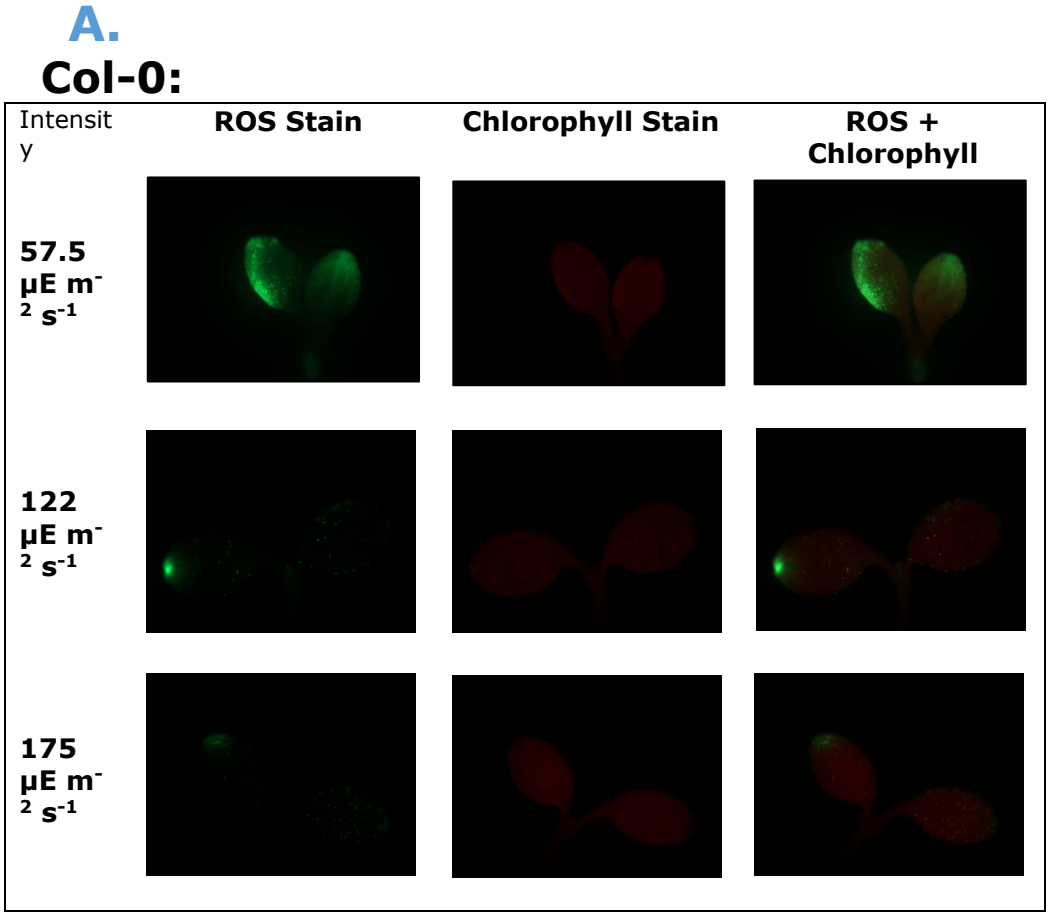

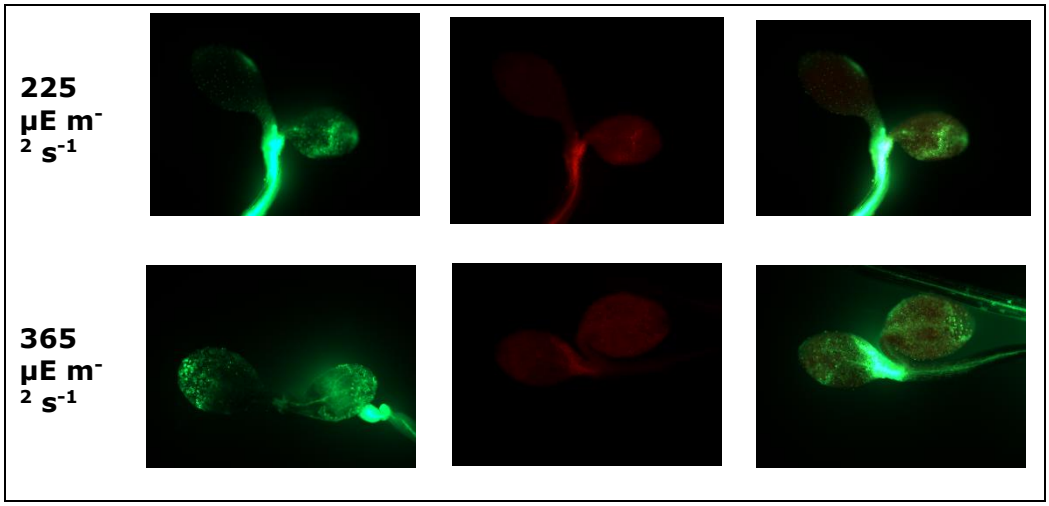
225 µE m-2 s-1
365 µE m-2 s-1

B

Sha

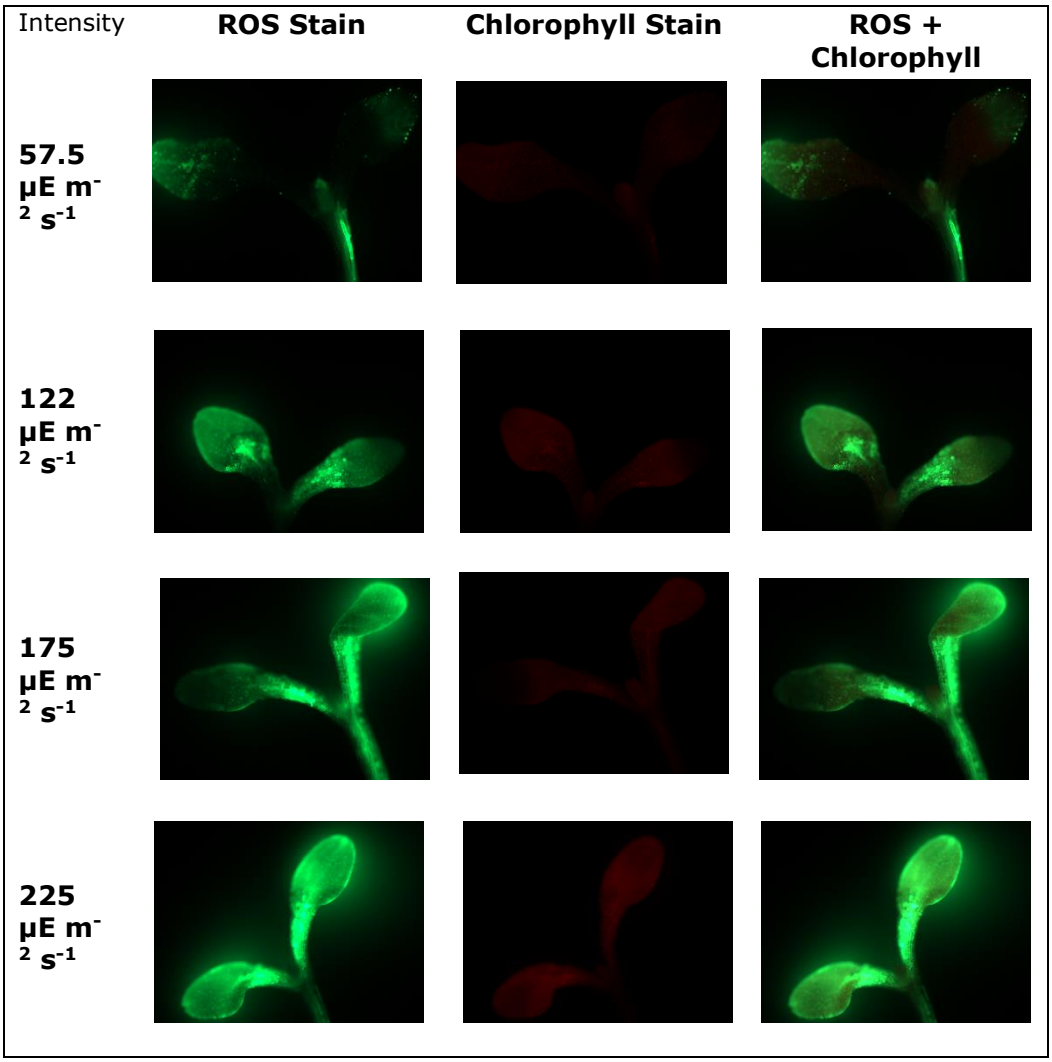
Intensity
ROS Stain
Chlorophyll Stain
ROS + Chlorophyll
57.5 µE m-2 s-1
122 µE m-2 s-1
175 µE m-2 s-1
225 µE m-2 s-1

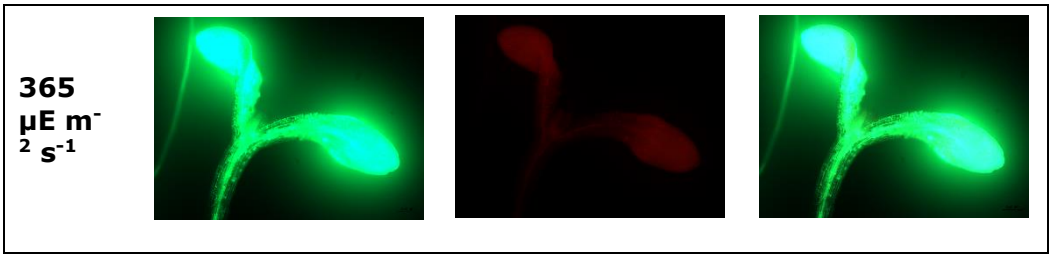

C

ROS + Chlorophyll Images

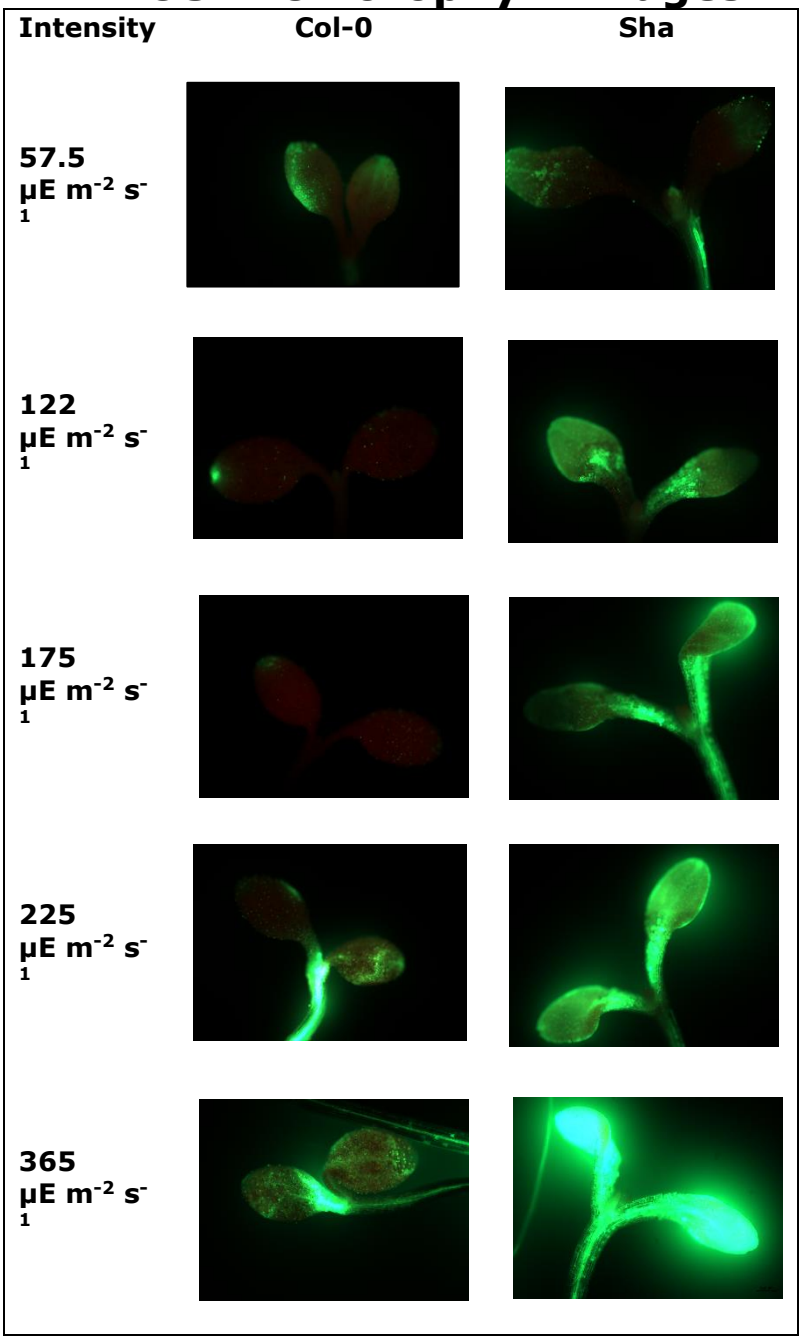

D

Intensity	Col-0	Sha
57.5 µE m^{-2} s^{-1}		
122 µE m^{-2} s^{-1}		
175 µE m^{-2} s^{-1}		
225 µE m^{-2} s^{-1}		
365 µE m^{-2} s^{-1}		

E

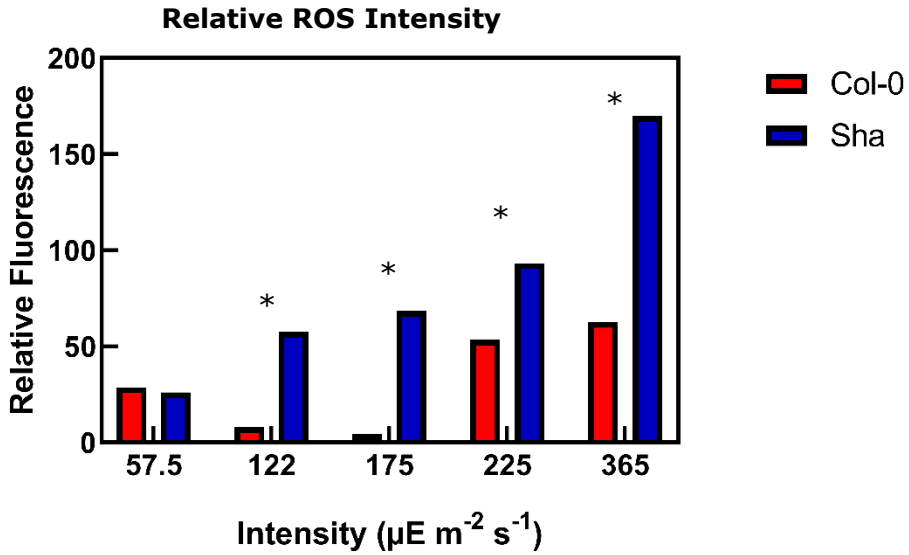

F

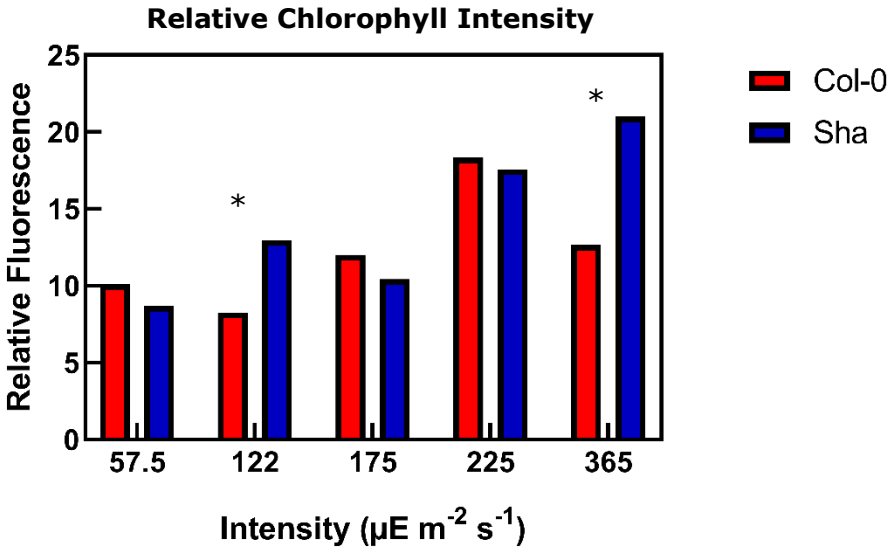

Figure 5:

(A) Stained images highlighting ROS and chlorophyll accumulation and distribution in Col-0 seedlings following exposure to 10 days in darkness and subsequent 5 days to light.

(B) Stained images highlighting ROS and chlorophyll accumulation and distribution in Sha seedlings following exposure to 10 days in darkness and subsequent 5 days to light.

(C) Comparison of ROS and chlorophyll accumulation between Col-0 and Sha seedlings following exposure to 10 days in darkness and subsequent 5 days to light.

(D) Images of Col-0 and Sha cotyledons following exposure to 10 days darkness and subsequent 5 days of light.

(E) Quantitative analysis comparing relative ROS fluorescence levels between Col-0 and Sha following exposure to 10 days in darkness and subsequent 5 days to light.

* indicates results between Col-0 and Sha from the same light intensity (μE m^{-2} s^{-1}) are significantly different from one another if the P-value was less or equal to 0.1 following a t-test.

(F) Quantitative analysis comparing relative chlorophyll fluorescence levels between Col-0 and Sha following exposure to 10 days in darkness and subsequent 5 days to light.

* indicates results between Col-0 and Sha from the same light intensity (μE m^{-2} s^{-1}) are significantly different from one another if the P-value was less or equal to 0.1 following a t-test.

3.02 Adaption to Altitude Impacts Seedling Development:
In order to examine how altitude adaption impacts other aspects of plant development, Col-0 and Sha seedlings were first grown in periods of 0, 6, 7 and 8 days of darkness. Seedlings were then transferred to light intensities of 460 μE m^{-2} s^{-1} and 621 μE m^{-2} s^{-1} and grown for 5 days. Figure 6A shows differences in chlorophyll accumulation between Col-0 and Sha following different exposures to darkness, with Col-0 producing elevated levels of chlorophyll to that of Sha following etiolation at all periods of time spent in darkness. Figure 6B shows the comparison of anthocyanin levels between Col-0 and Sha, as light intensity increases. The results show that for both the 460 μE m^{-2} s^{-1} and 621 μE m^{-2} s^{-1} intensities, Col-0 appears to accumulate more anthocyanin than Sha. Results show a significant difference in anthocyanin accumulation for 0, 7 and 8 days at 460 μE m^{-2} s^{-1}, with P values of 0.001487, 0.014065 and 0.00131 respectively. However, no significant difference was observed between Col-0 and Sha at 621 μE m^{-2} s^{-1} other than at 0 days etiolation, with P values being 0.01695, 0.881672, 0.236552 and 0.716849 for 0, 6, 7 and 8 days respectively. This trend of anthocyanin accumulation is also visually represented in Figure 5D where Col-0's cotyledons show a great amount of reddening as a result of anthocyanin accumulation, whereas Sha's cotyledons remain green/yellow. In Figure 6C I evaluated the phenotype of seedlings after exposure to 460 μE m^{-2} s^{-1}, as this was the light intensity in which there was the greatest difference in phenotype between the seedlings. In order to compare the seedlings, I split their appearance into 4 categories

dependent on the colour and phenotype of the cotyledons: "Arrested Growth", "Green", "Yellow" and "Dead". "Arrested Growth" was determined by a reddening of the cotyledons, due to excess anthocyanin accumulation. "Green" was for seedlings that were healthy and showed no sign of yellow or red colouration. Seedlings were determined "Yellow" if they had large amounts of yellowing in their cotyledons caused by excess ROS accumulation and chlorosis. Seedlings were determined "Dead" if they germinated and then did not survive following exposure to the elevated light intensity. I also compared survival between lines at varying periods of etiolation at both 460 µE m^{-2} s^{-1} and 621 µE m^{-2} s^{-1} (Figure 6D). For both Col-0 and Sha there was shown to be a decrease in survival as etiolation period was extended, however there was no significant difference between the two accessions suggesting altitude adaption does not impact seedling survival. However, for chlorophyll accumulation, anthocyanin accumulation and phenotype there are significant differences between Col-0 and Sha; showing adaptation of the accession to altitude plays a key role in seedling development.

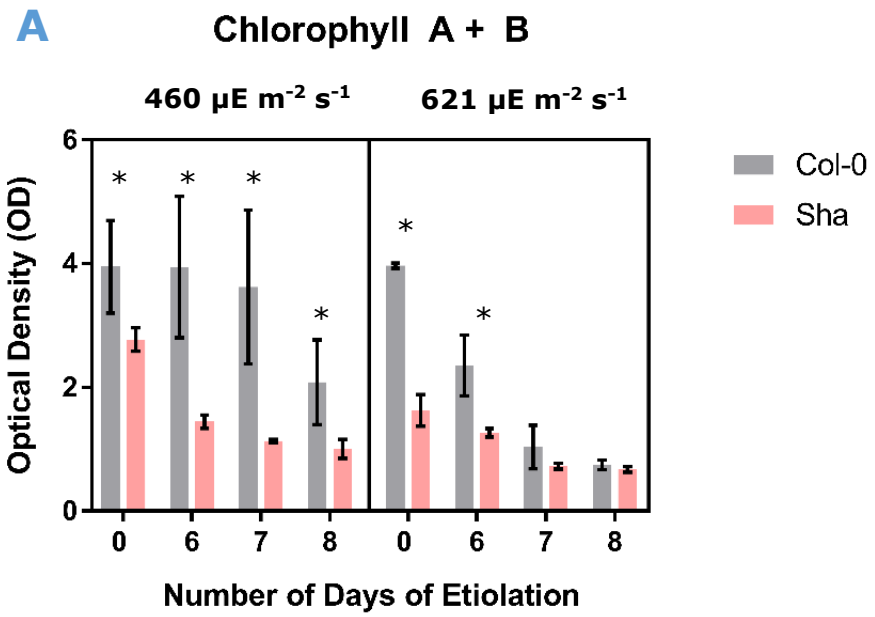

B

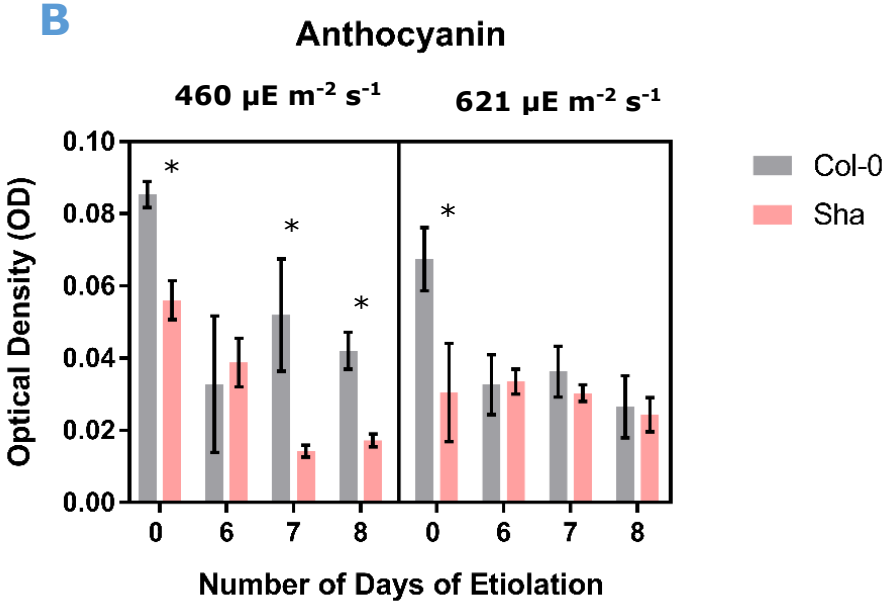
Anthocyanin
460 µE m-2 s-1
621 µE m-2 s-1
Optical Density (OD)
0.10
0.08
0.06
0.04
0.02
0.00
*
*
*
*
0
6
7
8
0
6
7
8
Number of Days of Etiolation
Col-0
Sha

C

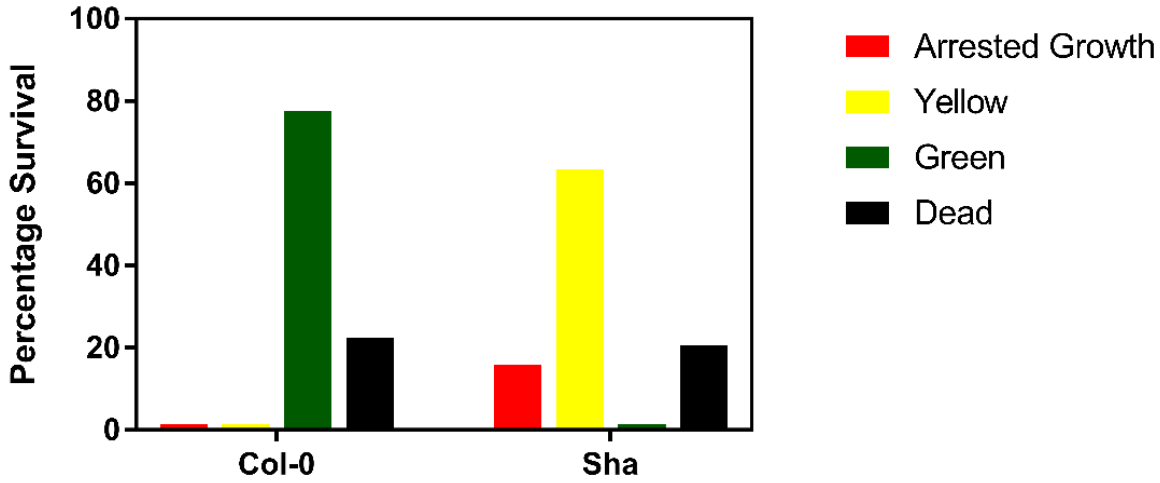
Percentage Survival
100
80
60
40
20
0
Col-0
Sha
Arrested Growth
Yellow
Green
Dead

D

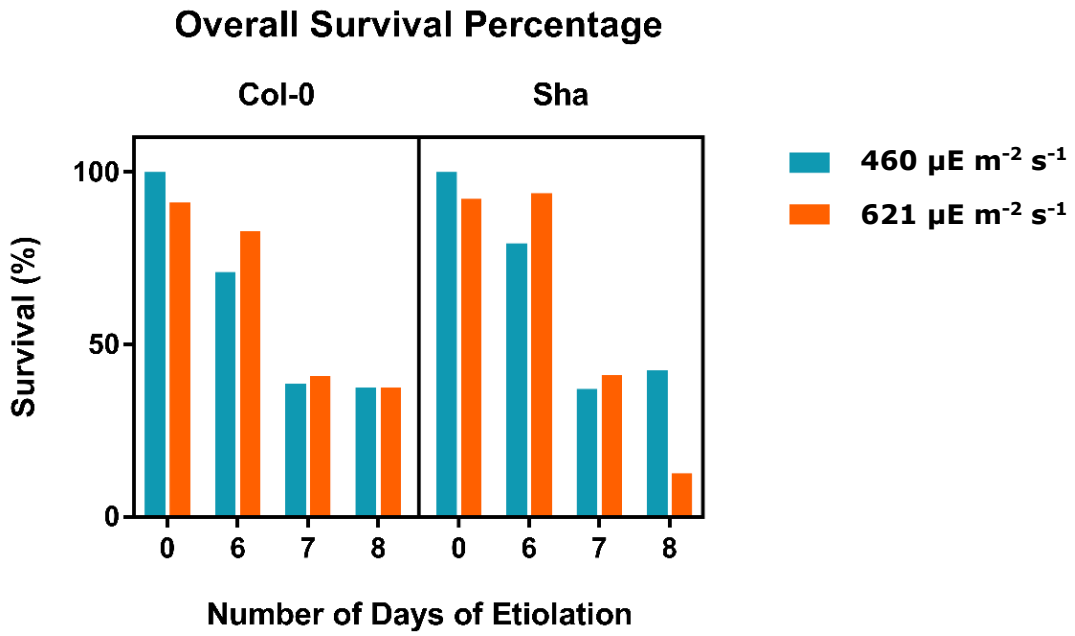

Figure 6:
Light Intensity Impacts Chlorophyll Accumulation and Physiological Development of *A. thaliana*.

(A) Relative chlorophyll A + B accumulation for Col-0 and Sha following varying periods of etiolation (0 days, 6 days, 7 days and 8 days) and exposure to differing light intensities (460 µE m^{-2} s^{-1} and 621 µE m^{-2} s^{-1}). Error bars indicate standard deviation (SD) from the mean.
* indicates results between Col-0 and Sha from the same period of etiolation are significantly different from one another if the P-value was less or equal to 0.1 following a t-test.

(B) Relative anthocyanin accumulation for Col-0 and Sha following varying periods of etiolation (0 days, 6 days, 7 days and 8 days) and exposure to differing light intensities (460 µE m^{-2} s^{-1} and 621 µE m^{-2} s^{-1}). Error bars indicate SD from the mean.
* indicates results between Col-0 and Sha from the same period of etiolation are significantly different from one another if the P-value was less or equal to 0.1 following a t-test.

(C) Percentage survival and physiological characteristics for Col-0 and Sha seedlings following 6 days of etiolation and placed at 460 µE m^{-2} s^{-1}**.**

(D) Comparison of survival for Col-0 and Sha seedlings following varying periods of etiolation (0 days, 6 days, 7 days and 8 days) and exposure to differing light intensities (460 µE m^{-2} s^{-1} and 621 µE m^{-2} s^{-1}).

3.03 Hyperoxia Impacts Plant Development

To determine the impact of destabilisation of ERFVIIs on ROS and chlorophyll levels I subjected a variety of seedlings of differing ERFVII stability, and mutants of the PRT6 N-degron pathway to hyperoxia (~27% v/v). Accessions from different altitudes (Col-0 – 100 masl, Sha – 3400 masl, Bdm – 2124 masl) and PRT6 N-degron pathway mutants (*prt6-1*, *erfVII*, *prt6erfVII*, Sha *prt6*, and *MA-HRE2*)were grown in darkness for 6 days and subsequently transferred to 460 µE m^{-2} s^{-1} for 5 days before fluorescent microcopy images and chlorophyll measurements were taken. 5 seedlings were from each line and each treatment were imaged, and the image shown is the most representative seedling that had the median amount of staining.

Results from Figure 7A-C show comparative ROS accumulation between accessions (Col-0, Sha, Bdm) and PRT6 N-degron pathway mutants (*prt6-1*, *erfVII*, *prt6erfVII*, Sha *prt6*, and *MA-HRE2*). Sha has significantly higher levels of ROS than that of Col-0, indicating that adaption to altitude and the environment is impacting plant development through ROS formation. Results from Figure 7D show that following exposure to hyperoxia chlorophyll levels decrease for all accessions (Col-0, Sha, Bdm) and PRT6 N-degron pathway mutants (*prt6-1*, *erfVII*, *prt6erfVII*, Sha *prt6*, and *MA-HRE2*). This is also visually represented through staining in Figures 7A-C. Results in Figure 7D show anthocyanin accumulation for accessions (Col-0, Sha, Bdm) and PRT6 N-degron pathway mutants (*prt6-1*, *erfVII*, *prt6erfVII*, Sha *prt6*, and *MA-HRE2*). Results in Figure 7D shows unexpected results, with anthocyanin levels varying heavily between accessions and between both normoxia and hyperoxia. For all lines it was hypothesised that during hyperoxia anthocyanin levels would increase compared to normoxia. It was hypothesised that increased destabilisation of ERFVIIs during hyperoxia would result in higher PCH and ROS accumulation, and thus require more anthocyanin quench additional ROS. This was true for Sha and Bdm, but was not the case for WT. For WT, higher levels of anthocyanin were shown in normoxia than in hyperoxia.

A

Normoxia	Bright Field	ROS	Chlorophyll
Col-0			
Sha		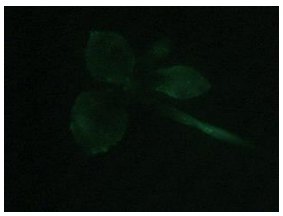	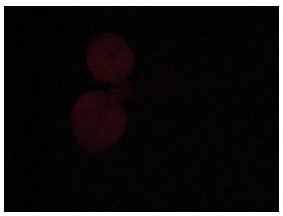
prt6-1		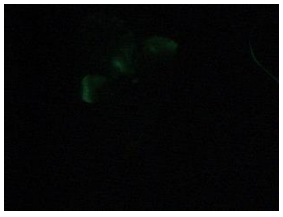	

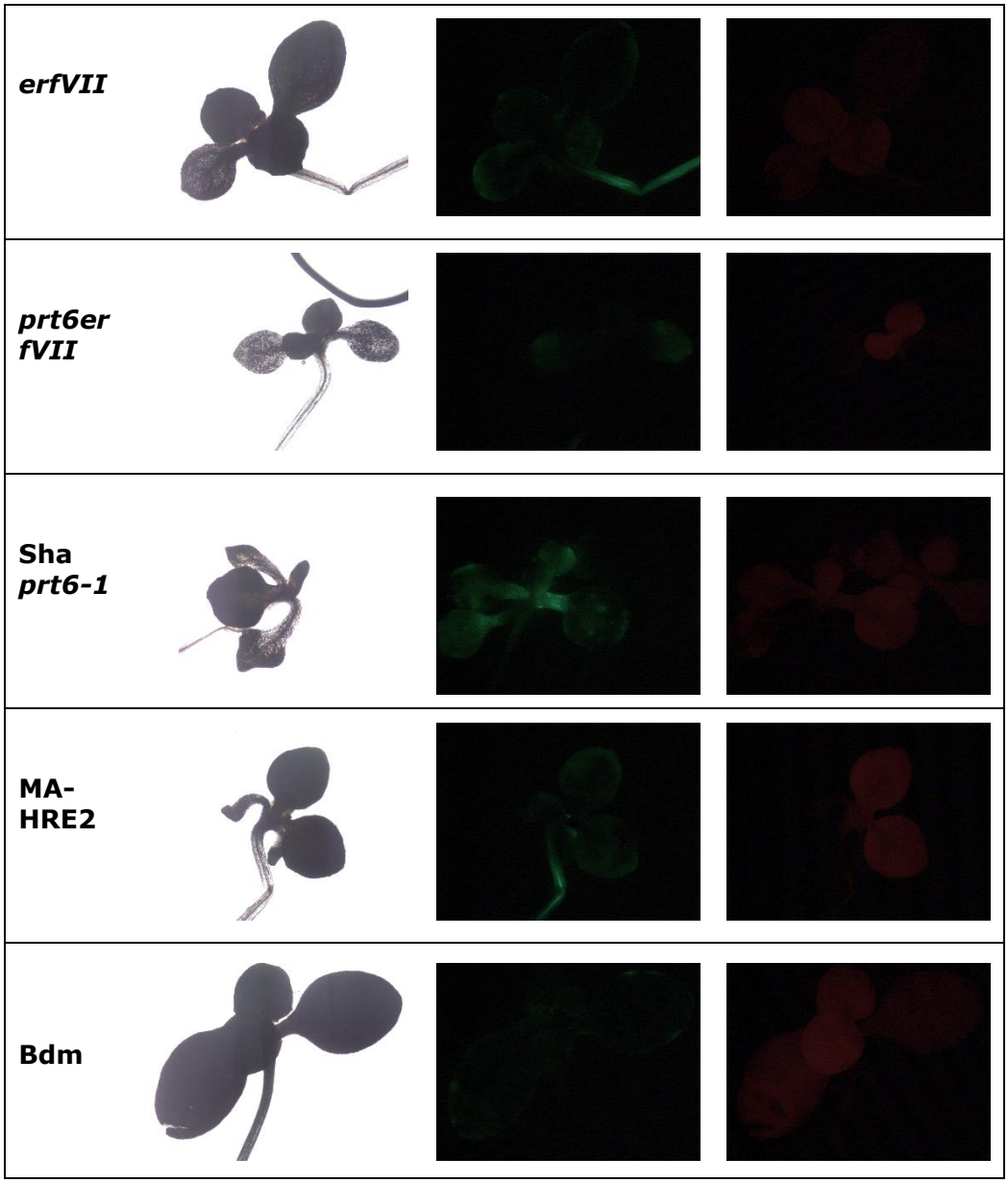
erfVII
prt6er fVII
Sha prt6-1
MA-HRE2
Bdm

B

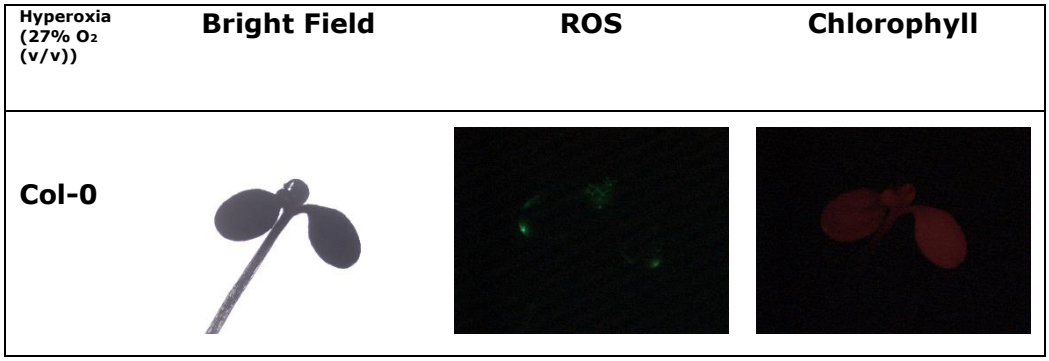
Hyperoxia (27% O2 (v/v))
Bright Field
ROS
Chlorophyll
Col-0

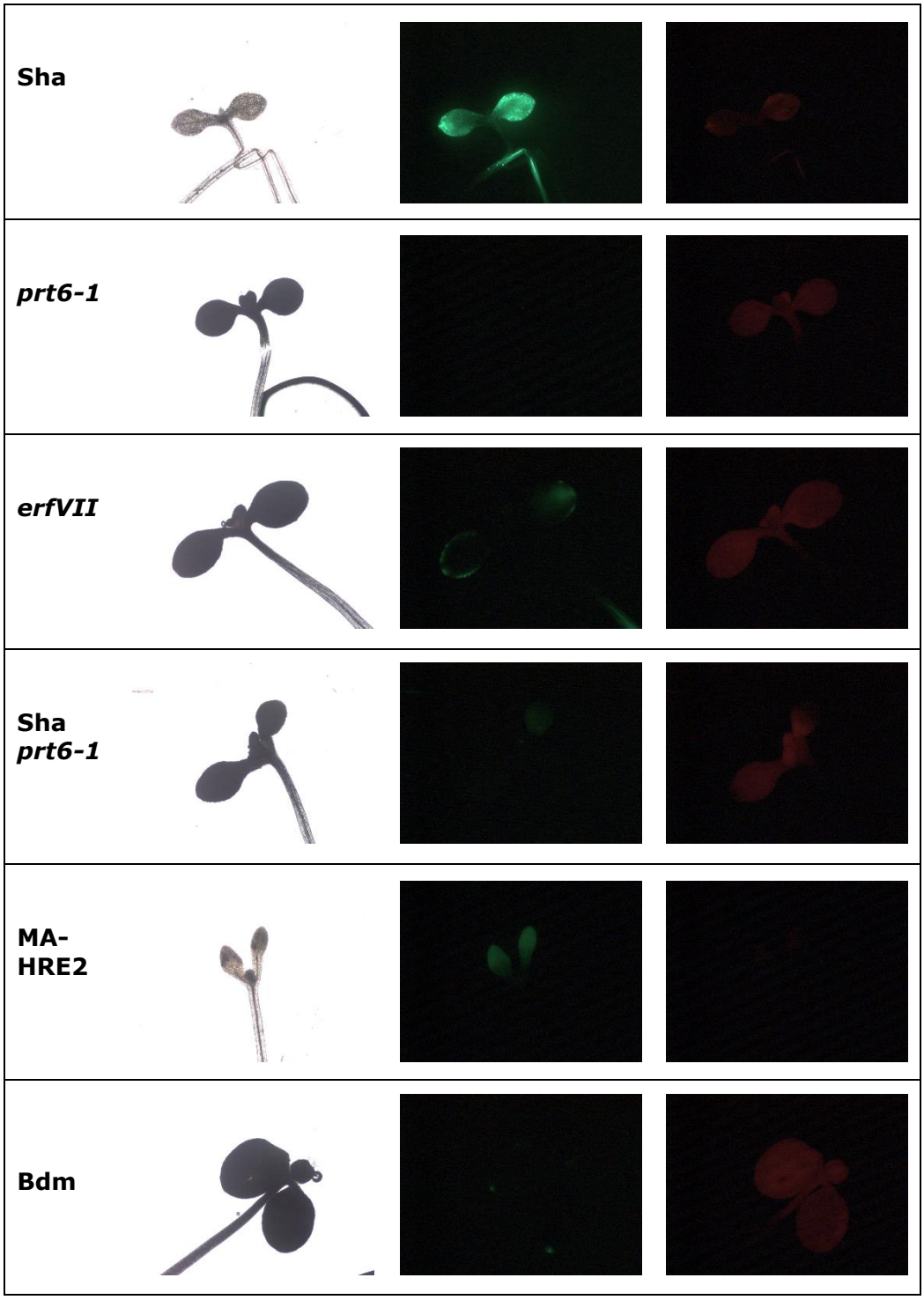
Sha
prt6-1
erfVII
Sha
prt6-1
MA-
HRE2
Bdm

C

ROS + Chlorophyll Images

	Normoxia	Hyperoxia (~27% O_2 (v/v))
Col-0	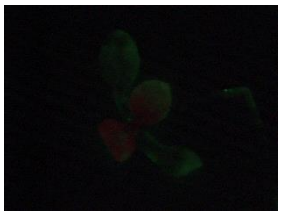	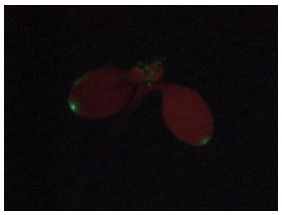
Sha	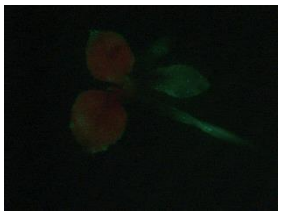	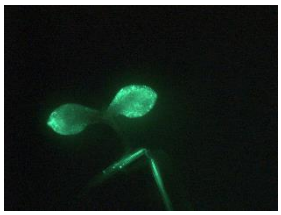
prt6-1	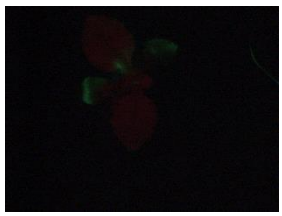	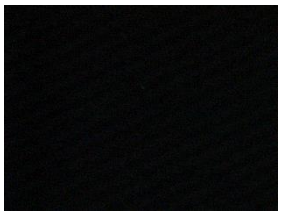
erfVII		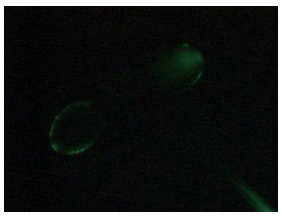
Sha *prt6-1*	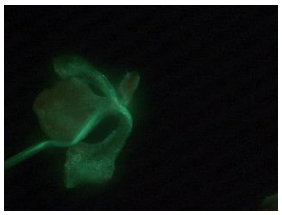	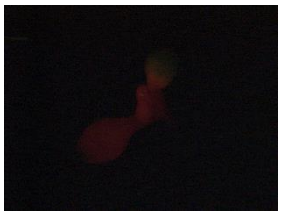
MA-HRE2	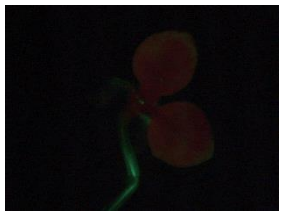	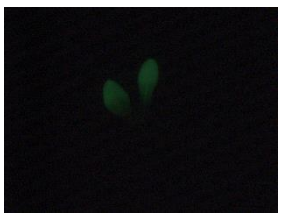


Bdm

D

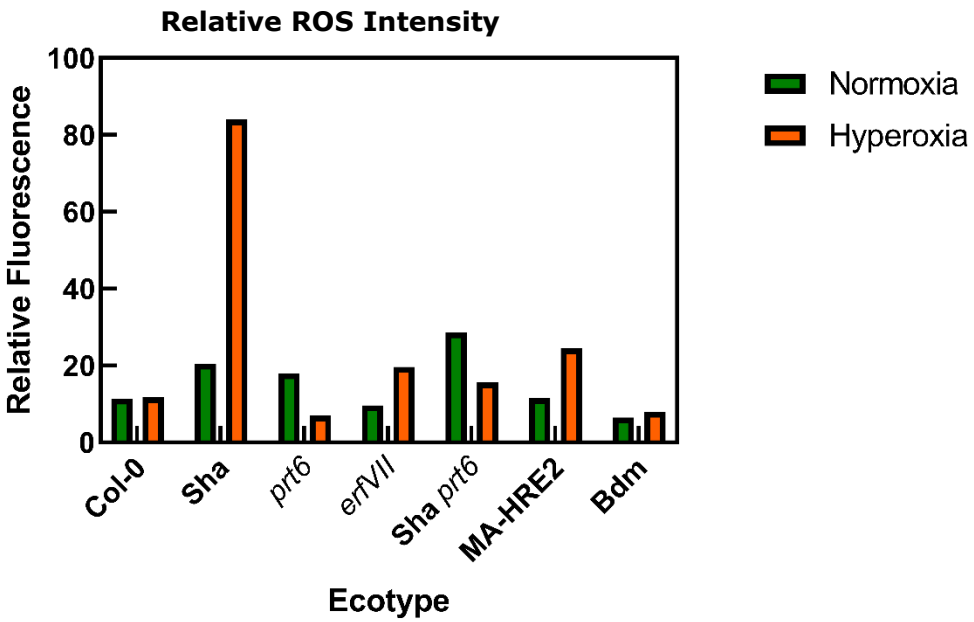
Relative ROS Intensity
Relative Fluorescence
100
80
60
40
20
0
Col-0
Sha
prt6
erfVII
Sha prt6
MA-HRE2
Bdm
Ecotype
Normoxia
Hyperoxia

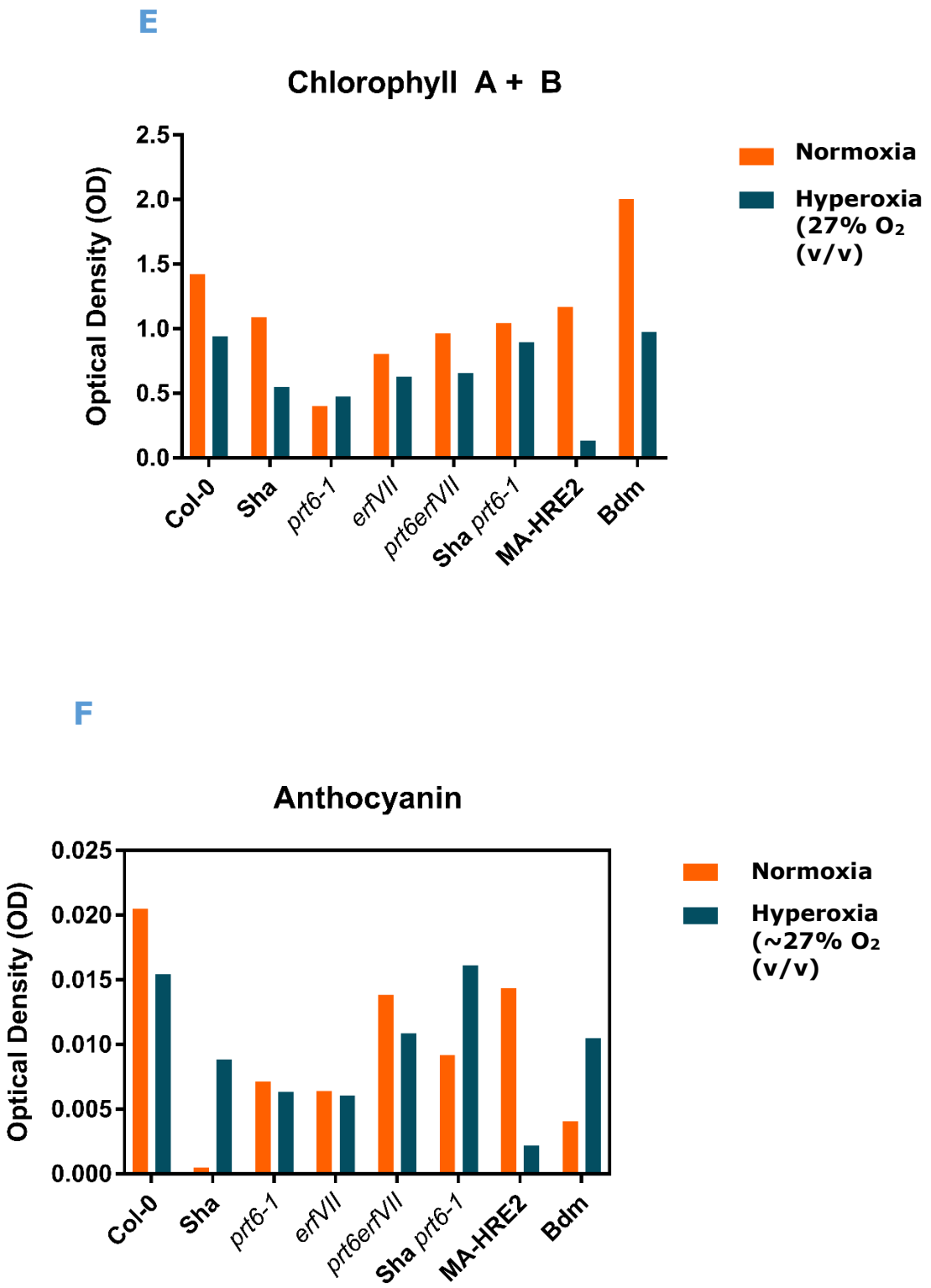

Figure 7
Hyperoxia at 27% O_2 (v/v) Impacts ERFVIIs Stabilisation and Plant Development in *A. thaliana*

(A) Stained images highlighting ROS and Chlorophyll accumulation in *A. thaliana* seedlings (Col-0, Sha, *prt6-1*, *erfVII*, *prt6erfVII*, Sha *prt6-1*, MA-HRE2, Bdm) when etiolated for 6 days under normoxia (21% O_2 (v/v)), and subsequently transferred to light (460 µE m^{-2} s^{-1}) for 5 days.

(B) Stained images highlighting ROS and Chlorophyll accumulation in *A. thaliana* seedlings (Col-0, Sha, *prt6-1*, *erfVII*, *prt6erfVII*, Sha *prt6-1*, MA-HRE2, Bdm) when etiolated for 6 days under hyperoxia (~27% O_2 (v/v)), and subsequently transferred to light (460 µE m^{-2} s^{-1}) for 5 days.

(C) Comparison of ROS and Chlorophyll accumulation between *A. thaliana* seedlings ((Col-0, Sha, *prt6-1*, *erfVII*, *prt6erfVII*, Sha *prt6-1*, MA-HRE2, Bdm) etiolated at normoxic (21% O_2 (v/v)) conditions against those etiolated at hyperoxic (~27% O_2 (v/v)) conditions.

(D) Quantitative analysis comparing relative ROS fluorescence levels in *A. thaliana* seedlings (Col-0, Sha, *prt6-1*, *erfVII*, *prt6erfVII*, Sha *prt6-1*, MA-HRE2, Bdm) when etiolated for 6 days under normoxia (21% O_2 (v/v)), and subsequently transferred to light (460 µE m^{-2} s^{-1}) for 5 days.

(E) Relative chlorophyll (chlorophyll *a* + *b*) levels (Optical Density) of *A. thaliana* (Col-0, Sha, *prt6-1*, *erfVII*, *prt6erfVII*, Sha *prt6-1*, MA-HRE2, Bdm) seedlings following etiolation for 6 days under hyperoxia (~27% O_2 (v/v)), and subsequently transferred to light (460 µE m^{-2} s^{-1}) for 5 days.

(F) Relative anthocyanin levels (Optical Density) of *A. thaliana* (Col-0, Sha, *prt6-1*, *erfVII*, *prt6erfVII*, Sha *prt6-1*, MA-HRE2, Bdm) seedlings following etiolation for 6 days under hyperoxia (~27% O_2 (v/v)), and subsequently transferred to light (460 µE m^{-2} s^{-1}) for 5 days

3.04 The Development of Transgenic Tools to Analyse RAP2.3 and its Role in the PRT6 N-degron Pathway

3.04.1 *Agrobacterium* Transformation of *promRAP2.3:MA-RAP2.3:GUS* and *promRAP2.3:MC-RAP2.3:GUS* :

From a stock of *promRAP2.3:MA-RAP2.3:GUS* and *promRAP2.3:MC-RAP2.3:GUS* I began the process of transferring these constructs to *A. thaliana* in order to analyse their expression, and the role of RAP2.3 in the PRT6 N-degron pathway. The *promRAP2.3:MA-RAP2.3:GUS* and *promRAP2.3:MA-RAP2.3:GUS* allow analysis of the RAP2.3 gene under its promoter, and allows for GUS staining to identify visualisation of the activity within the plant cells.

Agrobacterium competent cells were transformed *using promRAP2.3:MA-RAP2.3:GUS* and *promRAP2.3:MC-RAP2.3:GUS* DNA. The competent cells were then plated on selection plates containing rifampicin, spectinomycin and gentamicin (RGS). Rifampicin and spectinomycin were used to select for the *Agrobacterium* as the *Agrobacterium* strain used contains resistance to these antibiotics. Gentamicin was used to select for the plasmid as the plasmid contains the resistance gene for this antibiotic. Using this wide selection of antibiotics meant that any colonies that grew had to be resistant to all antibiotics, with resistance and growth only possible in *Agrobacterium* that had been transformed by the plasmid. Overnight cultures were then grown up of successful *Agrobacterium*

transformations in order to produce large volumes of single *Agrobacterium* clones containing the plasmid.

3.04.2 *Agrobacterium* transformation of promRAP2.3:MA-RAP2.3:GUS and promRAP2.3:MC-RAP2.3:GUS in to *A. thaliana*:

Next, I transformed *in vivo* into plants. I chose floral dipping (Clough and Bent, 1998) to transform *in vivo* over other transformation methods such as biolistics (Kikkert *et al.,* 2005) and the "Agrobacterium vacuum infiltration method" (Bechtold and Pelletier, 1998). Floral dipping provides numerous advantages over these other methods. Floral dipping is easily scalable and allowed the development of a large number of transgenic lines within a short period. Even though floral dipping does not give the highest transformation efficiency (1%), the large volume of seeds that are produced from *A. thaliana* ensures sufficient transgenic events occur in a single transformation event (Zhang *et al.,* 2006). Floral dipping also allows the maintenance of genomic stability within the *A. thaliana* transgenic plants which when using tissue-culture based transformation can be damaged (Labra *et al.,* 2004).

3.04.3 Screening of Transformants:

Following transformation plants were grown in short days (8 hours light, 16 hours darkness) for 1 month and dry seeds were collected. Hygromycin selection was then carried out on the T0 seeds (2.25). Hygromycin-resistant transformants were identified by their long hypocotyls (approximately 0.8-1 cm), whereas non-transformed seedlings had shorter hypocotyls (approximately 0.2-0.4 cm). Hygromycin resistant seedlings also had much larger cotyledons than non-transformants. Roots will also not develop in non-transformants. The phenotype of these T0 transgenic plants is hygromycin resistant (Hyg R), however the genotype of the seedlings is hemyzygous (R/0). In order to get true homozygous seeds these lines had to be taken to the T3 generation. Suspected transformed T0 seedlings were then transferred to a fresh plate to allow true leaves to emerge. Seedlings were then grown for 1-2 weeks to confirm that the T0 seeds were true transgenic lines, as non-transformants can also germinate following hygromycin selection and cotyledons can remain green for up to 1 month following germination. T0 seedlings were then transplanted to soil and plants grown under light for seed collection.

The seeds collected from growth of T0 plants are that of the T1 generation. The phenotype of T1 seedlings will be both Hyg R and Hyg r (hygromycin sensitive) at a ratio of 3:1 respectively. The genotype of the T1 seedlings will be a mixture of homozygous R/R (Hyg R), hemizygous R/0 (Hyg R) and homozygous r/r (Hyg r). Hygromycin selection (2.27) was then carried out on these seedlings to eliminate the r/r (Hyg r) individuals from the population. T1 seedlings were then transplanted to soil and plants grown under light for seed collection.

The seeds collected from growth of T1 plants are known as T2 generation plants. The phenotype of T2 generation plants is dependent on the genotype of the T1 progenitor. The only genotypes possible for the T1 progenitor now are that of homozygous R/R (Hyg R) and hemyzgous (R/0) as the homozygous r/r (Hyg r) have been eliminated. If the genotype of the T1 progenitor is that of homozygous R/R (Hyg R) then the phenotype of all T2 seedlings will also be homozygous R/R (Hyg R). However, if the T1 progenitor is hemzygous (R/0) then the genotype of the T2 plants will be a mixture of R/R, R/0 and r/r and the phenotype will be a mixture of Hyg R and Hyg r (3:1). This means that the majority of seedlings will now show hygromycin resistance. However, the lines were genotyped in order to get true homozygous R/R lines to take into the T3 generation. Seeds from the T3 generation plants were then harvested to use for PCH assays (3.05) and GUS staining (3.06). However, following the development of these seeds they are available to be used for a wide variety of experiments relating to the study of RAP2.3.

3.05 RAP2.3 is Essential in the Chlorophyll Tetrapyrrole Pathway and the Accumulation of PCH:

I carried out a PCH assay on T3 seeds in order to compare PCH accumulation between *promRAP2.3:MA-RAP2.3:GUS* in Sha, *promRAP2.3:MC-RAP2.3:GUS* in Sha Sha and Col-0 seedlings. It is known that ERFVIIs are important in the chlorophyll tetrapyrrole pathway in preventing the overaccumulation of PCH during hypoxic and skotomorphogenic environments (Abbas *et al.,* 2015). Through this PCH assay it allows me to further uncover the specific role of the RAP2.3 ERFVII in reducing PCH accumulation.

Seedlings were grown under 5 days complete darkness following stratification and germination. This period of darkness provides ample time for PCH levels to rise and accumulate as when in these conditions the chlorophyll tetrapyrrole pathway is restricted due to PIFs and reduced POR activity (Figure 3). Plants were not put in periods of darkness longer than 5 days as when placed in darkness longer than this there is potential for this to cause irreversible damage to the plant from excess PCH and ROS accumulation, as well as the plants may die as they may run out of ATP reserves without being able to photosynthesise. There was no light treatment as any light would begin the process of converting PCH to chlorophyll. Sha seedlings were used in conjunction to the *promRAP2.3:MA-RAP2.3* and *promRAP2.3:MC-RAP2.3:GUS* in Sha line as it allowed a comparison to be made of the effect of RAP2.3 stabilisation in the *promRAP2.3:MC-RAP2.3* line to that of the standard Sha accession. This allows confirmation that any differences in PCH are due to the expression of the RAP2.3 gene under its promoter. The Col-0 accession was used as a WT comparison to both *promRAP2.3:MA-RAP2.3* in Sha, *promRAP2.3:MA-RAP2.3:GUS* in Sha, and Sha.

Results in Figure 8 show a PCH assay comparing relative PCH levels between Col-0, Sha, promRAP2.3:MA-RAP2.3:GUS in Sha, promRAP2.3:MC-RAP2.3:GUS in Sha and Sha *prt6*. 2 lines of both the promRAP2.3:MA-RAP2.3:GUS in Sha and promRAP2.3:MC-RAP2.3:GUS in Sha were used to provide absolute confirmation of results, in the case that one of the T3 lines used were not completely homozygous. Following excitation at 440nm, the emission peak at 636 indicates relative PCH levels. Results show significantly higher PCH levels in Sha compared to all other lines and accessions used.

The emission between 650-700nm indicates potential slight light contamination within the samples. A peak at this emission (668nm) indicates the presence of chlorophyllide (Figure 3). In order for chlorophyllide to be present within the sample this would require the light activation of the POR enzyme. However, levels of chlorophyllide are extremely limited and do not rise above 0.01 for all samples (Figure 8) suggesting that any potential light contamination was extremely limited, and the results remain reliable. However, the experiment must be repeated to provide absolute confirmation of results.

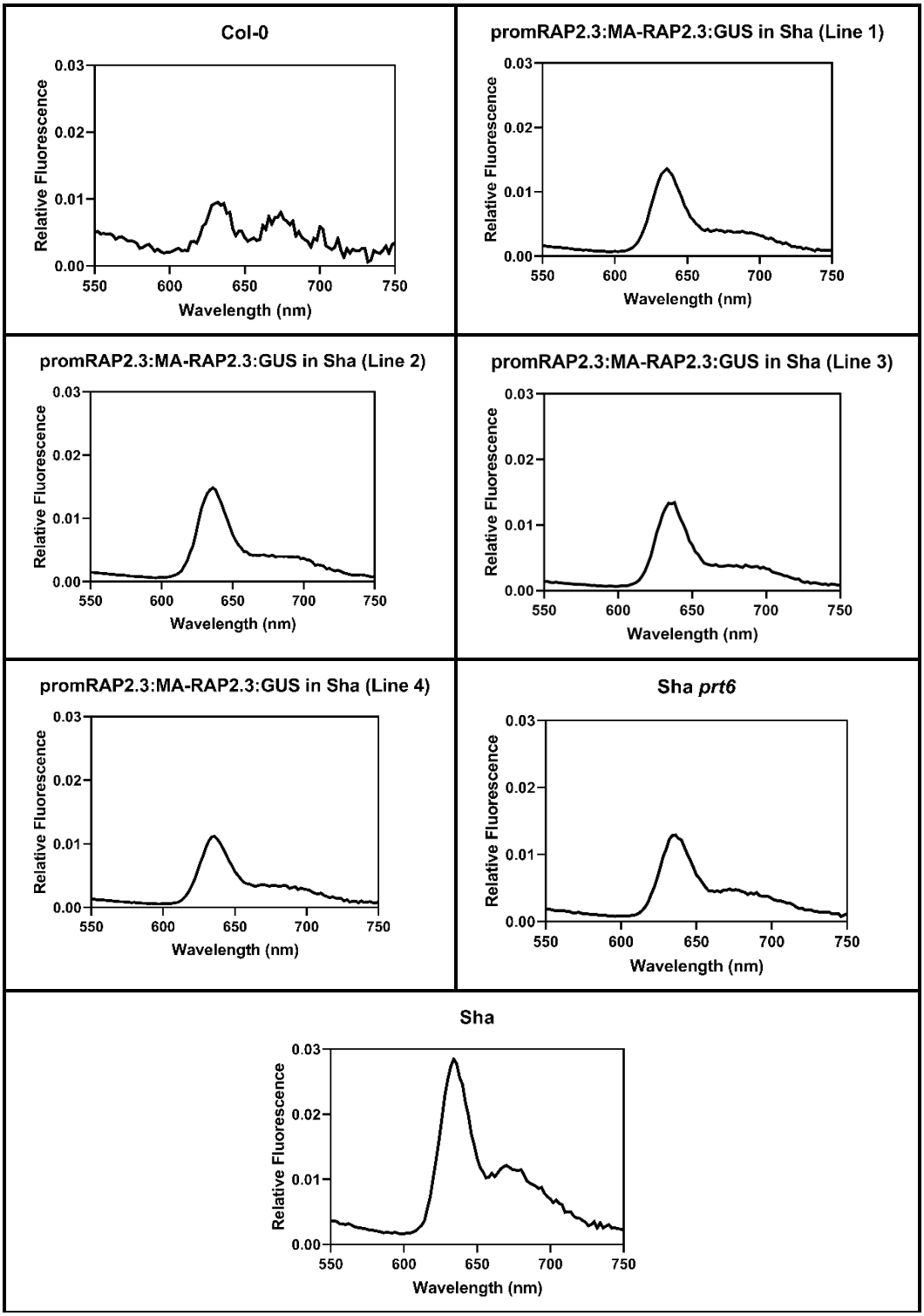
Col-0
promRAP2.3:MA-RAP2.3:GUS in Sha (Line 1)
promRAP2.3:MA-RAP2.3:GUS in Sha (Line 2)
promRAP2.3:MA-RAP2.3:GUS in Sha (Line 3)
promRAP2.3:MA-RAP2.3:GUS in Sha (Line 4)
Sha prt6
Sha
Relative Fluorescence
Wavelength (nm)
0.00
0.01
0.02
0.03
550
600
650
700
750

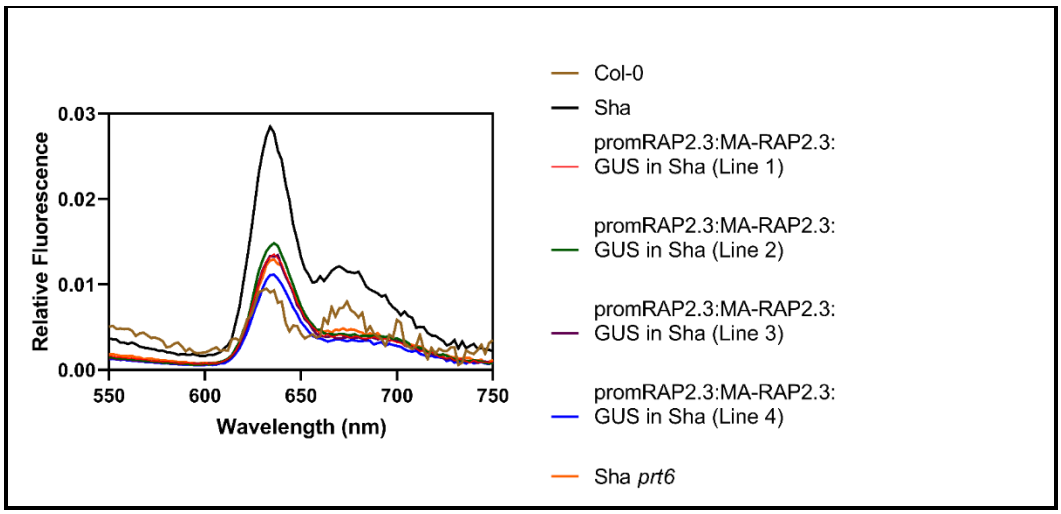

Figure 8:
Relative fluorescence and accumulation of PCH (excitation at 440nm; emission at 600-700nm) in *A. thaliana* lines (Col-0, Sha, *promRAP2.3:MA-RAP2.3:GUS* in Sha, *promRAP2.3:MA-RAP2.3:GUS* in Sha, and Sha *prt6*) using a gradient HPLC fluorescence detector.

3.06 Gene expression of RAP2.3 under its Promoter is Influenced by Etiolation and Light Availability

GUS staining was carried out to investigate how light availability impacted gene expression of RAP2.3 under its promoter. GUS staining was carried outs on *promRAP2.3:MA-RAP2.3:GUS* in Sha and *promRAP2.3:MC-RAP2.3:GUS* in Sha. 2 separate T3 lines of both *promRAP2.3:MA-RAP2.3:GUS* in Sha and *promRAP2.3:MC-RAP2.3:GUS* in Sha were used in order to ensure the results were repeatable, and weren't specific to one particular line that may not have been completely homozygous. GUS staining was carried out an seedlings that had undergone periods of 5 days and 7 days of etiolation following stratification and germination. Control staining was carried out on seedlings that had also undergone 5 days and 7 days of light following stratification and germination. 5 seedlings were from each line and each treatment were imaged, and the image shown is the most representative seedling that had the median amount of staining.

Results in Figure 9 show that extended periods of etiolation increase expression of the RAP2.3 gene, with the highest distribution of GUS activity for both *promRAP2.3:MA-RAP2.3:GUS* and *promRAP2.3:MC-RAP2.3:GUS* lines being after exposure to 7 days of darkness. These results suggest that light acts as a signal in regulating expression of RAP2.3, and Figure 9 shows that expression of RAP2.3 under its promoter is elevated with the presence of an alanine (*promRAP2.3:MA-RAP2.3:GUS*) over that of a cysteine (*promRAP2.3:MC-RAP2.3:GUS*) .

	*promRAP2.3:M**A**-RAP2.3:GUS* in Sha Line 1	*promRAP2.3:M**A**-RAP2.3:GUS* in Sha Line 2	*promRAP2.3:M**C**-RAP2.3:GUS* in Sha Line 1	*promRAP2.3:M**C**-RAP2.3:GUS* in Sha Line 2
5 Days Light (Control)	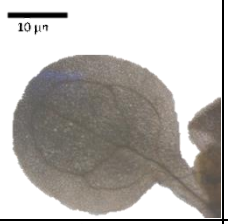	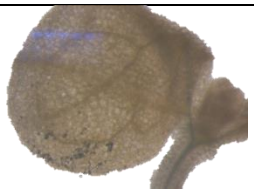		
5 Days Darkness				
7 Days Light (Control)				
7 Days Darkness				

Figure 9:
GUS staining of *A. thaliana* lines (*promRAP2.3:MA-RAP2.3:GUS* in Sha, *promRAP2.3:MC-RAP2.3:GUS* in Sha). Seedlings were either exposed to 5 days of darkness, 7 days of darkness, or were left in light. Following growth GUS staining was carried out to indicate expression of the RAP2.3 gene under its promoter and visualisation of this expression throughout the cotyledon (indicated by blue staining). 5 seedlings were from each line and each treatment were imaged, and the image shown is the most representative seedling that had the median amount of staining.

3.07 The Development of Transgenic Tools to Analyse RAP2.12 and the PRT6 N-degron Pathway:

RAP2.12 is an essential ERFVII TF that regulates a wide variety of responses within plants. RAP2.12 is constitutively expressed at RNA level throughout the entire plant and upregulated within leaves upon hypoxia (Licausi *et al.,* 2011). Hypoxia response is a key role of RAP2.12 in plants but RAP2.12 is also involved in a diverse range of processes such as: respiration, TCA cycle, amino acid metabolism, and the regulation of immune-regulatory metabolites (Paul *et al.,* 2016). At the beginning of the experiment I had available the RAP2.12 coding region starting at C^2 cloned into the Ubiquitin reference technique (1.10) plasmid to give the construct: $^{FLAG}DHFR^{HA}$-C^2-$RAP2.12^{HA}$.

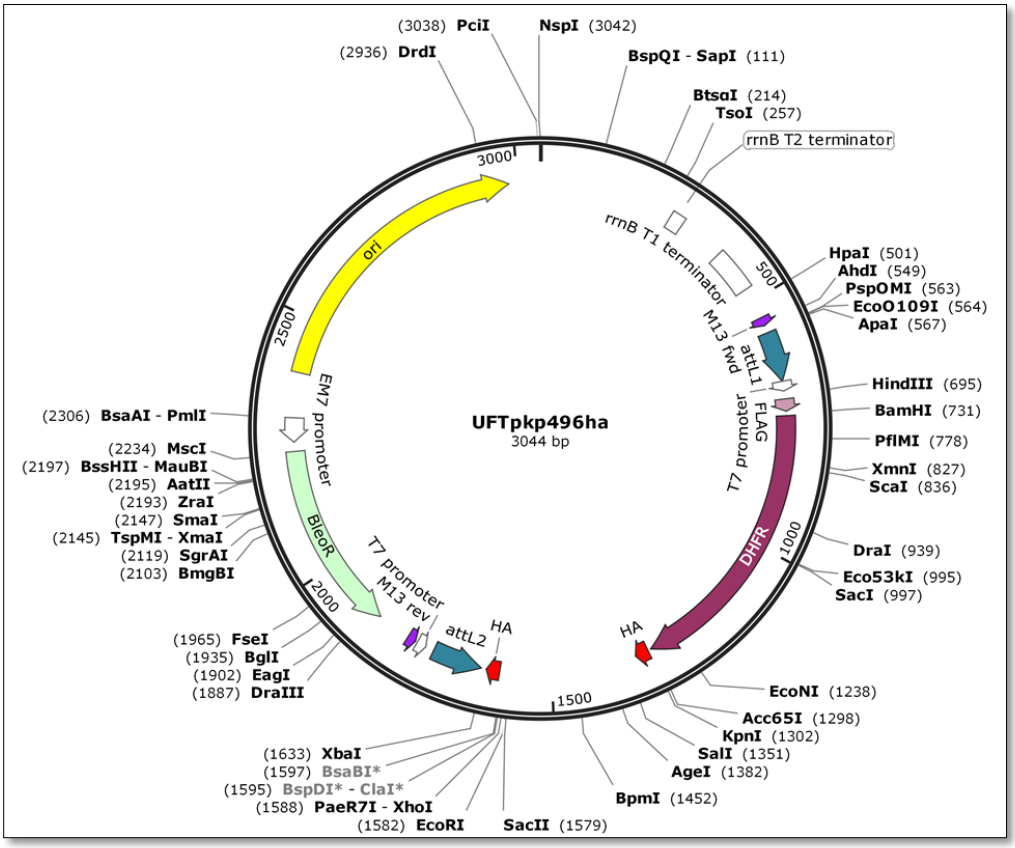

Figure 10:
UFT3XHA Vector Used for Cloning of C^2-RAP2.12

However, this was a plasmid stock and had to be re-checked and sequenced before transformations and *in vivo* work could take place. In order to re-check the plasmid stock, a polymerase chain reaction (PCR) (2.08) to amplify the stock of RAP2.12 was done. Following the amplification of the sample gel electrophoresis (2.09) was carried out to separate the DNA fragments according to size. The size of the bands was 39kDa which confirmed the presence of the RAP2.12 sample. In order to get the pure sample, RAP2.12 was extracted using a gel extraction kit as described (2.10). The RAP2.12 sample was then digested using SacII restriction enzyme (2.11) and ligated into the entry clone vector (2.12). This cloning reaction mixture was then transformed into competent *E. coli* cells (2.13). An LR reaction (2.14) was then carried out to transfer the cassette containing DHFR and Ubiquitin from the entry clone to the UFT3XHA destination vector in order to create a recombinant plasmid expression clone. Individual colonies from the LR reaction were then taken and cultured through shaking overnight at 37°C and the plasmid DNA was then isolated using a mini-prep kit (2.15). A confirmatory gel carried out and the plasmid DNA sequenced to confirm the presence of the C^2-RAP2.12.

3.07.1 *In Vitro* Assay of C^2-RAP2.12:

In order to confirm if C^2-RAP2.12 was a substrate of the Arg/N-degron pathway I carried out an *in vitro* assay and subsequent Western blots. The *in vitro* assay involved putting the C^2-RAP2.12-3xHA in to the rabbit reticulocyte lysate *in vitro* eukaryotic protein synthesis system, allowing translation to take place, then measuring relative protein abundance at 0, 30 and 120 minute time points. If C^2-RAP2.12 was a substrate of the PRT6 N-degron pathway, protein abundance (confirmed by Western blots) would decrease

throughout the time points as the protein is degraded. However, prior to carrying out an *in vitro* assay I first had to carry out Nandodrop Quantification (2.18) to find the required concentration of DNA required for an *in vitro* assay, as this must be 1200ng. Figure 11A shows an anti-HA Western blot of C^2-RAP2.12-3xHA with the assay either containing bortezomib and without bortezomib, and following translation, samples were taken at 0, 30 and 120 minute time points.

The lower band in Figure 11A is C^2-RAP2.12-3xHA and upper band is a lysate band used as a control. Lysate comes from the degradation of cells within the rabbit reticulocyte *in vitro* synthesis system and is not a substrate of the N-degron pathway so the band remains a constant throughout every time point, irrespective of bortezomib treatment. This means that if the C^2-RAP2.12-3xHA sample abundance decreases whilst the lysate band remains constant it confirms the C^2-RAP2.12-3xHA sample is actually being degraded, and the reduction in abundance is not due to a loading error.

Following incubation for 30 minutes at 30°C to allow for translation in the rabbit reticulocyte lysate *in vitro* eukaryotic protein synthesis system, cycohexamide was added to prevent further translation. A sample was then taken in order to get the initial amount of protein produced immediately following translation; this is the 0 minute sample. Samples were then taken at 30 and 120 minutes respectively in order to see protein abundance as time surpasses. Figure 11A confirms C^2-RAP2.12 as a substrate of the Arg/N-degron pathway and is being degraded. As the time points move from 0 to 120 in the treatment without bortezomib there is a clear reduction in C^2-RAP2.12 protein abundance, shown by how the C^2-RAP2.12 becomes fainter whilst the lysate control band remains constant. There is a slight reduction in abundance of C^2-RAP2.12 after 30 minutes, then at 120 minutes there is almost a complete absence of the protein indicating its almost full degradation (Figure 11A).

Figure 11A also shows Western blots for C^2-RAP2.12-3xHA *in vitro* samples treated with bortezomib. However, there is no decrease in protein abundance for samples treated with bortezomib (Figure 11A). There is no decrease in protein abundance for C^2-RAP2.12 because bortezomib is an inhibitor of the 26S proteasome. In the N-degron pathway following ubiquitination from the N-degron specialised E3 ligase PRT6 the protein substrate is degraded via the 26S proteasome. However, following bortezomib treatment this means that degradation is not possible via the 26S proteasome, resulting in C^2-RAP2.12 being unable to be degraded despite being ubiquitinated. As C^2-RAP2.12 abundance remains constant following bortezomib treatment this provides confirmation that C^2-RAP2.12 is a substrate of the Arg/N-degron pathway and is being degraded through the 26S proteasome.

A

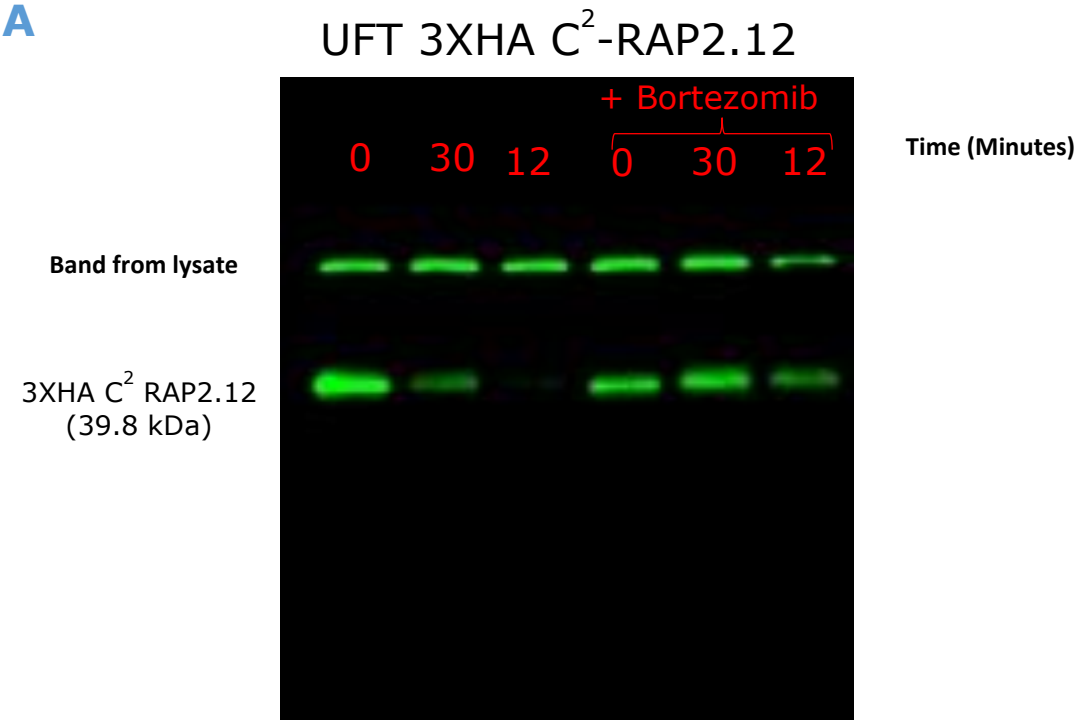

B

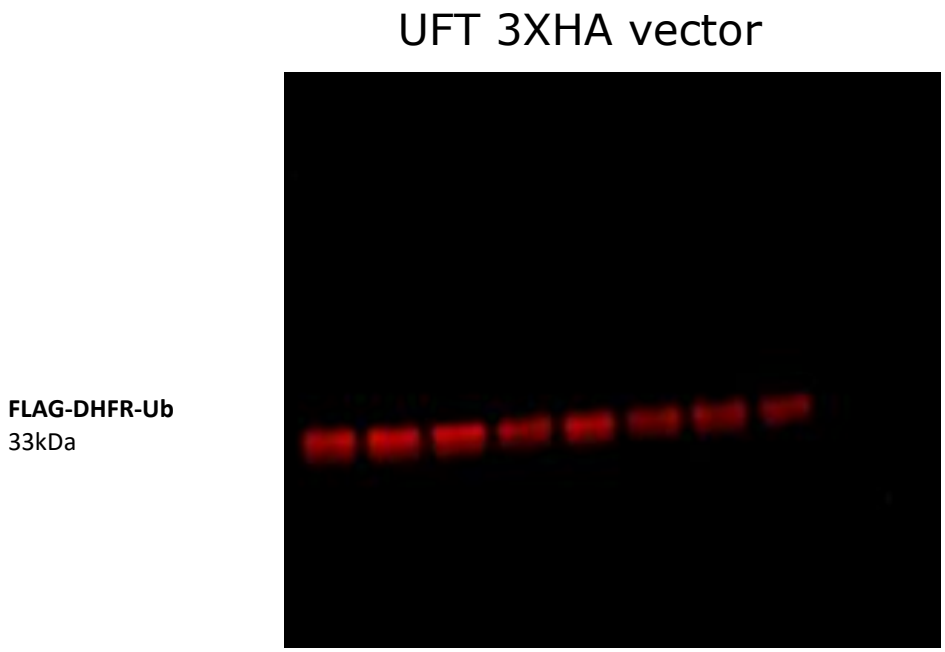

Figure 12:
UFT-C^2-RAP2.12 is a Substrate of the PRT6 N-degron Pathway

(A) Western blot of UFT-C^2-RAP2.12 showing the decrease in abundance of the protein (due to degradation) throughout the time course of non-bortezomib treated samples. Primary antibody antiHA (1:2000).

(B) Western blot of UFT-3XHA vector using the primary antibody antiFLAG (1:1000) to confirm presence of the vector.

3.07.2 Site-Directed Mutagenesis of C^2-RAP2.12 to A^2-RAP2.12:

In order to develop transgenic tools to analyse the role of RAP2.12 in the PRT6 N-degron pathway site-directed mutagenesis was carried out on C^2-RAP2.12 to convert the cysteine residue to a stable alanine. Alanine is a stabilising residue at the N-terminus meaning RAP2.12 is will no longer be degraded via the PRT6 N-degron pathway in this construct. Figure 12 shows the gel electrophoresis results from the site-directed mutagenesis, and the size of the bands in lanes 4 and 5 indicate site-directed mutagenesis was successful and the cysteine (C^2-RAP2.12) has been altered to an alanine (A-RAP2.12).

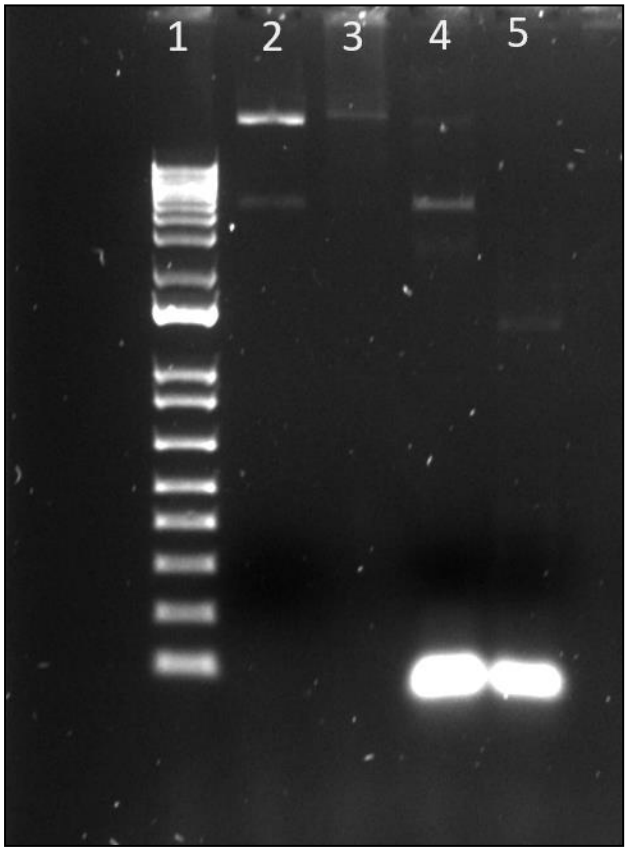

Figure 12:
Gel Electrophoresis for Confirmation of Successful Site-Directed Mutagenesis.
Lane: 1, molecular weight ladder; lane 2, control 1 (30ng template); lane 3, control 2 (30ng template + DpnI); lane 4, PCR reaction (A-RAP2.12); lane 5, PCR reaction (A-RAP2.12) + DpnI.

Chapter Four:

Discussion

4.01 Impact of Altitude Adaption on ROS Accumulation:

Results from 3.1 and Figure 5A-E show that altitude adaption impacts ROS and chlorophyll accumulation in seedlings, and if not adapted to the altitude that the seedling is grown at this can cause great amounts of ROS and chlorophyll accumulation. Seedlings from Figure 5A-E underwent a 10-day period of etiolation and were subsequently transferred to 5 days of light. Overaccumulation of ROS has been linked to PCH accumulation in etiolated seedlings (Huq *et al.,* 2004). PCH accumulates in darkness as the enzyme required to convert PCH to chlorophyllide (protochlorophyllide reductase - POR) is activated by light (Huq *et al.,* 2004). Prior results from Abbas *et al.,* 2015 show that stabilised ERFVIIs restrict the accumulation of ROS through regulating the control of PCH (Abbas *et al.,* 2015). Oxygen in *A. thaliana* is known to be sensed by ERFVIIs and the PRT6 N-degron pathway (Gibbs *et al.,* 2014). When Sha is grown normally it is grown at an oxygen concentration of approximately 18% (v/v) in comparison to Col-0 which is normally grown at an oxygen concentration of 21% (v/v). As Sha is acclimatised to being grown at low oxygen levels, I hypothesise that the ERFVIIs responsible for sensing oxygen are hypersensitive to oxidation and thus suffer greater degradation via the PRT6 N-degron pathway at normoxia (21% (v/v)) during this experiment. In the WT line (Col-0), I hypothesise that Col-0's ERFVIIs are less susceptible and hypersensitive to Cys oxidation and degradation via the PRT6 N-degron pathway, and therefore remain stable in order to coordinate responses associated with skotomorphogenesis.

4.02 Impact of Light Intensity on ROS Accumulation:

Results from 3.1 and Figure 5A-E show that increasing light intensity also increases ROS accumulation for both Col-0 and Sha. The PORA protein is rapidly degraded following light illumination (Ha *et al.,* 2017; Reinbothe *et al.,* 1995). This protein is essential for the conversion of PCH to chlorophyllide, and without its presence there will be greater amounts of PCH not bound to PORs. This free PCH then goes on to form ROS. As intensity increases from 57.5µE m^{-2} s^{-1} to 365 µE m^{-2} s^{-1} there is a vast increase in ROS accumulation (Figure 5C+D). ROS accumulation increases in proportion with intensity for both Col-0 and Sha in this way because even though they contain similar amounts of POR protein, I hypothesise that there is larger amounts of PCH in Sha due to the hypothesised hypersensitivity of Sha's ERFVIIs to oxidation following exposure to 21% oxygen (v/v)**.** I propose that this greater volume of PCH in Sha is then being converted to ROS, as there is greater amounts of free PCH not bound to the POR protein.

The N-terminal 35S:YFP-RAP2.3 has also been shown to be degraded in light, even under hypoxia independent of the Cys-2 N-degron (Abbas *et al.,* 2015; Gibbs *et al.,* 2015). This suggests that light may also be a signal regulating ERFVII stability. This may contribute to as to why as light intensity increases, ROS accumulation increases as ERFVII destabilisation increases. As light intensity increases, this may provide an additional signal to initiate the oxidation and destabilisation of ERFVIIs via the PRT6 N-degron pathway, hence the elevated ROS levels shown in the staining of Figure 5A-E as light intensity increases. However, ROS accumulation is not only controlled by ERFVIIs and light intensity, so ERFVIIs can not be confirmed as the sole reason for the elevated ROS levels in Figure 5A-E.

4.03 Impact of Altitude Adaption on Chlorophyll Accumulation:

Results from Figure 6A shows altitude adaption impacts chlorophyll accumulation as shown by Col-0 accumulating higher chlorophyll levels than that of Sha at both light intensities (460 µE m^{-2} s^{-1} and 621 µE m^{-2} s^{-1}) and at all periods of etiolation. During darkness chlorophyll biosynthesis is repressed (Huq *et al.,* 2004). Chlorophyll synthesis is supressed during darkness as the chlorophyll biosynthesis pathway is blocked after the formation of protochlorophyllide (PCH), as the reduction to chlorophyllide (the precursor of chlorophyll) requires light activation (op den Camp *et al.,* 2003). Once a critical mass of PCH has accumulated in dark grown cells, synthesis of Mg^{2+} porphyrins stops. Porphyrins are

essential in absorbing light and act as photosynthesisers (Meskauskiene *et al.,* 2001). If there is an overaccululation of PCH, this means that ROS production is favoured to that of chlorophyll upon transfer to light. ERFVII stability has been shown to restrict the accumulation of PCH (Abbas *et al.,* 2015). Similarly to 4.1, as Sha is acclimatised to being grown at low oxygen levels I hypothesise that the ERFVIIs responsible for sensing oxygen are hypersensitive to oxidation and thus suffer greater degradation via the PRT6 N-degron pathway at normoxia (21% (v/v)) during this experiment. With decreased stability of ERFVIIs, I hypothesise that Sha will then accumulate greater amounts of PCH. If Sha contains high amounts of PCH, this means that ROS production is favoured over chlorophyll production following the induction of light. This is opposed to in Col-0 where chlorophyll production will more favoured due to reduced PCH accumulation, resulting in elevated levels of chlorophyll to that of Sha, as shown in Figure 6A where there is a significant difference.

4.04 Impact of Altitude Adaption on Anthocyanin Accumulation:
Results from Figure 6B show altitude adaption impacts anthocyanin accumulation as shown by Col-0 accumulating higher anthocyanin levels to that of Sha. This difference in anthocyanin accumulation between the lines I believe is due to Col-0 being more adapted in coping with photosynthetic stress. As one of anthocyanin's prime roles is to protect the photosynthetic machinery of plants from excess light through absorbing blue and reflecting red light (Bac-Molenaar *et al.,* 2015; Zhang *et al.,* 2010), the production of anthocyanin's is beneficial to plants that are undergoing periods of high light that may cause photo-oxidative damage. I hypothesise that Sha is undergoing photo oxidative as a result of greater ERFVII destabilisation and PCH overaccumulation compared to that of Col-0, with the greater ROS production in Sha being to be due to the hypersensitivity of the Sha ERFVIIs. The amount of ROS in Sha's cotyledons greatly exceeds that of Col-0's, as shown in Figure 5C+D. As Sha has extremely high ROS levels with these levels being unquenchable by anthocyanin, I believe this is why see the reddening colour in Sha is absent. I believe in Sha the ROS levels are too high, and therefore unrecoverable, and chlorosis is already occurring in the cotyledons ahead of anthocyanin production. However, in Col-0 the ROS levels are not as excessive and are able recoverable, with the ROS to being quenched in part through anthocyanin production. I hypothesise that despite ERFVII destabilisation impacting PCH and ROS accumulation, anthocyanin accumulation is not also controlled through ERFVII accumulation and destabilisation. Anthocyanin is rather being produced as a response to the ROS production, which is being controlled through ERFVIIs.

As Sha is adapted at an altitude of 3400 masl, the atmosphere in which Sha is grown at is much thinner atmosphere meaning less UV light will be filtered. For every 1000 metres increase in altitude, UV levels increase by ~10-12%. This means that the conditions in which Sha is adapted to contain an extra 30-40% of UV light compared to that of Col-0. This is important as the lights used in these experiments to analyse Sha are emitting white light with minimal UV emissions. Anthocyanins are essential in sensing photosynthetic damage through protecting against the excess exposure to UV-B (Bac-Molenaar *et al.,* 2015; Zhang *et al.,* 2010). As Sha is normally grown in levels where there are higher amounts of UV-B due to the thinner atmosphere, this means that at the comparatively lower levels of UV-B exposure in the light source used during these experiments Sha may not sufficiently recognise the light signal to produce anthocyanin, despite the occurrence of ROS, hence the lower anthocyanin levels shown in Figure 6B.

4.05 Impact of Altitude Adaption on Phenotype of Seedlings:
Results from Figure 6C show altitude adaption has a significant impact on the phenotype of seedlings. Figure 6C shows that Sha had a much higher percentage of "Arrested growth" and "Yellow" phenotype than that of Col-0. The arrested growth phenotype is in part a result of anthocyanin accumulation in the seedlings as described in 4.04. I believe Sha has an increased anthocyanin accumulation because anthocyanin is a ROS scavenger. I

hypothesise that due to ERFVII hypersensitivity Sha has elevated levels of ROS compared to WT (4.01), I believe this is why there are higher levels of anthocyanin and thus the reddening phenotype. However, this does contradict results in Figure 6B where Sha was seen to have a lower anthocyanin accumulation in comparison to Col-0 at this intensity. The results taken in Figure 6C are evaluating the phenotype of the plants, so even though Col-0 may produce higher amounts of anthocyanin than Sha, the anthocyanin production in Col-0 was successful in quenching ROS and preventing further damage to the plant and preventing chlorosis; meaning the resultant greening and chlorophyll production was overriding to that of anthocyanin and the "Green" phenotype resulted.

I hypothesise the increased yellow phenotype in Sha compared to WT comes from an increased amount of chlorosis. ERFVIIs restrict the accumulation of ROS through controlling PCH accumulation and converting PCH to chlorophylls (Abbas *et al.,* 2015). When ERFVIIs have such high amounts of destabilisation as is occurring in Sha, this results in excess PCH accumulation. When there is excess PCH accumulation, the production of ROS is favoured to that of conversion to chlorophyll. Large ROS accumulation results in chlorosis and yellowing phenotype of cotyledons, as is shown in Sha (Figure 6C). I propose that whilst ROS is still being produced in Col-0, the levels are much lower in Col-0 due to Col-0 having increased ERFVII stability; restricting the accumulation of PCH and thus reduces the amount of ROS production. Hence, the much lower percentage of yellowing phenotype shown in comparison to Sha (Figure 6C). Col-0 also shows a much greater percentage of the "Green" phenotype compared to that of Sha. This is because with the reduced PCH accumulation, conversion of PCH to chlorophyll is favoured to conversion to ROS, which then results in the green colour of the cotyledons.

4.06 Impact of Altitude Adaption on Survival Rates of Seedlings:

Results from Figure 7E suggest that adaption to altitude does not impact survival rates of seedlings. For both Col-0 and Sha there was a decrease in survival as etiolation period was extended. As the time of etiolation is extended I this results in an increased amount of PCH accumulation, and thus ROS accumulation. It is this over accumulation of ROS that triggers necrosis and programmed cell death (PCD), resulting in a decrease in survival (Breusegem and Dat, 2006). There were not large differences in survival between Col-0 and Sha throughout changing periods of etiolation and light intensity. This suggests that despite Sha not being suitably adapted to normoxia and accumulating more ROS (Figure 5A-C), the elevated levels of ROS accumulated are not high enough to trigger necrosis and PCD, and the seedling is able to recover. The elevated ROS levels are only enough to trigger chlorosis, hence the difference in phenotype between the lines shown in Figure 6C where there is a far increased number of "yellow" seedlings. However, after a period of 7 days there is a drastic drop in survival for both WT and Sha to below 50% (Figure 6D). As there is little difference between Col-0 and Sha, I believe this drastic drop in survival is independent of adaption to altitude and proposed hypersensitivity of ERFVIIs and resultant stability, and is a result of the lack of photosynthetic activity to produce the ATP required for metabolic function.

4.07 Impact of Hyperoxia on ERFVIIs and Development of ROS Accumulation and Formation

Increasing oxygen concentration from normoxic (21%) to hyperoxic (27%) levels impacted ROS production, as shown in Figure 7A+B. As oxygen concentration increased, ROS production increased for almost all of lines, shown by the increasing intensity of the green ROS stain between the normoxic lines in Figure 7A and the hyperoxic lines in Figure 7B. I believe this increased ROS production is a result of destabilised ERFVIIs. As oxygen concentration increases, Cys oxidation of ERFVIIs also increases. Increased oxidation results in increased destabilisation and degradation of these ERFVIIs via the PRT6 N-

degron pathway. ERFVII stabilisation aids in dictating PCH accumulation and resultant ROS formation (Abbas *et al.,* 2015). In hyperoxia it is the increased oxygen concentration that is directly oxidising the Cys residue at the N-terminus of the ERFVII, resulting in its degradation via the PRT6 N-degron pathway and thus elevating PCH/ROS levels.

ROS levels during hyperoxia showed the greatest increase in Sha (Figure 7A+B). Sha already had elevated levels of ROS in comparison to WT due to the already destabilised nature of Sha's ERFVIIs during normoxia. However, following exposure to hyperoxic conditions ROS levels increase further. As shown by Sha's high ROS levels even at normoxia, this suggests that Sha's ERFVIIs are hypersensitive to Cys oxidation and resultant degradation by the 26S proteasome. When oxygen levels are increased to 27% it means that further Cys oxidation of ERFVIIs is taking place, resulting in degradation of Sha's ERFVIIs and increased PCH/ROS levels. This hypersensitivity of Sha's ERFVIIs to oxygen and resulting Cys oxidation is why the increase in oxygen concentration from 21% to 27% has such a considerable effect on ROS production in comparison to WT, where there is some increase in ROS production, but it is not as considerable of an increase compared to that of Sha.

Bdm's natural habitat is being grown in mesic grass and scrub land, meaning it is surrounded by shrubs, grasses, and herbs. In these conditions there is lots of competition for light due to the tall shrubbery surrounding the *A. thaliana*. As Bdm is from this elevated altitude it was hypothesised that Bdm's ERFVIIs would be more sensitive to elevated levels of oxygen resulting in increased Cys oxidation and elevated PCH and ROS production. However, ROS levels remain low and consistent throughout the varying oxygen concentrations (v/v) (Figure 7A-C). During this experiment Bdm was placed into light conditions of 460 µE m^{-2} s^{-1}. These light conditions are much higher than that of what would be experienced in the outside environment. These light conditions were also constant unlike in the outside environment where there are both periods of light and darkness. Bdm is adapted to being grown in a low light environment with great amount of competition for light. The POR enzyme required for the conversion of PCH to chlorophyllide, and continue the chlorophyll tetrapyrrole production pathway, is activated by light (Fujita and Bauer, 2000). It is possible that as Bdm has adapted to being grown in a low light environment, that following transfer to conditions where there are high light the POR enzyme is markedly activated and converts the excess amounts of PCH to chlorophyllide and continues the chlorophyll biosynthesis pathway, as shown by the high amounts of chlorophyll formed shown in Figure 7C. This means that despite the ERFVIIs in Bdm expected to be destabilised at these hyperoxic and high light conditions, Bdm is adapted to deal with excess amounts of PCH and ROS and convert this to chlorophyll through the adaption of heightened activity of the POR enzyme. Results from Figure 7A-C suggest ERFVII hypersensitivity and responsiveness varies between adaption to altitude between accessions, and surrounding oxygen concentration impacts accessions uniquely. Accessions such as Bdm where high ROS production may be expected to be high show low production, demonstrating that there may be other factors other than surrounding oxygen concentration that may influence ERFVII stability, as well as factors other than ERFVIIs may be important in controlling ROS accumulation.

4.08 The Impact of Hyperoxia on ERFVIIs and Chlorophyll Accumulation:

Hyperoxia was shown to decrease chlorophyll accumulation, as shown in Figure 8D. I propose that lower levels of chlorophyll during hyperoxia shown in Figure 8D arise from excessive PCH accumulation. During this experiment, the below ground environment was simulated with an extended period of total darkness of 6 days. However, this period of total darkness was also coupled with the seedlings being grown in a hyperoxic oxygen chamber with surrounding oxygen at 27%. These are opposing signals for below ground development, as when the seedling undergoes an extended period of total darkness below ground this is often coupled with lowered oxygen concentrations. During this extended

period of darkness, I propose the ERFVIIs of accessions within the hyperoxic chamber would have increased destabilisation to that of those grown in normoxia. Destabilisation of ERFVIIs restricts the ability of the seedling to control PCH accumulation (Abbas *et al.,* 2015). Following excess PCH accumulation, the tetrapyyrole pathway favours ROS production over conversion of PCH to chlorophyllide; hence, why chlorophyll levels are lower during hyperoxia.

4.09 The Impact of Hyperoxia on Anthocyanin Accumulation:

Figure 8E shows relative anthocyanin accumulation between accessions grown in normoxia and hyperoxia. Figure 8E shows unexpected results, with anthocyanin levels varying heavily between accessions and between both normoxia and hyperoxia. For all lines it was hypothesised that during hyperoxia anthocyanin levels would increase compared to normoxia. It was hypothesised that increased destabilisation of ERFVIIs during hyperoxia would result in higher PCH and ROS accumulation, and thus require more anthocyanin quench additional ROS. This was true for Sha and Bdm, but was not the case for WT. For WT, higher levels of anthocyanin were shown in normoxia than in hyperoxia.

Results in Figure 8E contradict those from Figure 8D where Col-0's chlorophyll results where chlorophyll levels were higher in hyperoxia than in normoxia. It would be predicted that as more chlorophyll was being produced during normoxia, it would be expected that ROS levels would be lower as the increased chlorophyll levels suggest that following transfer to light the PCH accumulated during darkness would be favoured to be converted to chlorophyll rather than to ROS. As a key role of anthocyanin is to quench ROS, it was hypothesised that anthocyanin levels would increase for all lines. However, anthocyanins are also responsible for other stresses, such as light stress. The difference in anthocyanin accumulation between accessions may be due to each individual accession's response to the high light (460 µE m^{-2} s^{-1}) placed in following complete darkness**.** However, this does not account as to why anthocyanin levels varied between normoxia and hyperoxia. These results must be repeated further to understand whether they are accurate, and if the same is true for a wider range of accessions.

4.10 Stability of RAP2.3 Impacts PCH Accumulation

The difference in PCH accumulation between Sha and *promRAP2.3:MA-RAP2.3:GUS* in Sha in Figure 8 confirms the role of RAP2.3's role in controlling PCH accumulation. For all *promRAP2.3:MA-RAP2.3:GUS* in Sha lines PCH accumulation was significantly lower. The only difference between Sha and *promRAP2.3:MA-RAP2.3:GUS* in Sha is the MA in *the promRAP2.3:MA-RAP2.3:GUS* lines is a stabilising residue and results in the RAP2.3 protein remaining stable and is not degraded via the PRT6 N-degron pathway. As this is the only difference between the lines, and this results in a drastic difference in PCH results, this provides confirmation that the stabilisation of RAP2.3 protein results in reduced PCH accumulation.

The Sha *prt6* line also shows significantly lower PCH levels to that of Sha (Figure 8). The Sha *prt6* (back crossed 8 times to Sha) is a mutant line of Sha that lacks the N-recognin E3 ligase PRT6 meaning degradation of ERFVIIs via the PRT6 N-degron pathway does not take place and ERFVIIs remain stable. In Sha *prt6* the stabilisation of ERFVIIs results in significantly lower PCH accumulation, once again providing confirmation of stabilised ERFVIIs role in restricting PCH accumulation. PCH levels in Sha *prt6* show no significant difference to that of the *promRAP2.3:MA-RAP2.3:GUS* in Sha lines. The difference between Sha *prt6* and *promRAP2.3:MA-RAP2.3:GUS* in Sha lines is that in *promRAP2.3:MA-RAP2.3:GUS* it is only the RAP2.3 that is a stabilised ERFVII, whereas in Sha *prt6* all ERFVIIs are unable to be degraded via the PRT6 N-degron pathway. However, despite only RAP2.3 being stable in *promRAP2.3:MA-RAP2.3:GUS* in Sha, there is no significant

difference as to when all ERFVIIs are stable. This suggests that RAP2.3 is the predominant ERFVII responsible in restricting PCH accumulation when stabilised, as even when other ERFVIIs are destabilised in *promRAP2.3:MA-RAP2.3:GUS* in Sha, PCH levels are not significantly different as to when all ERFVIIs are stable in Sha *prt6*. However, the potential role of other stabilised ERFVIIs in also reducing PCH accumulation must not be overlooked and must be further investigated.

4.11 Gene expression of RAP2.3 under its Promoter is Influenced by Etiolation and Light Availability to Mediate Skotomomorphogenic Response

Results from Figure 9 show GUS staining for both the *promRAP2.3:MA-RAP2.3:GUS* in Sha and *promRAP2.3:MC-RAP2.3:GUS* in Sha lines. Results show the presence of GUS staining at 5 days in light, whereas for the *promRAP2.3:MC-RAP2.3:GUS* line there is no blue staining. This shows that RAP2.3 is being expressed in *promRAP2.3:MA-RAP2.3:GUS* lines in light whereas it is not being expressed following the same treatment for *promRAP2.3:MA-RAP2.3:GUS*. However, there is only very limited amounts of GUS staining for the *promRAP2.3:MA-RAP2.3:GUS* line after 5 days in light, suggesting that even though the RAP2.3 gene is being expressed, it is at very low levels is only at the tip of the cotyledon. I hypothesise that the low level of RAP2.3 gene expression is because RAP2.3's primary role is in hypoxia response, and during this experiment *promRAP2.3:MA-RAP2.3:GUS* in Sha seedlings were grown in normoxia. Gene expression of RAP2.3 under its promoter is also low following 7 days of light treatment for the *promRAP2.3:MA-RAP2.3:GUS* line, where there is also small amounts of staining and gene expression (Figure 9).

Results show the highest amount of GUS staining in the *promRAP2.3:MA-RAP2.3:GUS* line after 7 days of etiolation (Figure 9). For both Line 1 and Line 2 of *promRAP2.3:MA-RAP2.3:GUS* there is a deep blue stain throughout the entire cotyledon, indicating high expression of RAP2.3 under its promoter. The highest amount of expression in which *promRAP2.3:MC-RAP2.3:GUS* in Sha showed expression of RAP2.3 under its promoter was also after 7 days of darkness. Results here suggest that exposing *promRAP2.3:MC-RAP2.3:GUS* line to 7 days of darkness increased expression of RAP2.3 under its promoter. With RAP2.3 expression being the highest at 7 days of darkness this shows that light availability plays a in dictating expression of RAP2.3 under its promoter.

During below ground during skotomorphogenesis, RAP2.3 is known to mediate apical hook opening (la Rosa *et al.,* 2014). RAP2.3 is involved in the mechanism with GA and ethylene to prevent premature opening of the apical hook during darkness (Abbas *et al.,* 2013; la Rosa *et al.,* 2014). This means that inducing expression of RAP2.3 following the longer period of darkness (7 days) will help prevent this premature opening of the apical hook. During below ground skotomorphogenesis, oxygen concentration may not always be as hypoxic as expected with surrounding oxygen concentration being dependent on the type and density of soil surrounding the seedling. ERFVII stability also being determined by light intensity may provide an additional another external signal to induce expression of RAP2.3 below ground, to prevent the premature opening of the apical hook during the darkness of skotomorphogenesis. However, there is little difference in RAP2.3 expression between the 5 days of light and the 5 days of darkness. I believe that is because that whilst light intensity may be a factor in dictating expression of RAP2.3 under its promoter, there needs to be a sustained period of darkness in order to enhance RAP2.3 expression substantially.

4.12 Future Work and Development with C^2-RAP2.12 and A^2-RAP2.12 *in vivo* in *A. thaliana*

Following the development of the C^2-RAP2.12 and A^2-RAP2.12 transgenic tools Next, *A. thaliana* accessions must be transformed to place these C^2-RAP2.12 and A^2-RAP2.12 transgenes *in vivo* to analyse their expression. *A. tumefaciens* mediated transformation should be carried out to convert the transgenes *in vivo* to *A. thaliana*. Following conversion *in vivo* further experiments relating to stability of RAP2.12 may be carried out. Western blotting should be used to analyse and compare stability between C^2-RAP2.12 and A^2-RAP2.12, with samples being able to be taken from actual plant material. Results are expected to be the same as *in vitro*, with plants containing A^2-RAP2 showing stability of RAP2.12 throughout the entire time course (0, 30, 120 minutes), and plant material from C^2-RAP2.12 being degraded via the PRT6 N-degron pathway.

Following confirmation of stability, transformed *A, thaliana* plants can be used in future experiments. Hypoxia tolerance can be investigated for C^2-RAP2.12, evaluating at what oxygen concentration stability of RAP2.12 occurs at and is no longer degraded by the PRT6 N-degron pathway. The stable A^2-RAP2.12 transgenic plants can also be used in a wide variety of experiments, removing the need for a hypoxia treatment to stabilise C^2-RAP2.12. Through the development of A^2-RAP2.12, the stable RAP2.12 allows for either a comparison of molecular pathways and phenotype to that of C^2-RAP2.12 and can be used to analyse RAP2.12 directly, and the effect that stabilisation has on the plant *in vivo*. This will be particularly important in investigating strategies to deal with flooding and submergence tolerance, where RAP2.12 also remains stable. As I have developed the transgene of the stable A^2-RAP2.12 this can now be placed into other *A. thaliana* accessions and the effects studied. For example, this construct can now be placed into accessions from various altitudes such as Sha in order to stabilise RAP2.12 at normoxic oxygen concentrations, and further investigate potential functions of the stabilisation of RAP2.12 during hypoxia.

Chapter Five:

Conclusion

5.01 Impact of Results:

The principle aim of this thesis was to investigate how altitudes from varying accessions have adapted to altitude, and throughout this thesis this has been confirmed. Results throughout this thesis have also shown that plants sense and adapt to the altitude that they grow at. Through work described throughout all experiments, it shows hypersensitivity of high altitude accessions (such as Sha) ERFVIIs to degradation via the PRT6 N-degron pathway. Even when grown in the same conditions as WT, Sha consistently shows results and phenotypes indicating the increased destabilisation of ERFVIIs. As plants were grown in the same conditions yet Sha showed results indicating increased destabilisation, this suggests that Sha has adapted to its growth at high altitude conditions with decreased oxygen concentration (v/v) in order for it to be effectively to be able to respond to changes in oxygen concentration at high altitudes. This suggests that plants have some sort of "altimeter" where they direct development in order to effectively respond to the elevated altitude and decreased oxygen concentration. However, in future research I would like to use other high-altitude accessions (e.g Sne and Vaz-0) in order to confirm this, as these lines would also show increased ERFVII destabilisation when grown at normoxia (27% v/v). Analysis of direct ERVII activity and levels must also be used in future experiments, as currently the direct impact of altitude on ERFVII stabilisation can only be hypothesised through the phenotypes associated with increased ERFVII destabilisation.

Results also confirm the essential role of RAP2.3 in the chlorophyll tetrapyrrole pathway. Prior results confirmed the general role of ERFVIIs in the chlorophyll tetrapyrrole pathway (Abbas *et al.,* 2015), but results here (Figure 8) confirm the specific role of stabilised RAP2.3 in controlling and reducing PCH accumulation. I hereby show the essential role of RAP2.3 in reducing and controlling PCH (and resultant ROS) accumulation, as if PCH accumulation is not controlled then health and survival of seedlings drastically suffers (Figure 6).

I have also developed transgenic tools that will be essential in further investigations of ERFVIIs. The transformation of C^2-RAP2.12 and A^2-RAP2.12 in vivo will provide a unique ability to analyse RAP2.12 stability, even during normoxia, which provides an invaluable tool to further analyse RAP2.12's importance in flooding where RAP2.12 also remains stable. The development of promRAP2.3:MA-RAP2.3:GUS and promRAP2.3:MA-RAP2.3:GUS lines allows for the ability to further analyse the activity of RAP2.3 and the result of its stability. Once again this provides a tool to analyse the role of RAP2.3 in hypoxia tolerance, as well as further investigating RAP2.3's role in PCH accumulation, as confirmed in Figure 8.

5.02 Limitations of Results:

One limitation of the results presented is the experimental design of only taking images and measuring results of young seedlings that were not older than 15 days. Following long term exposure to conditions seedlings may make a recovery, so the actual impact

of the changes in ROS, chlorophyll, anthocyanin and survival may only be temporary, and not impact seedling development and growth in the long term. Therefore, longer duration of time should be elapsed in future experiments before measurements are taken.

Another limitation of the results is that much of the changes in seedling development are attributed to ERFVIIs and their hypothesised hypersensitivity. However, in Figures 5-7 ERFVII levels and activity are not directly assessed. Despite results (high ROS levels) being typical of that of ERFVII destabilisation (Abbas et al., 2015), the conclusion that the results being solely due to proposed ERFVII destabilisation and hypersensitivity cannot be confirmed.

5.03 Future Research:

A key discovery throughout this thesis was the presence of plants containing an "altimeter", adapting to the altitude and surrounding oxygen availability in which they are grown at. The uncovering of this may provide a novel approach to improve food production and contribute towards ensuring global food security. Further understanding and harnessing of the mechanism behind altitude adaptation through hypersensivity of ERFVIIs may allow ERFVIIs to be manipulated to enable adaption of crops to growth at high altitudes. Mountains cover 25% of the worlds land surface and support approximately 12% of the world's population (FAO, 2015). However, currently growth of crops on mountains is uncommon due to yield being low as the crops are not suitably adapted to the environment. Manipulation of hypersensitivity of ERFVIIs will offer a new approach to growing crops at these previously non arable conditions. Root vegetables such as potatoes have been shown to grow well at high altitude due to optimal temperatures and growth conditions. These therefore offer the prime future targets for manipulation of ERFVIIs to further enhance yield and productivity of these vegetables. In future experiments other food crops such may also be targeted for adaption to be able to grow at altitude, however it is not just oxygen concentration that differs at altitude, other conditions such as temperature and soil structure are often vastly different. This means that correct selection of target crop species must be ensured to make sure the chosen crop species is able to grow in other biotic and abiotic factors, even if the crop is adapted to the oxygen concentration in which it can be grown at.

However, the most notable application of N-degron pathway research remains to be translating work done on hypoxia tolerance into manipulating crop tolerance to submergence and flooding events. Predictions suggest that in order to ensure food security there needs to be a doubling of agricultural productivity within the next two decades (Tester and Langridge, 2010). Achieving this level of agricultural productivity is becoming increasingly difficult due to the increased frequency of severe and unpredictable weather conditions such as flash floods (Bailey-Serres et al., 2012). Work displayed throughout this project enhance understanding ERFVII related plant development and potential transgenic routes to crop improvement to enhance hypoxia tolerance. If this work is successfully translated to high yielding crop species, such as wheat and barley, then this has potential to be a huge boost to ensuring global food security and ensuring the United Nations Millennium Development Goal of "eradicating extreme poverty and hunger and ensure environmental sustainability". Other benefits from successful translation of this work into high yielding crop species include: direct economic benefits to farmers by improving crop yields, maintaining stable crop prices for consumers, and reduction of dependency on subsidies for farmers.

Chapter Six:

References

Aarti, P.D., Tanaka, R., Tanaka, A., (2006) Effects of oxidative stress on chlorophyll biosynthesis in cucumber (Cucumis sativus) cotyledons. *Physiologia Plantarum* 128: 186–197.

Abbas, M., Alabadí, D., Blázquez, M.A., (2013) Differential growth at the apical hook: all roads lead to auxin. *Frontiers in Plant Science* 4: 441.

Abbas, M., Berckhan, S., Rooney, D.J., Gibbs, D.J., Vicente Conde, J., Sousa Correia, C., Bassel, G.W., Marín-de la Rosa, N., León, J., Alabadí, D., Blázquez, M.A., Holdsworth, M.J., (2015) Oxygen Sensing Coordinates Photomorphogenesis to Facilitate Seedling Survival. *Current Biology* 25: 1483–1488.

Achard, P., Baghour, M., Chapple, A., Hedden, P., Van Der Straeten, D., Genschik, P., Moritz, T., Harberd, N.P., 2007. The plant stress hormone ethylene controls floral transition via DELLA-dependent regulation of floral meristem-identity genes. *Proceedings of the National Academy of Sciences of the United States of America* 104: 6484–6489.

Ádám, A.L., Nagy, Z.Á., Kátay, G., Mergenthaler, E., Viczián, O., (2018) Signals of Systemic Immunity in Plants: Progress and Open Questions. *International Journal of Molecular Sciences* 19.

Aksnes, H., Drazic, A., Marie, M., Arnesen, T., (2016) First Things First: Vital Protein Marks by N-Terminal Acetyltransferases. *Trends in Biochemical Sciences* 41: 746–760.

An, F., Zhang, X., Zhu, Z., Ji, Y., He, W., Jiang, Z., Li, M., Guo, H., (2012) Coordinated regulation of apical hook development by gibberellins and ethylene in etiolated Arabidopsis seedlings. Cell Research. 22: 915–927.

Apel, K., Hirt, H., (2004) Reactive oxygen species: metabolism, oxidative stress, and signal transduction. Annual Review of Plant Biology 55: 373–399.

Archacki, R., Buszewicz, D., Sarnowski, T.J., Sarnowska, E., Rolicka, A.T., Tohge, T., Fernie, A.R., Jikumaru, Y., Kotlinski, M., Iwanicka-Nowicka, R., Kalisiak, K., Patryn, J., Halibart-Puzio, J., Kamiya, Y., Davis, S.J., Koblowska, M.K., Jerzmanowski, A., (2013) BRAHMA ATPase of the SWI/SNF chromatin remodeling complex acts as a positive regulator of gibberellin-mediated responses in arabidopsis. *PLoS ONE* 8: 585-588.

Aristov, Yu.I., Restuccia, G., Tokarev, M.M., Buerger, H.-D., Freni, A., (2000) Selective Water Sorbents for Multiple Applications. 11. CaCl2 Confined to Expanded Vermiculite. *Reaction Kinetics and Catalysis Letters* 71: 377–384.

Armstrong, W., Strange, M., Cringle, S., Beckett, P., (1994) Microelectrode and Modeling Study of Oxygen Distribution in Roots. *Annals of Botany* 74: 287–299.

Armstrong, W., Webb, T., Darwent, M., Beckett, P.M., (2009) Measuring and interpreting respiratory critical oxygen pressures in roots. *Annals of Botany* 103: 281–293.

Arnell, N.W., Brown, S., Gosling, S.N., Gottschalk, P., Hinkel, J., Huntingford, C., Lloyd-Hughes, B., Lowe, J.A., Nicholls, R.J., Osborn, T.J., Osborne, T.M., Rose, G.A., Smith, P., Wheeler, T.R., Zelazowski, P., (2016) The impacts of climate change across the globe: A multi-sectoral assessment. *Climatic Change* 134: 457–474.

Asada, K., (1994) Production and action of active oxygen species in photosynthetic tissues. Causes of photooxidative stress and amelioration of defense systems in plants. 77-104.

Bachmair, A., Finley, D., Varshavsky, A., (1986) In vivo half-life of a protein is a function of its amino-terminal residue. Science *234*: 179–186.

Bac-Molenaar, J.A., Fradin, E.F., Rienstra, J.A., Vreugdenhil, D., Keurentjes, J.J.B., (2015) GWA Mapping of Anthocyanin Accumulation Reveals Balancing Selection of MYB90 in Arabidopsis thaliana. *PLoS ONE* 10: 143-212.

Bailey-Serres, J., Lee, S.C., Brinton, E., (2012) Waterproofing Crops: Effective Flooding Survival Strategies. *Plant Physiology* 160: 1698–1709.

Bailey-Serres, J., Voesenek, L. a. C.J., (2008) Flooding stress: acclimations and genetic diversity. *Annual Review of Plant Biology* 59: 313–339.

Baskin, J.M., Baskin, C.C., (2004) A classification system for seed dormancy. *Seed Science Research* 14: 1–16.

Bechtold, N., Pelletier, G., (1998) In planta Agrobacterium-mediated transformation of adult Arabidopsis thaliana plants by vacuum infiltration. *Methods in Molecular Biology* 82: 259–266.

Beligni, M.V., Lamattina, L., (2000) Nitric oxide stimulates seed germination and de-etiolation, and inhibits hypocotyl elongation, three light-inducible responses in plants. *Planta* 210: 215–221.

Bent, A., (2006) Arabidopsis thaliana floral dip transformation method. *Methods in Molecular Biology* 343: 87–103.

Bethke, P.C., Gubler, F., Jacobsen, J.V., Jones, R.L., (2004) Dormancy of Arabidopsis seeds and barley grains can be broken by nitric oxide. *Planta* 219: 847–855.

Bethke, P.C., Libourel, I.G.L., Aoyama, N., Chung, Y.-Y., Still, D.W., Jones, R.L., (2007) The Arabidopsis aleurone layer responds to nitric oxide, gibberellin, and abscisic acid and is sufficient and necessary for seed dormancy. *Plant Physiology* 143: 1173–1188.

Bigham, A.W., Lee, F.S., (2014) Human high-altitude adaptation: forward genetics meets the HIF pathway. *Genes & Development* 28: 2189–2204.

Borisjuk, L., Rolletschek, H., (2009) The oxygen status of the developing seed. *New Phytologist* 182: 17–30.

Brahimi-Horn, C., Mazure, N., Pouysségur, J., (2005) Signalling via the hypoxia-inducible factor-1alpha requires multiple posttranslational modifications. *Cell Signalling* 17: 1–9.

Branco-Price, C., Kaiser, K.A., Jang, C.J.H., Larive, C.K., Bailey-Serres, J., (2008) Selective mRNA translation coordinates energetic and metabolic adjustments to cellular oxygen deprivation and reoxygenation in Arabidopsis thaliana. *The Plant Journal* 56: 743–755.

Breusegem, F.V., Dat, J.F., (2006) Reactive Oxygen Species in Plant Cell Death. *Plant Physiology* 141: 384–390.

Bruick, R.K., (2003) Oxygen sensing in the hypoxic response pathway: regulation of the hypoxia-inducible transcription factor. *Genes & Development* 17: 2614–2623.

Bui, L.T., Giuntoli, B., Kosmacz, M., Parlanti, S., Licausi, F., (2015) Constitutively expressed ERF-VII transcription factors redundantly activate the core anaerobic response in Arabidopsis thaliana. Plant *Science* 236: 37–43.

Chang, K.N., Zhong, S., Weirauch, M.T., Hon, G., Pelizzola, M., Li, H., Huang, S.-S.C., Schmitz, R.J., Urich, M.A., Kuo, D., Nery, J.R., Qiao, H., Yang, A., Jamali, A., Chen, H., Ideker, T., Ren, B., Bar-Joseph, Z., Hughes, T.R., Ecker, J.R., (2013) Temporal transcriptional response to ethylene gas drives growth hormone cross-regulation in Arabidopsis. *eLife* 2: 675.

Chen, S.-J., Wu, X., Wadas, B., Oh, J.-H., Varshavsky, A., (2017) An N-end rule pathway that recognizes proline and destroys gluconeogenic enzymes. *Science* 355.

Clough, S.J., Bent, A.F., (1998) Floral dip: a simplified method for Agrobacterium-mediated transformation of Arabidopsis thaliana. *The Plant Journal* 16: 735–743.

Colmer, T.D., Voesenek, L. a. C.J., (2009) Flooding tolerance: suites of plant traits in variable environments. *Functional Plant Biology* 36: 665–681.

Cutler, S.R., Rodriguez, P.L., Finkelstein, R.R., Abrams, S.R., (2010) Abscisic acid: emergence of a core signaling network. *Annual Review of Plant Biology* 61: 651–679.

Davydov, I.V., Varshavsky, A., (2000) RGS4 is arginylated and degraded by the N-end rule pathway in vitro. *Journal of Biological Chemistry* 275: 22931–22941.

Dawood, T., Rieu, I., Wolters-Arts, M., Derksen, E.B., Mariani, C., Visser, E.J.W., (2014) Rapid flooding-induced adventitious root development from preformed primordia in Solanum dulcamara. *AoB Plants* 6.

de Marchi, R., Sorel, M., Mooney, B., Fudal, I., Goslin, K., Kwaśniewska, K., Ryan, P.T., Pfalz, M., Kroymann, J., Pollmann, S., Feechan, A., Wellmer, F., Rivas, S., Graciet, E., (2016) The N-end rule pathway regulates pathogen responses in plants. *Scientific Reports* 6: 26020.

Denton, M.L., Schuster, K.J., Rockwell, B.A., (2006) Accurate measure of laser irradiance threshold for near-infrared photo-oxidation with a modified confocal microscope. *Journal of Microscopy* 221: 164–171.

Desikan, R., Griffiths, R., Hancock, J., Neill, S., (2002) A new role for an old enzyme: nitrate reductase-mediated nitric oxide generation is required for abscisic acid-induced stomatal closure in Arabidopsis thaliana. *Proceedings of the National Academy of Sciences of the United States of America* 99: 16314–16318.

Desjardins, P., Conklin, D., (2010) NanoDrop Microvolume Quantitation of Nucleic Acids. *Journal of Visualized Experiments.*

Dissmeyer, N., (2017) Conditional Modulation of Biological Processes by Low-Temperature Degrons. *Methods in Molecular Biology* 1669: 407–416.

Domingos, P., Prado, A.M., Wong, A., Gehring, C., Feijo, J.A., (2015) Nitric Oxide: A Multitasked Signaling Gas in Plants. *Molecular Plant Cell Signaling* 8: 506–520.

Dougan, D.A., Micevski, D., Truscott, K.N., (2012) The N-end rule pathway: From recognition by N-recognins, to destruction by AAA+proteases. *Biochimica et Biophysica Acta* 1823: 83–91.

Drew, M.C., (1997) OXYGEN DEFICIENCY AND ROOT METABOLISM: Injury and Acclimation Under Hypoxia and Anoxia. *Annual Review of Plant Biology* 48: 223–250.

Drew, M.C., He, C.J., Morgan, P.W., (2000) Programmed cell death and aerenchyma formation in roots. *Trends in Plant Science* 5: 123–127.

Duplan, V., Rivas, S., (2014) E3 ubiquitin-ligases and their target proteins during the regulation of plant innate immunity. *Frontiers in Plant Science* 5: 42.

Durst, R.A., Staples, B.R., (1972) Tris-tris-HCl: a standard buffer for use in the physiologic pH range. *Clinical Chemistry* 18: 206–208.

Eckardt, N.A., (2007) GA Signaling: Direct Targets of DELLA Proteins. *The Plant Cell* 19: 2970.

Efroni, I., Han, S.-K., Kim, H.J., Wu, M.-F., Steiner, E., Birnbaum, K.D., Hong, J.C., Eshed, Y., Wagner, D., (2013) Regulation of leaf maturation by chromatin-mediated modulation of cytokinin responses. *Developmental Cell* 24: 438–445.

Eysholdt-Derzsó, E., Sauter, M., (2017) Root Bending Is Antagonistically Affected by Hypoxia and ERF-Mediated Transcription via Auxin Signaling1. *Plant Physiology* 175: 412–423.

Finley, D., Ulrich, H.D., Sommer, T., Kaiser, P., (2012) The ubiquitin-proteasome system of Saccharomyces cerevisiae. *Genetics* 192: 319–360.

Frigerio, M., Alabadí, D., Pérez-Gómez, J., García-Cárcel, L., Phillips, A.L., Hedden, P., Blázquez, M.A., (2006) Transcriptional regulation of gibberellin metabolism genes by auxin signaling in Arabidopsis. *Plant Physiology* 142: 553–563.

Fujita, Y., Bauer, C.E., (2000) Reconstitution of Light-independent Protochlorophyllide Reductase from Purified Bchl and BchN-BchB Subunits IN VITRO CONFIRMATION OF NITROGENASE-LIKE FEATURES OF A BACTERIOCHLOROPHYLL BIOSYNTHESIS ENZYME. *Journal Biological Chemistry* 275: 23583–23588.

Fukao, T., Bailey-Serres, J., (2008) Submergence tolerance conferred by Sub1A is mediated by SLR1 and SLRL1 restriction of gibberellin responses in rice. *Proceedings of the National Academy of Sciences of the United States of America* 105: 16814–16819.

Fukao, T., Xu, K., Ronald, P.C., Bailey-Serres, J., (2006) A variable cluster of ethylene response factor-like genes regulates metabolic and developmental acclimation responses to submergence in rice. *Plant Cell* 18: 2021–2034.

Fukao, T., Yeung, E., Bailey-Serres, J., 2011. The submergence tolerance regulator SUB1A mediates crosstalk between submergence and drought tolerance in rice. *Plant Cell* 23, 412–427.

Ganguly, A., Lee, S.H., Cho, M., Lee, O.R., Yoo, H., Cho, H.-T., (2010) Differential auxin-transporting activities of PIN-FORMED proteins in Arabidopsis root hair cells. *Plant Physiology* 153: 1046–1061.

Garriga, M., Retamales, J.B., Romero-Bravo, S., Caligari, P.D.S., Lobos, G.A., (2014) Chlorophyll, anthocyanin, and gas exchange changes assessed by spectroradiometry in Fragaria chiloensis under salt stress. *Journal of Integrative Plant Biology* 56: 505–515.

Garzón, M., Eifler, K., Faust, A., Scheel, H., Hofmann, K., Koncz, C., Yephremov, A., Bachmair, A., 2007. PRT6/At5g02310 encodes an Arabidopsis ubiquitin ligase of the N-end rule pathway with arginine specificity and is not the CER3 locus. *FEBS Letters* 581: 3189–3196.

Gasch, P., Fundinger, M., Müller, J.T., Lee, T., Bailey-Serres, J., Mustroph, A., (2016) Redundant ERF-VII Transcription Factors Bind to an Evolutionarily Conserved cis-Motif to Regulate Hypoxia-Responsive Gene Expression in Arabidopsis. *The Plant Cell* 28: 160–180.

Gelvin, S.B., (2003) Agrobacterium-Mediated Plant Transformation: the Biology behind the "Gene-Jockeying" Tool. Microbiol Molecular Biology Review 67: 16–37.

Gibbs, D.J., Bacardit, J., Bachmair, A., Holdsworth, M.J., (2014a) The eukaryotic N-end rule pathway: conserved mechanisms and diverse functions. *Trends in Cell Biology* 24: 603–611.

Gibbs, D.J., Conde, J.V., Berckhan, S., Prasad, G., Mendiondo, G.M., Holdsworth, M.J., (2015) Group VII Ethylene Response Factors Coordinate Oxygen and Nitric Oxide Signal Transduction and Stress Responses in Plants. *Plant Physiology* 169: 23–31.

Gibbs, D.J., Lee, S.C., Isa, N.M., Gramuglia, S., Fukao, T., Bassel, G.W., Correia, C.S., Corbineau, F., Theodoulou, F.L., Bailey-Serres, J., Holdsworth, M.J., (2011) Homeostatic response to hypoxia is regulated by the N-end rule pathway in plants. *Nature* 479: 415–418.

Gibbs, D.J., Md Isa, N., Movahedi, M., Lozano-Juste, J., Mendiondo, G.M., Berckhan, S., Marín-de la Rosa, N., Vicente Conde, J., Sousa Correia, C., Pearce, S.P., Bassel, G.W., Hamali, B., Talloji, P., Tomé, D.F.A., Coego, A., Beynon, J., Alabadí, D., Bachmair, A., León, J., Gray, J.E., Theodoulou, F.L., Holdsworth, M.J., (2014b) Nitric oxide sensing in plants is mediated by proteolytic control of group VII ERF transcription factors. *Molecular Cell* 53: 369–379.

Gibbs, D.J., Tedds, H.M., Labandera, A.-M., Bailey, M., White, M.D., Hartman, S., Sprigg, C., Mogg, S.L., Osborne, R., Dambire, C., Boeckx, T., Paling, Z., Voesenek, L.A.C.J., Flashman, E., Holdsworth, M.J., (2018) Oxygen-dependent proteolysis regulates the stability of angiosperm polycomb repressive complex 2 subunit VERNALIZATION 2. *Nature Communications* 9: 5438.

Giuntoli, B., Perata, P., (2018) Group VII Ethylene Response Factors in Arabidopsis: Regulation and Physiological Roles. *Plant Physiology* 176: 1143–1155.

Giuntoli, B., Shukla, V., Maggiorelli, F., Giorgi, F.M., Lombardi, L., Perata, P., Licausi, F., (2017) Age-dependent regulation of ERF-VII transcription factor activity in Arabidopsis thaliana. *Plant Cell Environment* 40: 2333–2346.

Gonzalez-Guzman, M., Pizzio, G.A., Antoni, R., Vera-Sirera, F., Merilo, E., Bassel, G.W., Fernández, M.A., Holdsworth, M.J., Perez-Amador, M.A., Kollist, H., Rodriguez, P.L., (2012) Arabidopsis PYR/PYL/RCAR Receptors Play a Major Role in Quantitative Regulation of Stomatal Aperture and Transcriptional Response to Abscisic Acid. *Plant Cell* 24: 2483–2496.

Graciet, E., Mesiti, F., Wellmer, F., (2010) Structure and evolutionary conservation of the plant N-end rule pathway. *The Plant Journal* 61: 741–751.

Graciet, E., Walter, F., Ó'Maoiléidigh, D.S., Pollmann, S., Meyerowitz, E.M., Varshavsky, A., Wellmer, F., (2009) The N-end rule pathway controls multiple functions during Arabidopsis shoot and leaf development. *Proceedings of the National Academy of Sciences of the United States of America* 106: 13618–13623.

Gravot, A., Richard, G., Lime, T., Lemarié, S., Jubault, M., Lariagon, C., Lemoine, J., Vicente, J., Robert-Seilaniantz, A., Holdsworth, M.J., Manzanares-Dauleux, M.J., (2016) Hypoxia response in Arabidopsis roots infected by Plasmodiophora brassicae supports the development of clubroot. *BMC Plant Biology* 16: 251.

Grotewold, E., (2006) The genetics and biochemistry of floral pigments. *Annual Review of Plant Biology* 57: 761–780.

Ha, J.-H., Lee, H.-J., Jung, J.-H., Park, C.-M., (2017) Thermo-Induced Maintenance of Photo-oxidoreductases Underlies Plant Autotrophic Development. *Developmental Cell* 41: 170-179.

Haddad, J.J., (2004) Oxygen sensing and oxidant/redox-related pathways. *Biochemical and Biophysical Research Communications* 316: 969–977.

Han, S.-K., Sang, Y., Rodrigues, A., Wu, M.-F., Rodriguez, P.L., Wagner, D., (2012) The SWI2/SNF2 chromatin remodeling ATPase BRAHMA represses abscisic acid responses in the absence of the stress stimulus in Arabidopsis. *Plant Cell* 24: 4892–4906.

Hartman, S., Liu, Z., van Veen, H., Vicente, J., Reinen, E., Martopawiro, S., Zhang, H., van Dongen, N., Bosman, F., Bassel, G.W., Visser, E.J.W., Bailey-Serres, J., Theodoulou, F.L., Hebelstrup, K.H., Gibbs, D.J., Holdsworth, M.J., Sasidharan, R., Voesenek, L.A.C.J., (2019) Ethylene-mediated nitric oxide depletion pre-adapts plants to hypoxia stress. *Nature Communications* 10.

Hattori, Y., Nagai, K., Furukawa, S., Song, X.-J., Kawano, R., Sakakibara, H., Wu, J., Matsumoto, T., Yoshimura, A., Kitano, H., Matsuoka, M., Mori, H., Ashikari, M., (2009) The ethylene response factors SNORKEL1 and SNORKEL2 allow rice to adapt to deep water. *Nature* 460: 1026–1030.

Heyes, D.J., Hunter, C.N., (2005) Making light work of enzyme catalysis: protochlorophyllide oxidoreductase. *Trends in Biochemical Sciences* 30: 642–649.

Hinz, M., Wilson, I.W., Yang, J., Buerstenbinder, K., Llewellyn, D., Dennis, E.S., Sauter, M., Dolferus, R., (2010) Arabidopsis RAP2.2: An Ethylene Response Transcription Factor That Is Important for Hypoxia Survival. *Plant Physiology* 153: 757–772.

Hirano, K., Kouketu, E., Katoh, H., Aya, K., Ueguchi-Tanaka, M., Matsuoka, M., (2012) The suppressive function of the rice DELLA protein SLR1 is dependent on its transcriptional activation activity. *The Plant Journal* 71: 443–453.

Ho, Q.T., Verboven, P., Verlinden, B.E., Schenk, A., Delele, M.A., Rolletschek, H., Vercammen, J., Nicolaï, B.M., (2010) Genotype effects on internal gas gradients in apple fruit. *Journal of Experimental Botany* 61: 2745–2755.

Hoch, W.A., Zeldin, E.L., McCown, B.H., (2001) Physiological significance of anthocyanins during autumnal leaf senescence. *Tree Physiology* 21: 1–8.

Hoffmann-Benning, S., Kende, H., (1992) On the Role of Abscisic Acid and Gibberellin in the Regulation of Growth in Rice. *Plant Physiology* 99: 1156–1161.

Holdsworth, M.J., (2017) First hints of new sensors. *Nature Plants* 3: 767–768.

Holdsworth, M.J., Bentsink, L., Soppe, W.J.J., (2008) Molecular networks regulating Arabidopsis seed maturation, after-ripening, dormancy and germination. *New Phytologist* 179: 33–54.

Holman, T.J., Jones, P.D., Russell, L., Medhurst, A., Ubeda Tomás, S., Talloji, P., Marquez, J., Schmuths, H., Tung, S.-A., Taylor, I., Footitt, S., Bachmair, A., Theodoulou, F.L., Holdsworth, M.J., (2009) The N-end rule pathway promotes seed germination and establishment through removal of ABA sensitivity in Arabidopsis. *Proceedings of the National Academy of Sciences of the United States of America* 106: 4549–4554.

Hughes, N.M., Vogelmann, T.C., Smith, W.K., (2008) Optical effects of abaxial anthocyanin on absorption of red wavelengths by understorey species: revisiting the back-scatter hypothesis. *Journal of Experimental Botany* 59: 3435–3442.

Huq, E., Al-Sady, B., Hudson, M., Kim, C., Apel, K., Quail, P.H., (2004) Phytochrome-interacting factor 1 is a critical bHLH regulator of chlorophyll biosynthesis. *Science* 305: 1937–1941.

Hwang, C.-S., Shemorry, A., Varshavsky, A., (2010) N-terminal acetylation of cellular proteins creates specific degradation signals. *Science* 327: 973–977.

Jasinski, S., Piazza, P., Craft, J., Hay, A., Woolley, L., Rieu, I., Phillips, A., Hedden, P., Tsiantis, M., (2005) KNOX action in Arabidopsis is mediated by coordinate regulation of cytokinin and gibberellin activities. *Current Biology* 15: 1560–1565.

Jiang, Y.-F., Chou, C.-H., Lin, E.-C., Chiu, C.-H., (2011) Molecular characterization of hypoxia and hypoxia-inducible factor 1 alpha (HIF-1α) from Taiwan voles (Microtus kikuchii). *Comparative Biochemistry and Physiology*. 158: 183–188.

Josse, E.-M., Halliday, K.J., (2008) Skotomorphogenesis: the dark side of light signalling. *Current Biology* 18: 1144-1146.

Jung, K.-H., Seo, Y.-S., Walia, H., Cao, P., Fukao, T., Canlas, P.E., Amonpant, F., Bailey-Serres, J., Ronald, P.C., (2010) The submergence tolerance regulator Sub1A mediates stress-responsive expression of AP2/ERF transcription factors. *Plant Physiology* 152: 1674–1692.

Juntawong, P., Girke, T., Bazin, J., Bailey-Serres, J., (2014) Translational dynamics revealed by genome-wide profiling of ribosome footprints in Arabidopsis. *PNAS* 111, 203–212.

Kende, H., van der Knaap, E., Cho, HT., (1998) Deepwater rice: A model plant to study stem elongation. *Plant Physiology* 118, 1105–1110.

Kim, J.-M., Seok, O.-H., Ju, S., Heo, J.-E., Yeom, J., Kim, D.-S., Yoo, J.-Y., Varshavsky, A., Lee, C., Hwang, C.-S., (2018) Formyl-methionine as an N-degron of a eukaryotic N-end rule pathway. *Science* 362.

Kim, S., Schlicke, H., Ree, K.V., Karvonen, K., Subramaniam, A., Richter, A., Grimm, B., Braam, J., (2013) Arabidopsis Chlorophyll Biosynthesis: An Essential Balance between the Methylerythritol Phosphate and Tetrapyrrole Pathways. *The Plant Cell* 25: 4984.

Kim, Y., Tsuda, K., Igarashi, D., Hillmer, R.A., Sakakibara, H., Myers, C.L., Katagiri, F., (2014) Mechanisms underlying robustness and tunability in a plant immune signaling network. *Cell Host Microbe* 15: 84–94.

Kliebenstein, D.J., (2014) Orchestration of plant defense systems: genes to populations. *Trends in Plant Science* 19: 250–255.

Koren, I., Timms, R.T., Kula, T., Xu, Q., Li, M.Z., Elledge, S.J., (2018) The Eukaryotic Proteome Is Shaped by E3 Ubiquitin Ligases Targeting C-Terminal Degrons. *Cell* 173: 1622-1635.

Kosmacz, M., Parlanti, S., Schwarzländer, M., Kragler, F., Licausi, F., Van Dongen, J.T., (2015) The stability and nuclear localization of the transcription factor RAP2.12 are dynamically regulated by oxygen concentration. *Plant Cell Environment* 38: 1094–1103.

Kovacs, I., Lindermayr, C., (2013) Nitric oxide-based protein modification: formation and site-specificity of protein S-nitrosylation. Frontiers in Plant Science 4: 137.

Kovinich, N., Kayanja, G., Chanoca, A., Otegui, M.S., Grotewold, E., (2015) Abiotic stresses induce different localizations of anthocyanins in Arabidopsis. *Plant Signal Behaviours* 10.

Kovinich, N., Kayanja, G., Chanoca, A., Riedl, K., Otegui, M.S., Grotewold, E., (2014) Not all anthocyanins are born equal: distinct patterns induced by stress in Arabidopsis. *Planta* 240: 931–940.

Křeček, P., Skůpa, P., Libus, J., Naramoto, S., Tejos, R., Friml, J., Zažímalová, E., (2009) The PIN-FORMED (PIN) protein family of auxin transporters. *Genome Biology* 10: 249.

Kume, A., (2017) Importance of the green color, absorption gradient, and spectral absorption of chloroplasts for the radiative energy balance of leaves. *Journal of Plant Research* 130: 501–514.

la Rosa, N.M., Sotillo, B., Miskolczi, P., Gibbs, D.J., Vicente, J., Carbonero, P., Oñate-Sánchez, L., Holdsworth, M.J., Bhalerao, R., Alabadí, D., Blázquez, M.A., (2014) Large-Scale Identification of Gibberellin-Related Transcription Factors Defines Group VII ETHYLENE RESPONSE FACTORS as Functional DELLA Partners. *Plant Physiology* 166: 1022–1032.

Labra, M., Vannini, C., Grassi, F., Bracale, M., Balsemin, M., Basso, B., Sala, F., (2004) Genomic stability in Arabidopsis thaliana transgenic plants obtained by floral dip. *Theoretical and Applied Genetics* 109: 1512–1518.

Lee, J.H., Schöffl, F., (1997). GUS activity staining — a powerful tool in plant molecular biology, *Plant Molecular Biology Manual*. Springer Netherlands, Dordrecht, pp. 23–32.

Levy, J.S., Taylor, B.R., (2003) Effects of pulp mill solids and three composts on early growth of tomatoes. *Bioresource Technology* 89: 297–305.

Licausi, F., Dongen, J.T.V., Giuntoli, B., Novi, G., Santaniello, A., Geigenberger, P., Perata, P., (2010) HRE1 and HRE2, two hypoxia-inducible ethylene response factors, affect anaerobic responses in Arabidopsis thaliana. *The Plant Journal* 62: 302–315.

Licausi, F., Kosmacz, M., Weits, D.A., Giuntoli, B., Giorgi, F.M., Voesenek, L.A.C.J., Perata, P., van Dongen, J.T., (2011) Oxygen sensing in plants is mediated by an N-end rule pathway for protein destabilization. *Nature* 479, 419–422.

Liu, Y., Shi, L., Ye, N., Liu, R., Jia, W., Zhang, J., (2009) Nitric oxide-induced rapid decrease of abscisic acid concentration is required in breaking seed dormancy in Arabidopsis. *New Phytologist* 183: 1030–1042.

Lozano-Juste, J., León, J., (2011) Nitric oxide regulates DELLA content and PIF expression to promote photomorphogenesis in Arabidopsis. Plant Physiologist 156: 1410–1423.

Lu, D., Lin, W., Gao, X., Wu, S., Cheng, C., Avila, J., Heese, A., Devarenne, T.P., He, P., Shan, L., (2011) Direct ubiquitination of pattern recognition receptor FLS2 attenuates plant innate immunity. *Science* 332: 1439–1442.

Lumba, S., Toh, S., Handfield, L.-F., Swan, M., Liu, R., Youn, J.-Y., Cutler, S.R., Subramaniam, R., Provart, N., Moses, A., Desveaux, D., McCourt, P., (2014) A Mesoscale Abscisic Acid Hormone Interactome Reveals a Dynamic Signaling Landscape in Arabidopsis. *Developmental Cell* 29: 360–372.

Mancuso, S., Boselli, M., (2002) Characterisation of the oxygen fluxes in the division, elongation and mature zones of Vitis roots: influence of oxygen availability. *Planta* 214: 767–774.

Mano, J., Ohno, C., Domae, Y., Asada, K., (2001) Chloroplastic ascorbate peroxidase is the primary target of methylviologen-induced photooxidative stress in spinach leaves: its relevance to

monodehydroascorbate radical detected with in vivo ESR. *Biochimica et Biophysica Acta* 1504: 275–287.

Marino, D., Froidure, S., Canonne, J., Ben Khaled, S., Khafif, M., Pouzet, C., Jauneau, A., Roby, D., Rivas, S., (2013) Arabidopsis ubiquitin ligase MIEL1 mediates degradation of the transcription factor MYB30 weakening plant defence. *Nature Communication* 4: 1476.

Marino, D., Peeters, N., Rivas, S., (2012) Ubiquitination during plant immune signaling. *Plant Physiology* 160: 15–27.

Maxim, L.D., Niebo, R., McConnell, E.E., (2014) Perlite toxicology and epidemiology – a review. *Inhalation Toxicology* 26: 259–270.

Mazzella, M.A., Casal, J.J., Muschietti, J.P., Fox, A.R., (2014) Hormonal networks involved in apical hook development in darkness and their response to light. Frontiers in Plant Science 5: 52.

Mendiondo, G.M., Gibbs, D.J., Szurman-Zubrzycka, M., Korn, A., Marquez, J., Szarejko, I., Maluszynski, M., King, J., Axcell, B., Smart, K., Corbineau, F., Holdsworth, M.J., (2016) Enhanced waterlogging tolerance in barley by manipulation of expression of the N-end rule pathway E3 ligase PROTEOLYSIS6. *Plant Biotechnology Journal* 14: 40–50.

Meskauskiene, R., Nater, M., Goslings, D., Kessler, F., op den Camp, R., Apel, K., (2001). FLU: A negative regulator of chlorophyll biosynthesis in Arabidopsis thaliana *Proceedings of the National Academy of Sciences of the United States of America* 98: 12826–12831.

Müller, M., Munné-Bosch, S., (2015) Ethylene Response Factors: A Key Regulatory Hub in Hormone and Stress Signaling. *Plant Physiology* 169: 32–41.

Muneer, S., Kim, E.J., Park, J.S., Lee, J.H., (2014) Influence of Green, Red and Blue Light Emitting Diodes on Multiprotein Complex Proteins and Photosynthetic Activity under Different Light Intensities in Lettuce Leaves (Lactuca sativa L.*). International Journal of Molecular Science* 15: 4657–4670.

Mur, L.A.J., Mandon, J., Persijn, S., Cristescu, S.M., Moshkov, I.E., Novikova, G.V., Hall, M.A., Harren, F.J.M., Hebelstrup, K.H., Gupta, K.J., (2013) Nitric oxide in plants: an assessment of the current state of knowledge. *AoB Plants* 5: 52.

Murashige, T., Skoog, F., (1962) A Revised Medium for Rapid Growth and Bio Assays with Tobacco Tissue Cultures. *Physiologia Plantarum* 15: 473–497.

Mustroph, A., Zanetti, M.E., Jang, C.J.H., Holtan, H.E., Repetti, P.P., Galbraith, D.W., Girke, T., Bailey-Serres, J., (2009) Profiling translatomes of discrete cell populations resolves altered cellular priorities during hypoxia in Arabidopsis. *PNAS* 106: 18843–18848.

Nakano, T., Suzuki, K., Fujimura, T., Shinshi, H., (2006) Genome-Wide Analysis of the ERF Gene Family in Arabidopsis and Rice. *Plant Physiology* 140: 411–432.

Ohme-Takagi, M., Shinshi, H., (1995) Ethylene-inducible DNA binding proteins that interact with an ethylene-responsive element. *Plant Cell* 7: 173–182.

Okamuro, J.K., Caster, B., Villarroel, R., Van Montagu, M., Jofuku, K.D., (1997) The AP2 domain of APETALA2 defines a large new family of DNA binding proteins in Arabidopsis. *Proceedings of the National Academy of Sciences of the United States of America* 94: 7076–7081.

Olsen, K.M., Lea, U.S., Slimestad, R., Verheul, M., Lillo, C., (2008) Differential expression of four Arabidopsis PAL genes; PAL1 and PAL2 have functional specialization in abiotic environmental-triggered flavonoid synthesis. *Journal of Plant Physiology* 165: 1491–1499.

op den Camp, R.G.L., Przybyla, D., Ochsenbein, C., Laloi, C., Kim, C., Danon, A., Wagner, D., Hideg, É., Göbel, C., Feussner, I., Nater, M., Apel, K., (2003) Rapid Induction of Distinct Stress Responses after the Release of Singlet Oxygen in Arabidopsis. *Plant Cell* 15: 2320–2332.

Ou, B., Yin, K.-Q., Liu, S.-N., Yang, Y., Gu, T., Wing Hui, J.M., Zhang, L., Miao, J., Kondou, Y., Matsui, M., Gu, H.-Y., Qu, L.-J., (2011) A high-throughput screening system for Arabidopsis transcription factors and its application to Med25-dependent transcriptional regulation. *Molecular Plant* 4: 546–555.

Papdi, C., Pérez-Salamó, I., Joseph, M.P., Giuntoli, B., Bögre, L., Koncz, C., Szabados, L., (2015) The low oxygen, oxidative and osmotic stress responses synergistically act through the ethylene response factor VII genes RAP2.12, RAP2.2 and RAP2.3. *The Plant Journal* 82: 772–784.

Park, S.-E., Kim, J.-M., Seok, O.-H., Cho, H., Wadas, B., Kim, S.-Y., Varshavsky, A., Hwang, C.-S., (2015) Control of mammalian G protein signaling by N-terminal acetylation and the N-end rule pathway. *Science* 347: 1249–1252.

Paul, M.V., Iyer, S., Amerhauser, C., Lehmann, M., Dongen, J.T. van, Geigenberger, P., (2016) Oxygen Sensing via the Ethylene Response Transcription Factor RAP2.12 Affects Plant Metabolism and Performance under Both Normoxia and Hypoxia. *Plant Physiology* 172: 141–153.

Peirats-Llobet, M., Han, S.-K., Gonzalez-Guzman, M., Jeong, C.W., Rodriguez, L., Belda-Palazon, B., Wagner, D., Rodriguez, P.L., (2016) A Direct Link between Abscisic Acid Sensing and the Chromatin-Remodeling ATPase BRAHMA via Core ABA Signaling Pathway Components. Molecular Plant 9: 136–147.

Perrar, A., Dissmeyer, N., Huesgen, P.F., (2019) New beginnings and new ends: methods for large-scale characterization of protein termini and their use in plant biology. Journal of Experimental Botany 70: 2021–2038.

Piatkov, K., Graciet, E., Varshavsky, A., (2013) Ubiquitin Reference Technique and Its Use in Ubiquitin-Lacking Prokaryotes. *PLoS One* 8.

Piatkov, K.I., Vu, T.T.M., Hwang, C.-S., Varshavsky, A., (2015) Formyl-methionine as a degradation signal at the N-termini of bacterial proteins. *Microbial Cell* 2: 376–393.

Pickart, C.M., Eddins, M.J., (2004) Ubiquitin: structures, functions, mechanisms. *Biochimica et Biophysica Acta* 1695: 55–72.

Pucciariello, C., Perata, P., (2017) New insights into reactive oxygen species and nitric oxide signalling under low oxygen in plants. *Plant Cell Environment* 40: 473–482.

Raskin, I., Kende, H., (1984) Role of gibberellin in the growth response of submerged deep water rice. *Plant Physiology* 76: 947–950.

Raz, V., Ecker, J.R., (1999) Regulation of differential growth in the apical hook of Arabidopsis. *Development* 126: 3661–3668.

Reinbothe, C., Apel, K., Reinbothe, S., (1995) A light-induced protease from barley plastids degrades NADPH:protochlorophyllide oxidoreductase complexed with chlorophyllide. *Molecular and Cellular Biology* 15: 6206–6212.

Riber, W., Müller, J.T., Visser, E.J.W., Sasidharan, R., Voesenek, L.A.C.J., Mustroph, A., (2015) The Greening after Extended Darkness1 Is an N-End Rule Pathway Mutant with High Tolerance to Submergence and Starvation. *Plant Physiology* 167: 1616–1629.

Riechmann, J.L., Meyerowitz, E.M., (1998) The AP2/EREBP family of plant transcription factors. *Biological Chemistry* 379: 633–646.

Rodrigues, C., Vandenberghe, L.P. de S., Oliveira, J. de, Soccol, C.R., (2012) New perspectives of gibberellic acid production: a review. *Critical Reviews in Biotechnology* 32: 263–273.

Rolletschek, H., Weschke, W., Weber, H., Wobus, U., Borisjuk, L., (2004) Energy state and its control on seed development: starch accumulation is associated with high ATP and steep oxygen gradients within barley grains. *Journal of Experimental Botany* 55: 1351–1359.

Rosa, N.M. la, Sotillo, B., Miskolczi, P., Gibbs, D.J., Vicente, J., Carbonero, P., Oñate-Sánchez, L., Holdsworth, M.J., Bhalerao, R., Alabadí, D., Blázquez, M.A., (2014) Large-Scale Identification of Gibberellin-Related Transcription Factors Defines Group VII ETHYLENE RESPONSE FACTORS as Functional DELLA Partners. *Plant Physiology* 166: 1022–1032.

Sauter, M., (2013) Root responses to flooding. *Current Opinions in Plant Biology* 16: 282–286.

Sauter, M., (2000) Rice in deep water: “how to take heed against a sea of troubles.” *Naturwissenschaften* 87: 289–303.

Setter, T.L., Bhekasut, P., Greenway, H., (2010) Desiccation of leaves after de-submergence is one cause for intolerance to complete submergence of the rice cultivar IR 42. *Functional Plant Biology* 37: 1096.

Shabala, S., Shabala, L., Barcelo, J., Poschenrieder, C., (2014) Membrane transporters mediating root signalling and adaptive responses to oxygen deprivation and soil flooding. *Plant Cell Environment* 37: 2216–2233.

Sharma, B., Joshi, D., Yadav, P.K., Gupta, A.K., Bhatt, T.K., (2016) Role of Ubiquitin-Mediated Degradation System in Plant Biology. *Frontiers in Plant Science* 7.

Shemorry, A., Hwang, C.-S., Varshavsky, A., (2013) Control of protein quality and stoichiometries by N-terminal acetylation and the N-end rule pathway. *Molecular Cell* 50: 540–551.

Sperling, U., van Cleve, B., Frick, G., Apel, K., Armstrong, G.A., (1997) Overexpression of light-dependent PORA or PORB in plants depleted of endogenous POR by far-red light enhances seedling survival in white light and protects against photooxidative damage. *The Plant Journal* 12: 649–658.

Sriram, S.M., Kim, B.Y., Kwon, Y.T., (2011) The N-end rule pathway: emerging functions and molecular principles of substrate recognition. *Nature Reviews Molecular Cell Biology* 12: 735–747.

Szabó, I., Bergantino, E., Giacometti, G.M., (2005) Light and oxygenic photosynthesis: energy dissipation as a protection mechanism against photo-oxidation. *EMBO Reports* 6: 629–634.

Terry, M.J., Smith, A.G., (2013) A model for tetrapyrrole synthesis as the primary mechanism for plastid-to-nucleus signaling during chloroplast biogenesis. *Frontiers in Plant Science* 4.

Tester, M., Langridge, P., (2010) Breeding Technologies to Increase Crop Production in a Changing World. *Science* 327: 818–822.

Tobias, J.W., Shrader, T.E., Rocap, G., Varshavsky, A., (1991) The N-end rule in bacteria. *Science* 254: 1374–1377.

Triantaphylidès, C., Havaux, M., (2009) Singlet oxygen in plants: production, detoxification and signaling. *Trends in Plant Science* 14: 219–228.

van Dongen, J.T., Licausi, F., 2015. Oxygen Sensing and Signaling. *Annual Review of Plant Biology* 66: 345–367.

Varshavsky, A., (2019) N-degron and C-degron pathways of protein degradation. *PNAS* 116: 358–366.

Varshavsky, A., (2011) The N-end rule pathway and regulation by proteolysis. *Protein Science* 20: 1298–1345.

Varshavsky, A., (2005) Regulated protein degradation. Trends in Biochemistry. *Science* 30: 283–286.

Varshavsky, A., (1991) Naming a targeting signal. *Cell* 64: 13–15.

Vicente, J., Mendiondo, G.M., Movahedi, M., Peirats-Llobet, M., Juan, Y., Shen, Y., Dambire, C., Smart, K., Rodriguez, P.L., Charng, Y., Gray, J.E., Holdsworth, M.J., (2017) The Cys-Arg/N-End Rule Pathway Is a General Sensor of Abiotic Stress in Flowering Plants. *Current Biology* 27: 3183-3190.

Vicente, J., Mendiondo, G.M., Pauwels, J., Pastor, V., Izquierdo, Y., Naumann, C., Movahedi, M., Rooney, D., Gibbs, D.J., Smart, K., Bachmair, A., Gray, J.E., Dissmeyer, N., Castresana, C., Ray, R.V., Gevaert, K., Holdsworth, M.J., (2019) Distinct branches of the N-end rule pathway modulate the plant immune response. *New Phytologist* 221: 988–1000.

Vicente, J., Mendiondo, G.M., Pauwels, J., Pastor, V., Izquierdo, Y., Naumann, C., Movahedi, M., Rooney, D., Gibbs, D.J., Smart, K., Bachmair, A., Gray, J.E., Dissmeyer, N., Castresana, C., Ray, R.V., Gevaert, K., Holdsworth, M.J., (2018) Distinct branches of the N-end rule pathway modulate the plant immune response. *New Phytologist*.

Vicente, J.A., Peixoto, F., Lopes, M.L., Madeira, V.M., (2001) Differential sensitivities of plant and animal mitochondria to the herbicide paraquat. *Journal of Biochemical and Molecular Toxicology* 15: 322–330.

Voesenek, L. a. C.J., Colmer, T.D., Pierik, R., Millenaar, F.F., Peeters, A.J.M., (2006) How plants cope with complete submergence. *New Phytologist* 170: 213–226.

Voesenek, L. a. C.J., Sasidharan, R., (2013) Ethylene – and oxygen signalling – drive plant survival during flooding. *Plant Biology* 15: 426–435.

Wang, F., Chen, Z.-H., Shabala, S., (2017) Hypoxia Sensing in Plants: On a Quest for Ion Channels as Putative Oxygen Sensors. *Plant Cell Physiology* 58: 1126–1142.

Weits, D.A., Giuntoli, B., Kosmacz, M., Parlanti, S., Hubberten, H.-M., Riegler, H., Hoefgen, R., Perata, P., van Dongen, J.T., Licausi, F., (2014) Plant cysteine oxidases control the oxygen-dependent branch of the N-end-rule pathway. *Nature Communications* 5: 3425.

Weits, D.A., Kunkowska, A.B., Kamps, N.C.W., Portz, K.M.S., Packbier, N.K., Venza, Z.N., Gaillochet, C., Lohmann, J.U., Pedersen, O., Dongen, J.T. van, Licausi, F., (2019) An apical hypoxic niche sets the pace of shoot meristem activity. *Nature* 569: 714–717.

Welsch, R., Maass, D., Voegel, T., DellaPenna, D., Beyer, P., (2007) Transcription Factor RAP2.2 and Its Interacting Partner SINAT2: Stable Elements in the Carotenogenesis of Arabidopsis Leaves. *Plant Physiology* 145: 1073–1085.

White, M.D., Klecker, M., Hopkinson, R.J., Weits, D.A., Mueller, C., Naumann, C., O'Neill, R., Wickens, J., Yang, J., Brooks-Bartlett, J.C., Garman, E.F., Grossmann, T.N., Dissmeyer, N., Flashman, E., (2017) Plant cysteine oxidases are dioxygenases that directly enable arginyl transferase-catalysed arginylation of N-end rule targets. *Nature Communications* 8.

Wu, S.-H., (2014) Gene expression regulation in photomorphogenesis from the perspective of the central dogma. *Annual Review of Plant Biology* 65: 311–333.

Xu, K., Xu, X., Fukao, T., Canlas, P., Maghirang-Rodriguez, R., Heuer, S., Ismail, A.M., Bailey-Serres, J., Ronald, P.C., Mackill, D.J., (2006) Sub1A is an ethylene-response-factor-like gene that confers submergence tolerance to rice. *Nature* 442: 705–708.

Xu, R., Li, Q.Q., (2008) Protocol: Streamline cloning of genes into binary vectors in Agrobacterium via the Gateway® TOPO vector system. *Plant Methods* 4: 4.

Xu, Z., Rothstein, S.J., (2018) ROS-Induced anthocyanin production provides feedback protection by scavenging ROS and maintaining photosynthetic capacity in Arabidopsis. *Plant Signal Behaviours* 13.

Yang, S., Li, C., Zhao, L., Gao, S., Lu, J., Zhao, M., Chen, C.-Y., Liu, X., Luo, M., Cui, Y., Yang, C., Wu, K., (2015) The Arabidopsis SWI2/SNF2 Chromatin Remodeling ATPase BRAHMA Targets Directly to PINs and Is Required for Root Stem Cell Niche Maintenance. *Plant Cell* 27: 1670–1680.

Yoshida, S., Ito, M., Callis, J., Nishida, I., Watanabe, A., (2002) A delayed leaf senescence mutant is defective in arginyl-tRNA:protein arginyltransferase, a component of the N-end rule pathway in Arabidopsis. *Plant Journal* 32: 129–137.

Zeng, F., Konnerup, D., Shabala, L., Zhou, M., Colmer, T.D., Zhang, G., Shabala, S., (2014) Linking oxygen availability with membrane potential maintenance and K+ retention of barley roots: implications for waterlogging stress tolerance. *Plant Cell Environment* 37: 2325–2338.

Zhang, H., Gannon, L., Hassall, K.L., Deery, M.J., Gibbs, D.J., Holdsworth, M.J., van der Hoorn, R.A.L., Lilley, K.S., Theodoulou, F.L., (2018a) N-terminomics reveals control of Arabidopsis seed storage proteins and proteases by the Arg/N-end rule pathway. *New Phytologist* 218: 1106–1126.

Zhang, H., Gannon, L., Jones, P.D., Rundle, C.A., Hassall, K.L., Gibbs, D.J., Holdsworth, M.J., Theodoulou, F.L., (2018b) Genetic interactions between ABA signalling and the Arg/N-end rule pathway during Arabidopsis seedling establishment. *Scientific Reports* 8: 15192.

Zhang, K.-M., Yu, H.-J., Shi, K., Zhou, Y.-H., Yu, J.-Q., Xia, X.-J., (2010) Photoprotective roles of anthocyanins in Begonia semperflorens. *Plant Science* 179: 202–208.

Zhang, X., Henriques, R., Lin, S.-S., Niu, Q.-W., Chua, N.-H., (2006) Agrobacterium -mediated transformation of Arabidopsis thaliana using the floral dip method. *Nature Protocols* 1: 641.

Zhang, Y., Zheng, S., Liu, Z., Wang, L., Bi, Y., (2011) Both HY5 and HYH are necessary regulators for low temperature-induced anthocyanin accumulation in Arabidopsis seedlings. *Journal of Plant Physiology* 168: 367–374

Zhao, Y., Wei, T., Yin, K.-Q., Chen, Z., Gu, H., Qu, L.-J., Qin, G., (2012) Arabidopsis RAP2.2 plays an important role in plant resistance to Botrytis cinerea and ethylene responses. *New Phytologist* 195: 450–460.

Supplementary Information:

Forward primer:	5′-GAAACCCGCGGTGGTTGTGGAGGAGCTATAATAT-3′
Reverse primer:	5′-TTTTCCGCGGGAAGACTCCTCCAATCATG-3′

S1: Forward and Reverse Primers used for PCR amplification of truncated RAP2.12

Forward primer:	5'-ATTATAGCTCCTCCAGCACCACCGCGGAGCCTTAG-3'
Reverse primer:	5′-CTAAGGCTCCGCGGTGGTGCTGGAGGAGCTATAAT-3'

S2: Forward and Reverse Primers used for Site-Directed Mutagenesis of C^2-RAP2.12

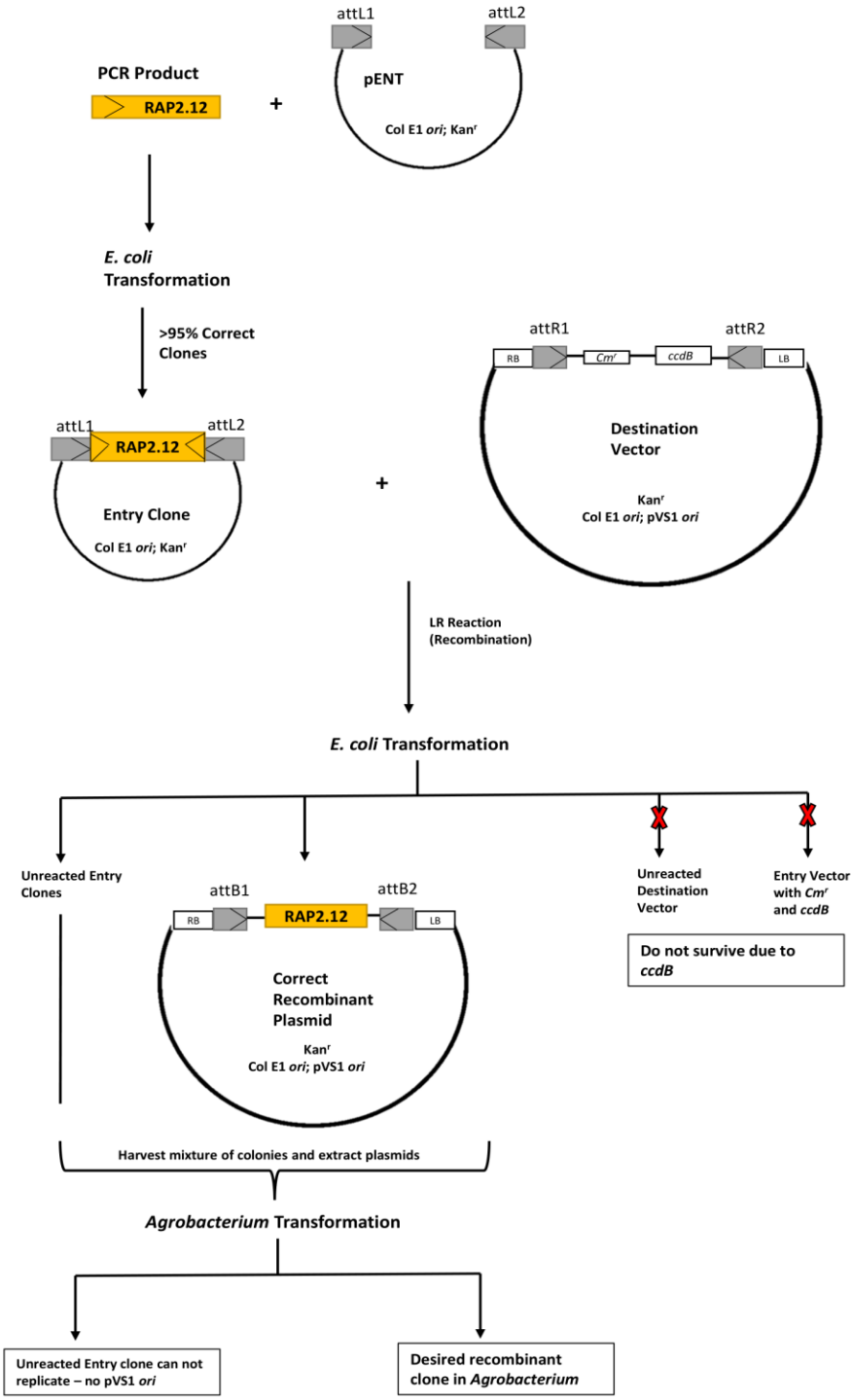

S3: Schematic of the PCR gene cloning to *Agrobacterium* using Gateway Cloning

Col E1 *ori*: origin of replication for E. coli; pVS1 ori: origin of replication for Agrobacterium; RB: right border of T-DNA; LB: left border of T-DNA; attL, attR, attB: recombination sites.